

THE INVESTIGATION OF WAVE-STRUCTURE INTERACTIONS FOR
THE COOLING WATER INTAKE STRUCTURE OF THE
DIABLO CANYON NUCLEAR POWER PLANT

by

Fredric Raichlen
Civil Engineer

Pacific C
77
San Fra

— NOTICE —

THE ATTACHED FILES ARE OFFICIAL RECORDS OF THE
DIVISION OF DOCUMENT CONTROL. THEY HAVE BEEN
CHARGED TO YOU FOR A LIMITED TIME PERIOD AND
MUST BE RETURNED TO THE RECORDS FACILITY
BRANCH 016. PLEASE DO NOT SEND DOCUMENTS
CHARGED OUT THROUGH THE MAIL. REMOVAL OF ANY
PAGE(S) FROM DOCUMENT FOR REPRODUCTION MUST
BE REFERRED TO FILE PERSONNEL.

DEADLINE RETURN DATE

50-275

1/10/83

830 1120 280

RECORDS FACILITY BRANCH

December 1982

8301120293 830110
PDR ADOCK 05000275
P PDR

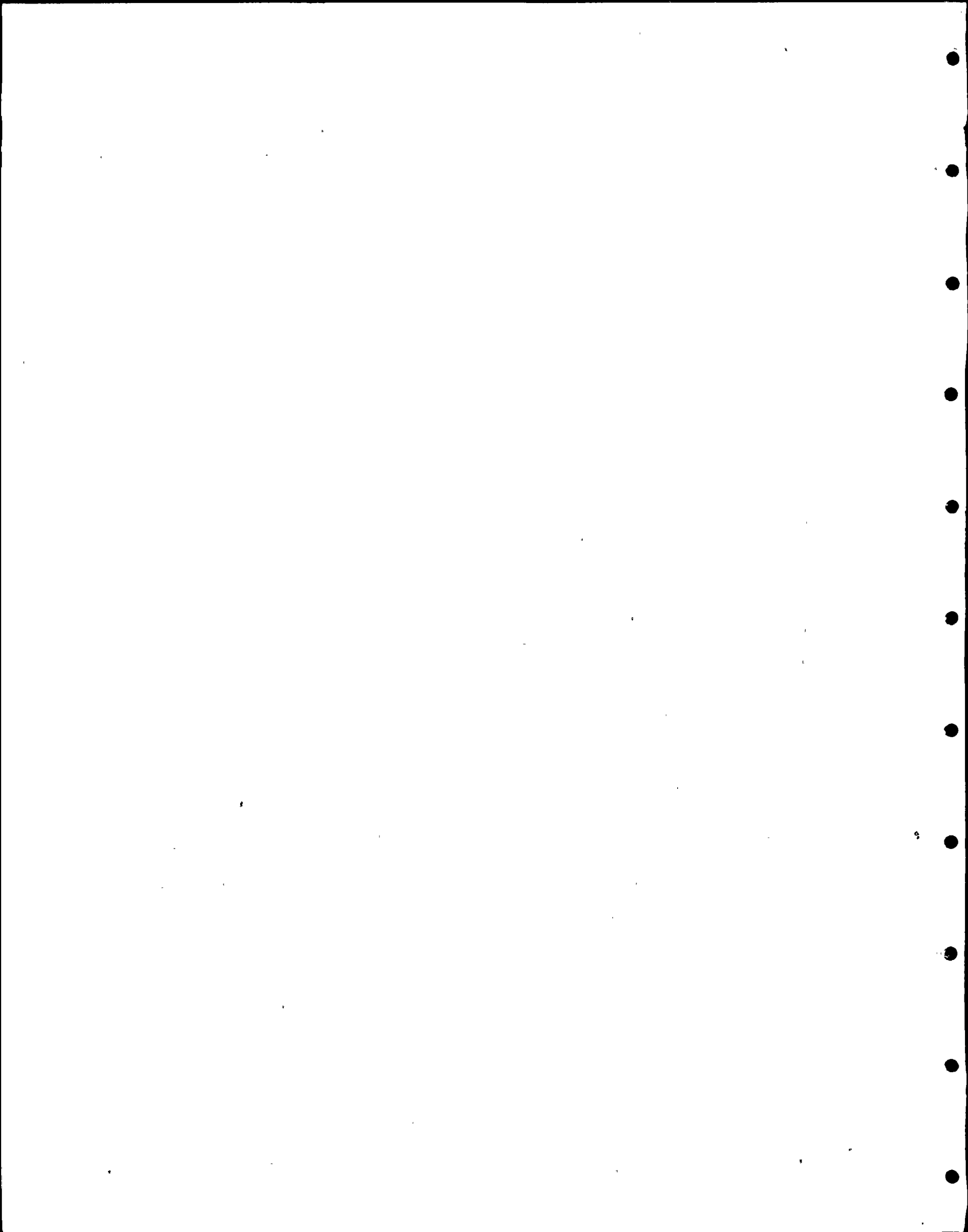


TABLE OF CONTENTS

	<u>Page</u>
List of Figures	
List of Tables	
Summary	1
1. Introduction	6
2. Experimental Equipment and Procedures	12
2.1 General Considerations	12
2.2 Wave Generators	14
2.3 Wave Measurements	21
2.4 Pressure Measurements	23
2.5 Auxiliary Saltwater Pump Forebay Model	27
2.6 Velocity Measurements	34
2.7 Data Acquisition and Analysis	34
2.8 Experimental Program	36
2.8.1 Wave-Induced Loads on the Curtain Wall	36
2.8.2 Wave-Induced Loads on the Auxiliary Saltwater Pump Forebays	37
2.8.3 Velocities at the Entrance to the Auxiliary Saltwater Pump Forebays	39
3. Presentation and Discussion of Results	40
3.1 Wave-Induced Loads on the Curtain Wall	40
3.1.1 Pressures on the curtain wall for the condition of: tsunami, high tide, meteorological tide, and 1981 ⁺ storm; (+17 ft MLLW)	55
3.1.2 Pressures on the curtain wall for the condition of: maximum tide and limit waves; (+7.5 ft MLLW)	74
3.2 Wave-Induced Loads on the Auxiliary Saltwater Pump Forebays	83
3.2.1 Pressures on the ceiling of the ASWP forebays for the conditions of: tsunami, high tide, meteorological tide, and 1981 ⁺ storm; (+17 ft MLLW)	85
3.2.2 Pressures on the ceiling of the ASWP forebays for the condition of: maximum tide and limit waves; (+7.5 ft MLLW)	88
3.2.3 Pressures on the ceiling of the ASWP forebays for the condition of: minimum tide and limit waves, and minimum tide and 1981 ⁺ storm; (-2 ft MLLW)	94

3.3	Velocities at the Entrance to the Auxiliary Saltwater Pump Forebays	101
3.3.1	Velocities at the entrance to the ASWP forebays for the condition of: tsunami, high tide, meteorological tide, and 1981 ⁺ storm; (+17 ft MLLW)	101
3.3.2	Velocities at the entrance to the ASWP forebays for the condition of: maximum tide (and minimum tide) and limit waves: (+7.5 ft MLLW and -2 ft MLLW)	105
4.	Conclusions	111
5.	References	113

List of Figures

<u>Figure</u>		<u>Page</u>
1	Energy Density Spectra as Measured by NOAA Buoy No. 46011	9
2	Basin Boundaries and Bathymetric Contours in Model (after Lillevang, Raichlen, and Cox, 1982)	13
3	Typical Cross-Sections of Degraded Breakwaters in the Model (after Lillevang, Raichlen, and Cox, 1982)	15
4a	Plan View of Cooling Water Intake Structure at Invert Elevation -28.9 ft MLLW	16
4b	Elevation of Cooling Water Intake Structure: Section A	17
4c	Elevation of Cooling Water Intake Structure: Section B	18
4d	Elevation of Cooling Water Intake Structure: Section C	19
5	Locations of Wavemaker and Wave Gages for Waves from the South (203°) (after Lillevang, Raichlen, and Cox, 1982)	22
6	Typical Wave Gage Calibration	24
7a	Vertical Location of Pressure Transducers in the Curtain Wall	26
7b	Pressure Transducers Mounted in the Pressure Block	26
8a	Curtain Wall Pressure Block and Calibration Block	28
8b	An Example of Pressure Cell Calibration Using (i) Air as the Pressure Media, (ii) Water Alone by Submergence of the Pressure Block	29
9a	Model of the Auxiliary Saltwater Pump Forebays	30
9b	Schematic Drawing of Forebays and Pressure Cell Locations	32
10	Model of the Cooling Water Intake Structure With the Forebay Section Attached	33
11	Typical Minature Current Meter Calibration	35
12	Ponding for Various Azimuth Directions and Offshore Wave Conditions as Measured at Locations R and S for Degraded Breakwater, +17 ft MLLW	42
13	Spectrum of Waves in Model Compared to Measured Spectrum for Storm of 1/28/81 at 1800 hrs GMT	46

List of Figures (cont'd)

14	Typical Time Histroy of Waves at Wavemaker During 1981 ⁺ Storm at +17 ft MLLW Water Level	48
15	Waves from Storm (1981 ⁺), +17 ft MLLW, 203°Az	50
16	Waves for T=16 sec, H _B =18 ft, +7.5 ft MLLW, 203°Az	51
17	Waves for T=16 sec, H _B =36 ft, +7.5 ft MLLW, 203°Az	52
18	Section of Oscillograph Trace for Run 130: 1981 ⁺ Storm, +17 ft MLLW, 225°Az, Center Panel Instrumented	53
19	Maximum Pressures Measured on Centerline During Storm of 1981 ⁺ Storm, +17 ft MLLW, 203°Az	57
20	Maximum Pressures Measured on Centerline During Storm of 1981 ⁺ Storm, +17 ft MLLW, 225°Az	58
21	Maximum Pressures Measured at West Corner During Storm of 1981 ⁺ , +17 ft MLLW, 225°Az	59
22	Normalized Wave Height Frequency Distirbution: 1981 ⁺ storm, +17 ft MLLW, 203°Az	61
23	Normalized Pressure Frequency Distribution: 1981 ⁺ storm, +17 ft MLLW, 203°Az	62
24	Normalized Head Difference Frequency Distribution: 1981 ⁺ storm, +17 ft MLLW, 203°Az	63
25	Normalized Wave Height Frequency Distribution: 1981 ⁺ storm, +17 ft MLLW, 225°Az, West Corner	65
26	Normalized Pressure Frequency Distribution: 1981 ⁺ storm, +17 ft MLLW, 225°Az, West Corner	66
27	Normalized Head Difference Frequency Distribution: 1981 ⁺ storm, +17 ft MLLW, 225°Az, West Corner	67
28	Normalized Pressure Frequency Distribution: 1981 ⁺ storm, +17 ft MLLW, 225°Az, Center	68
29	Normalized Head Difference Frequency Distribution: 1981 ⁺ storm, +17 ft MLLW, 225°Az, Center	69
30	Maximum Pressure Measured on Centerline for Periodic Waves: +7.5 ft. MLLW T=16 sec, H _B =41 ft., 225°Az	75
31	Variation of Total Pressure With Offshore Wave Height: +7.5 ft. MLLW, T=12 sec, 203°Az, Centerline	77

List of Figures (cont'd)

32	Variation of Total Pressure With Offshore Wave Height: +7.5 ft. MLLW, T=12 sec, 225°Az, Centerline	78
33	Variation of Total Pressure With Offshore Wave Height: +7.5 ft. MLLW, T=12 sec, 225°Az, Corner	79
34	Variation of Total Pressure With Offshore Wave Height: +7.5 ft. MLLW, T=16 sec, 203°Az, Centerline	80
35	Variation of Total Pressure With Offshore Wave Height: +7.5 ft MLLW, T=16 sec, 225°Az, Centerline	81
36	Variation of Total Pressure With Offshore Wave Height: +7.5 ft MLLW, T=16 sec, 225°Az, West Corner	82
37	Normalized Pressure Frequency Distribution on Forebay Ceiling: 1981 ⁺ storm, +17 ft. MLLW, 203°Az, unvented	86
38	Normalized Pressure Frequency Distribution on Forebay Ceiling: 1981 ⁺ storm, +17 ft. MLLW, 203°Az, vented (Moderate)	87
39	Total Pressure on Forebay Ceiling vs. Wave Height: +7.5 ft MLLW, T=12 sec, 203°Az, Unvented	89
40	Total Pressure on Forebay Ceiling vs. Wave Height: +7.5 ft. MLLW, T=12 sec, 203°Az, Vented (Moderate)	90
41	Total Pressure on Forebay Ceiling vs. Wave Height: +7.5 ft MLLW, T=16 sec, 203°Az, Unvented	91
42	Total Pressure on Forebay Ceiling vs. Wave Height: +7.5 ft MLLW, T=16 sec, 203°Az, Vented (Moderate)	92
43	Total Pressure on Forebay Ceiling vs. Wave Height: -2 ft MLLW, T=12 sec, 203°Az, Unvented	95
44	Total Pressure on Forebay Ceiling vs. Wave Height: -2 ft MLLW, T=12 sec, 203°Az, Vented (Moderate)	96
45	Total Pressure on Forebay Ceiling vs. Wave Height: -2 ft. MLLW, T=16 sec, 203°Az, Unvented	98
46	Total Pressure on Forebay Ceiling vs. Wave Height: -2 ft MLLW, T=16 sec, 203°Az, Vented (Moderate)	99
47	Normalized Pressure Frequency Distribution on Forebay Ceiling: 1981 ⁺ storm, -2 ft MLLW, 203°Az, Unvented, Vented (Moderate), Vented (Full)	100
48	Normalized Velocity Frequency Distribution at Entrance to ASWP Forebay: 1981 ⁺ storm, +17 ft MLLW, 203°Az, Unvented	102

List of Figures (cont'd)

49	Sequential Photographs of: (a) Dye injected at entrance to forebay, (b) Dye diffused through forebay, 5 min (prototype) later	104
50	Velocity at Entrance to ASWP Forebay: +7.5 ft. MLLW, T=12 sec, 203°Az, Unvented	106
51	Velocity at Entrance to ASWP Forebay: +7.5 ft MLLW, T=16 sec, 203°Az, Unvented	106
52	Velocity at Entrance to ASWP Forebay: -2 ft MLLW, T=12 sec, 203°Az, Unvented	108
53	Velocity at Entrance to ASWP Forebay: -2 ft MLLW, T=16 sec, 203°Az, Unvented	108
54	Velocity at Entrance to ASWP Forebay: -2 ft MLLW, T=16 sec, 203°Az, Vented (Moderate)	109

List of Figures (cont'd)

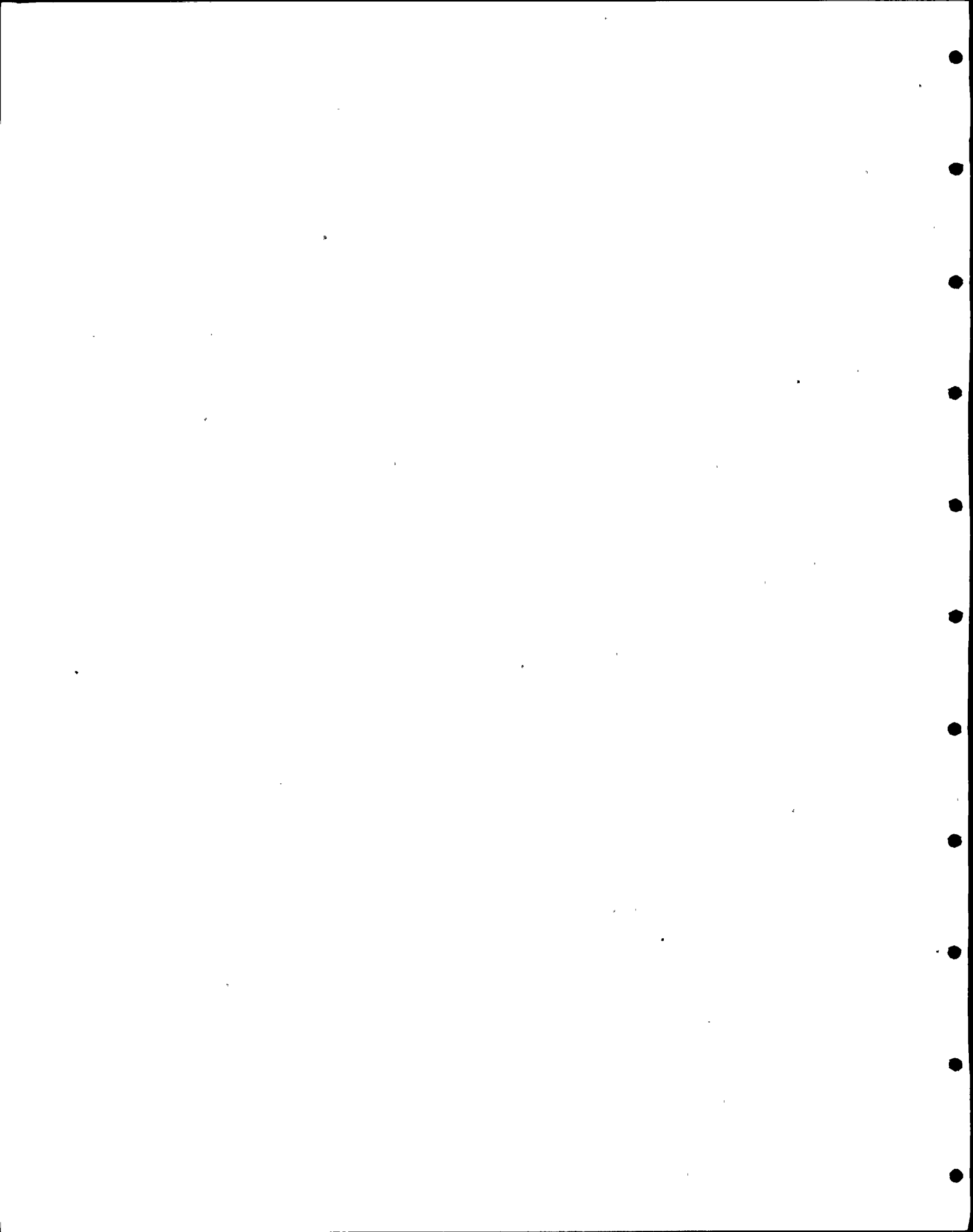
32	Variation of Total Pressure With Offshore Wave Height: +7.5 ft. MLLW, T=12 sec, 225°Az, Centerline	78
33	Variation of Total Pressure With Offshore Wave Height: +7.5 ft. MLLW, T=12 sec, 225°Az, Corner	79
34	Variation of Total Pressure With Offshore Wave Height: +7.5 ft. MLLW, T=16 sec, 203°Az, Centerline	80
35	Variation of Total Pressure With Offshore Wave Height: +7.5 ft MLLW, T=16 sec, 225°Az, Centerline	81
36	Variation of Total Pressure With Offshore Wave Height: +7.5 ft MLLW, T=16 sec, 225°Az, West Corner	82
37	Normalized Pressure Frequency Distribution on Forebay Ceiling: 1981 ⁺ storm, +17 ft. MLLW, 203°Az, unvented	86
38	Normalized Pressure Frequency Distribution on Forebay Ceiling: 1981 ⁺ storm, +17 ft. MLLW, 203°Az, vented (Moderate)	87
39	Total Pressure on Forebay Ceiling vs. Wave Height: +7.5 ft MLLW, T=12 sec, 203°Az, Unvented	89
40	Total Pressure on Forebay Ceiling vs. Wave Height: +7.5 ft. MLLW, T=12 sec, 203°Az, Vented (Moderate)	90
41	Total Pressure on Forebay Ceiling vs. Wave Height: +7.5 ft MLLW, T=16 sec, 203°Az, Unvented	91
42	Total Pressure on Forebay Ceiling vs. Wave Height: +7.5 ft MLLW, T=16 sec, 203°Az, Vented (Moderate)	92
43	Total Pressure on Forebay Ceiling vs. Wave Height: -2 ft MLLW, T=12 sec, 203°Az, Unvented	95
44	Total Pressure on Forebay Ceiling vs. Wave Height: -2 ft MLLW, T=12 sec, 203°Az, Vented (Moderate)	96
45	Total Pressure on Forebay Ceiling vs. Wave Height: -2 ft. MLLW, T=16 sec, 203°Az, Unvented	98
46	Total Pressure on Forebay Ceiling vs. Wave Height: -2 ft MLLW, T=16 sec, 203°Az, Vented (Moderate)	99
47	Normalized Pressure Frequency Distribution on Forebay Ceiling: 1981 ⁺ storm, -2 ft MLLW, 203°Az, Unvented, Vented (Moderate), Vented (Full)	100
48	Normalized Velocity Frequency Distribution at Entrance to ASWP Forebay: 1981 ⁺ storm, +17 ft MLLW, 203°Az, Unvented	102

List of Figures (cont'd)

49	Sequential Photographs of: (a) Dye injected at entrance to forebay, (b) Dye diffused through forebay, 5 min (prototype) later	104
50	Velocity at Entrance to ASWP Forebay: +7.5 ft. MLLW, T=12 sec, 203°Az, Unvented	106
51	Velocity at Entrance to ASWP Forebay: +7.5 ft MLLW, T=16 sec, 203°Az, Unvented	106
52	Velocity at Entrance to ASWP Forebay: -2 ft MLLW, T=12 sec, 203°Az, Unvented	108
53	Velocity at Entrance to ASWP Forebay: -2 ft MLLW, T=16 sec, 203°Az, Unvented	108
54	Velocity at Entrance to ASWP Forebay: -2 ft MLLW, T=16 sec, 203°Az, Vented (Moderate)	109

LIST OF TABLES

	<u>Page</u>
Table 1 Data on Irregular Storm Waves from Measurements and Hindcasts	45



Summary

This report describes results of hydraulic model experiments conducted to define wave-induced effects at the intake structure of the Diablo Canyon Nuclear Power Plant: (1) loads acting on the curtain wall, (2) loads acting on the ceilings of the Auxiliary Saltwater Pump forebays, and (3) velocities at the entrance to the Auxiliary Saltwater Pump (ASWP) forebays. Observations within the forebays are presented and discussed.

The three-dimensional hydraulic model was basically the same as that discussed in the report by Lillevang, Raichlen, and Cox (1982) used for earlier wave force measurements on the ASWP air vents and for experiments related to the west breakwater repair. The model is constructed to an undistorted scale of 1:45. For the current test program the cooling water intake structure was modified to accurately model the ASWP forebays. Pressures were measured using 1/4 in. diameter flush-mounted pressure cells. Velocities were measured using miniature propeller meters. Water surface displacements were measured using capacitance wave gages. Waves were generated in the model basin by hydraulically driven piston type wave generators capable of generating either periodic or irregular waves. Where appropriate the wave machine trajectory for periodic waves was based upon cnoidal wave theory.

Two major sets of conditions were simulated and investigated in the model corresponding to conditions which have been identified by the Nuclear Regulatory Commission as "design flood events". These were:

(i) A probable maximum tsunami combined with storm waves of mean annual severity and high tide with anomaly. For these conditions the NRC defined the maximum still water level to be 15.5 ft MLLW; however, for the

experiments a more severe condition of +17 ft MLLW was used. Also for the mean annual storm, a more severe case was used in the laboratory experiments. Irregular waves based on the recorded wave spectrum of the storm of January 28, 1981 at 1800 hrs GMT were used. However, the storm simulated in the model was much more intense and corresponds to storm waves with a return period of about 41 years and a period of the peak energy of nearly 16 sec. It is denoted herein as the 1981⁺ storm.

(ii) A maximum credible wave event combined with high tide with anomaly. (A still water surface elevation of +7.5 ft MLLW was used in the model compared to 6.3 ft MLLW proposed by the NRC.) In lieu of defining a maximum credible wave event, the concept of limit waves as described by Lillevang, Raichlen, and Cox (1982) was used. Limit waves refer to the limiting height of waves occurring shoreward of the breakwaters in the intake basin which were observed in the model, i.e., as the height of waves generated near the wave machines increased, a maximum wave height was reached in the intake basin.

In all experiments a "degraded" breakwater condition was used. As defined in experiments reported by Lillevang, Raichlen, and Cox (1982) this condition was postulated to result from the combined effect of a seismic event and wave events with no repair attempted so that the crests of both the east and the west breakwaters were levelled to an elevation of zero ft relative to mean lower low water (MLLW). The seaward slopes below the crest level were as originally constructed and the basin side of each breakwater was widened to include the material above elevation zero in the undisturbed cross-section. A shoreward side slope of 1.5 horizontal to 1 vertical was assumed. The cross-section was maintained with moderate repair during the testing program by fixing its shape with

a wide mesh net passing over the section and held in place by weights.

Two wave directions were used in these experiments: southerly waves with a direction of 203° in a depth of about 100 ft and southwesterly waves with a direction of 225° in the same depth; the corresponding directions in deep water are 180° and 225° , respectively. The southerly direction was considered because it provided the most direct incidence on the intake structure with waves travelling between natural terrain features, over the two breakwaters, and through the breakwater gap. The southwesterly direction was used because of the minimal effect on the waves of refraction due to the offshore bathymetry when waves approach the site from this direction. Further details on the choice of wave directions are given in the 1982 supplemental letter to the report by Lillevang, Raichlen, and Cox (1982).

In order to define the loading on the curtain wall, pressures were measured at seven elevations on the centerline of the intake structure for the southerly and southwesterly wave directions and at the west corner of the structure for the southwesterly waves. Simultaneous with these measurements, the water surface elevation was measured as a function of time on the front face of the curtain wall and at the bar screen deck opening. These measurements provided data from which estimates of the wave-induced loads acting on the front face of the curtain wall could be made due to the "design flood events".

Pressures were measured at selected locations on the ceiling of the ASWP forebays for the "design flood events" described earlier. This was investigated for three conditions of venting of the ASWP forebays: unvented or an airtight ceiling, moderate venting where an opening equivalent to a 5.6 in. diameter hole existed in the floor of the main pump room, and

fully vented where an opening in the floor of the main pump room equivalent to a 17 in. diameter hole was considered.

Velocities were measured at the entrance to the ASWP forebays under the wave and tide conditions described. In addition, observations were made of injected dye to assist in defining internal velocities in the forebays. Plastic cubes with a specific gravity of about 1.3 were used to assist in defining the potential for entrainment of missiles within the ASWP forebays.

The major conclusions which were reached as a result of this investigation are as follows:

- a. For all conditions tested, no impact pressures were observed on the seaward face of the curtain wall of the cooling water intake structure.
- b. In general, the pressure distributions observed were somewhat less than hydrostatic relative to the water level at the front of the curtain wall which occurred simultaneously with the maximum pressures.
- c. For irregular waves and a still water level of +17 ft MLLW, the frequency distribution of wave heights and pressure on the curtain wall appears to follow a Rayleigh distribution.
- d. For the 1981⁺ storm and a water surface elevation of +17 ft MLLW, the maximum total pressure measured on the front face of the curtain wall which occurs on the centerline at the lowest elevation was 44 ft. The probable maximum total pressure, obtained from the measurements and probability theory, would be about 59 ft.
- e. For the pressures measured for the maximum credible wave event at a tide of +7.5 ft MLLW, treated using the limit wave concept, the loading on the centerline of the front face of the curtain wall was significantly less than for the conditions at +17 ft MLLW. The maximum total pressure measured at the lowest elevation was about 27 ft.
- f. Impact pressures may occur on the underside of the deck of the intake structure. Tests indicated the pressures would be mitigated by removing the deck section abutting the parapet wall or installing wedge-shaped fillets under the deck in the corner formed by the deck and the curtain wall.
- g. Impact pressures may occur on the ceiling of the ASWP forebay for the fully vented condition. Tests indicated that these pressures would be mitigated by restricting the venting to the moderately vented condition, or eliminating leaks, i.e., the unvented condition.
- h. For the 1981⁺ storm and a +17 ft MLLW still water level the pressures measured on the ceilings of the four ASWP forebays with the structure vented or unvented were similar. The maximum total pressure measured was 56 ft and the estimated probable maximum total pressure was between 88 ft and 97 ft.

- i. For still water levels of +7.5 ft MLLW and -2 ft MLLW and for 12 sec and 16 sec periodic limit waves the total pressures measured on the ceiling of the auxiliary saltwater pump forebays were less than 64 ft. For -2 ft MLLW and the 1981⁺ storm the probable maximum pressure would be less than about 57 ft if the chamber is unvented or less than about 73 ft if it is vented by a small opening. (The maximum pressures measured were 30 ft for the unvented case and 41 ft for the moderately vented case.)
- j. For +17 ft MLLW and the 1981⁺ storm the maximum measured velocity at the ASWP forebay entrances was about 4 fps and the probable maximum velocity inferred from measured cumulative frequency distributions would be between 4.0 fps and 7.8 fps. At extreme high tide (+7.5 ft MLLW) and at extreme low tide (-2 ft MLLW) using limit periodic waves for all conditions investigated the maximum velocities measured were less than 1 fps.
- k. Photographs and visual observations of dye demonstrate the velocities in the forebays are less than those at the forebay entrance.
- l. Plastic cubes with a specific gravity of about 1.3 moved only slowly along the floor of the ASWP forebays during irregular wave exposure indicating that missile entrainment would be extremely unlikely.

1. INTRODUCTION

The Nuclear Regulatory Commission (NRC) has requested information on wave-induced loads acting on the Cooling Water Intake Structure of the Diablo Canyon Nuclear Power Plant. The wave loads investigated were those acting on the curtain wall of the intake structure and on the ceiling of the auxiliary saltwater pump (ASWP) forebays. The latter includes the floor of the main cooling water pump room located adjacent to the ASWP rooms. The impetus for investigating these locations was a concern that, due to wave impacts, pressures would be large enough to exceed the structural capacity for these portions of the structure. It was hypothesized that excessive loads could produce damage which could lead to the flooding of the ASWP rooms. In addition, a question was raised as to whether missiles could be entrained in the ASWP forebays by interior currents generated by outside storm waves.

Experiments were conducted in the existing three-dimensional hydraulic model of the Diablo Canyon site to specifically investigate these questions and the results of these experiments related to the above questions will be discussed in this report. Certain aspects of this study rely on data acquired in prior model studies of the Diablo Canyon Nuclear Power Plant which were related to defining wave-induced forces which could act on the ASWP air intake structures located on the deck of the cooling water intake structure as well as defining measures to prevent water ingestion into the ASWP room due to the overtopping of the seaward parapet wall by waves. The original purpose for which the three-dimensional model was built was to define remedial methods for the reconstruction of the damaged portion of the west breakwater which provides one seaward limit of the cooling water intake basin. The results relating to the forces on the ASWP air intake

structures are presented in the report of Lillevang, Raichlen, and Cox (1982); the results dealing with the repair of the west breakwater are to be presented in a forthcoming report.

The conditions for the experimental program are based on the results of a meeting with staff members of the NRC and PG and E staff on September 25, 1981 where it was proposed to test the design flood events with the conditions of the east and the west breakwater crests degraded to an elevation of MLLW. The design flood events are defined as:

- (i) A probable maximum tsunami combined with storm waves of mean annual severity and high tide with anomaly.
- (ii) A maximum credible wave event combined with high tide with anomaly.

In the series of tests related to Case (i), the water level has been defined as consisting of a maximum change in water level relative to the plant due to the tsunami of 8.5 ft with a maximum astronomical tide of 7.5 ft and a meteorological tide of 1 ft resulting in a total still water surface elevation relative to mean low low water (MLLW) of +17 ft. This is more severe than the NRC's SER which states +15.5 ft MLLW for the event. (Hwang and Brandsma (1974) indicate that this level exists for only a relatively short period of time (of the order of 2 to 3 minutes). This should be kept in mind when considering maximum water level conditions.) The storm consisting of waves of mean annual severity (a yearly recurrence interval) has not been defined for this site. Waves from a storm with a much longer recurrence interval were imposed upon the model. Wave measurements were available for the storm of January 28, 1981 from oceanographic buoy no. 46011 maintained by the National Oceanic and Atmospheric Administration (NOAA), located at latitude 34°52"N and longitude 120°52"W

in about 600 ft of water. It was this storm which damaged the west breakwater at the plant site. The buoy transmitted, on an hourly basis, energy density spectra of waves in terms of the energy density (m^2/hz) for each of fifty frequency bands. From these data it was determined that the significant wave height at the buoy for waves from the storm of January 28, 1981 at 1800 hours Greenwich Mean Time (GMT) was 22.74 ft. Examples of spectra obtained from this buoy are presented in Figure 1. When this spectrum for 1800 hrs GMT is refracted and shoaled in accordance with linear theory, a significant wave height of about 21.8 ft is obtained at a position near the tip of the west breakwater away from the influence of certain extreme bottom features. Thus, the result of both refraction and shoaling for the direction of this storm is to reduce the significant wave height somewhat from that measured in 600 ft of water at the buoy. The direction of this storm was determined from hindcast studies conducted in connection with the breakwater repair phase of the Diablo Canyon model investigation (see Strange, 1982), and from a numerical refraction model; the direction was determined to be about 249° in a depth of 100 ft. In a study connected with the breakwater investigation regarding the probability of recurrence of storms at the Diablo Canyon site it was determined by Borgman (1982) that this storm would have a recurrence interval of about 15.6 years. This storm was simulated in the model (although scaled to a greater intensity) and used in combination with the tsunami, high tide, and meteorological tide event to define the various forces and internal velocities which were of interest at the intake structure. Thus, a more severe condition was imposed in the model than had been proposed originally by the NRC, and the storm simulated in the model, in accordance with Borgman (1982), is estimated to have a recurrence interval of 41 years.

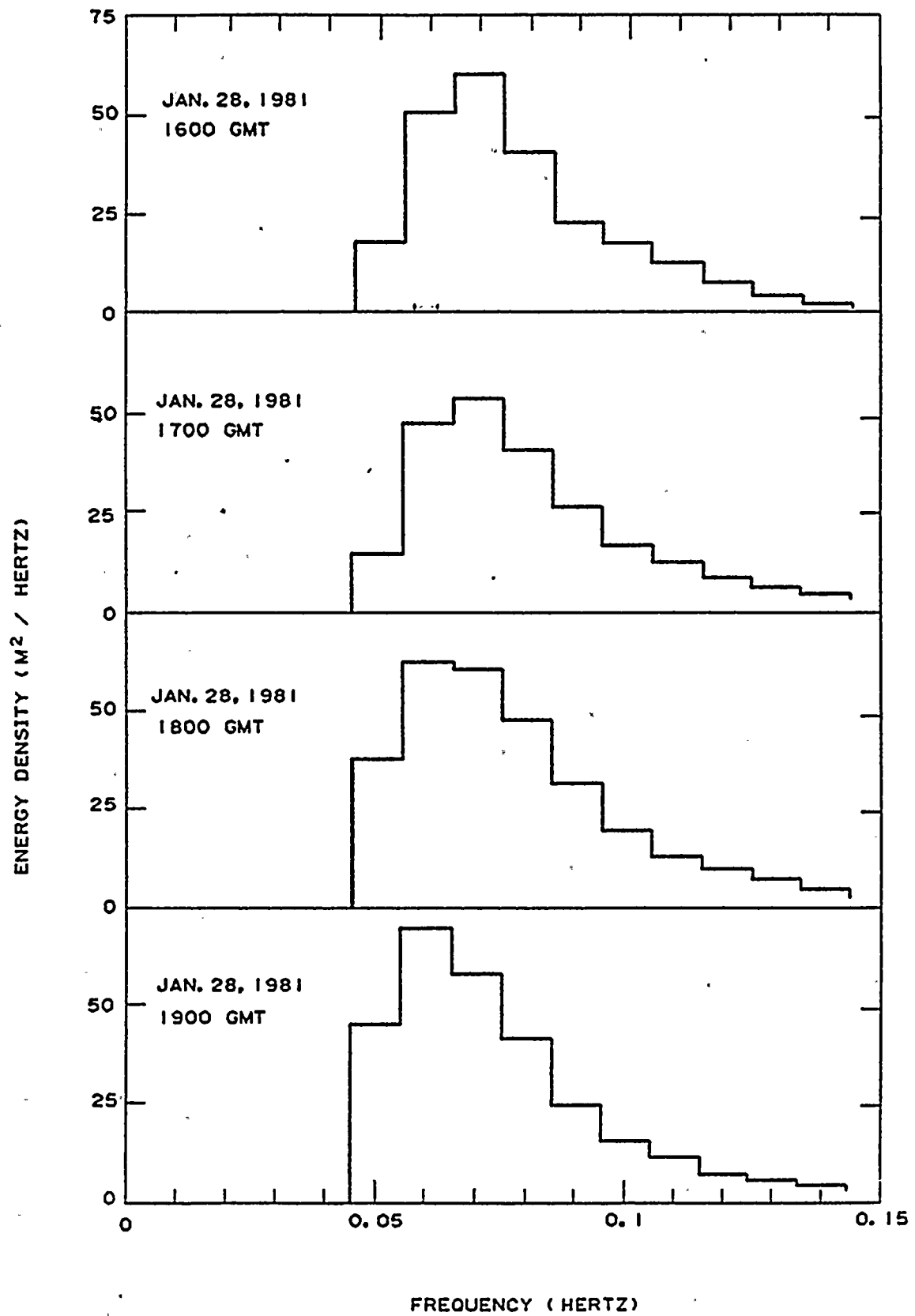


FIGURE 1 Energy Density Spectra as Measured by NOAA Buoy No. 46011

With regard to Case (ii) (the maximum credible wave event imposed with a +7.5 ft high tide) an extreme test condition was contrived. Rather than defining the "maximum credible wave event" the approach taken in the study dealing with the forces on the ASWP air intake structures was employed. This was described by Lillevang, Raichlen, and Cox (1982) as the "limit wave" approach where it was realized that waves impinging on the cooling water intake structure were limited in height by the effects of the degraded breakwater and the nearshore terrain in the basin in front of the intake. Therefore, in the model such conditions were imposed using regular waves with periods corresponding to the range of periods realized at the site and with maximum wave heights. Thus, "limit" periodic waves were used in the model for the extreme high tide experiments, i.e., a still water level of +7.5 ft MLLW.

Two wave directions were used for all experiments. The first direction in deep water was 180° which due to refraction caused by the offshore bathymetry becomes 203° at the location of the wave machines in the model. The second was for a direction in deep water of 225° which because of refraction for the wave period range of interest results in a wave direction at the wave machines which is unchanged, i.e., 225° . Although hindcast studies indicate important historic storms tend to approach from westerly directions, the southerly (203°) direction was considered of primary importance because it provided the most direct incidence on the intake structure with waves traveling between natural terrain features and through the breakwater gap most directly as well as overtopping both breakwaters. The direction of 225° was used because of the minimal effect on the waves of the bathymetry seaward of the -80 ft MLLW to -100 ft MLLW contours. Certain other aspects of the influence of direction

of the incident waves on the structure will be discussed more fully in Section 3.1.

A detailed quantitative study of wave-induced loads on the curtain wall was preceded by an exploratory investigation where the occurrence of significant impact pressures was investigated. Such intense pressures of short duration were not observed. Therefore, a more structured experimental program was developed; the results of this aspect of the program are the subject of this report.

2. EXPERIMENTAL EQUIPMENT AND PROCEDURES

2.1 General Considerations

The experiments were conducted in the same model basin using the intake model (with certain modifications) that was used in earlier studies reported by Lillevang, Raichlen, and Cox (1982). Therefore, the equipment will be described here only briefly; the interested reader is referred to the cited publication for a more complete description of the system.

The model basin is 120 ft long, 80 ft wide, and 4 ft deep. The boundaries of the basin are oriented in a north-south, east-west direction with regard to the power plant coordinates; the general layout and the basin boundaries can be seen in Figure 2. The nearshore contorted bathymetry and the bathymetry to a depth of -100 ft MLLW was carefully modelled at an undistorted scale of 1:45, using offshore surveys obtained from several sources. About one-third of the area of the model basin was kept at a depth of -100 ft MLLW to provide room for maneuvering and positioning the wave machines; this region had a thicker floor to accommodate the weight of the wave generators.

All experiments for which results are reported herein were conducted with the east and the west breakwaters in a "degraded" condition. The crest elevation of the breakwaters was maintained at zero ft elevation with reference to mean lower low water (MLLW). It was assumed that the breakwaters reached this configuration by having material originally located above MLLW moved onto the basin side of the cross-section. Thus, the seaward slopes below MLLW remained as originally constructed and the

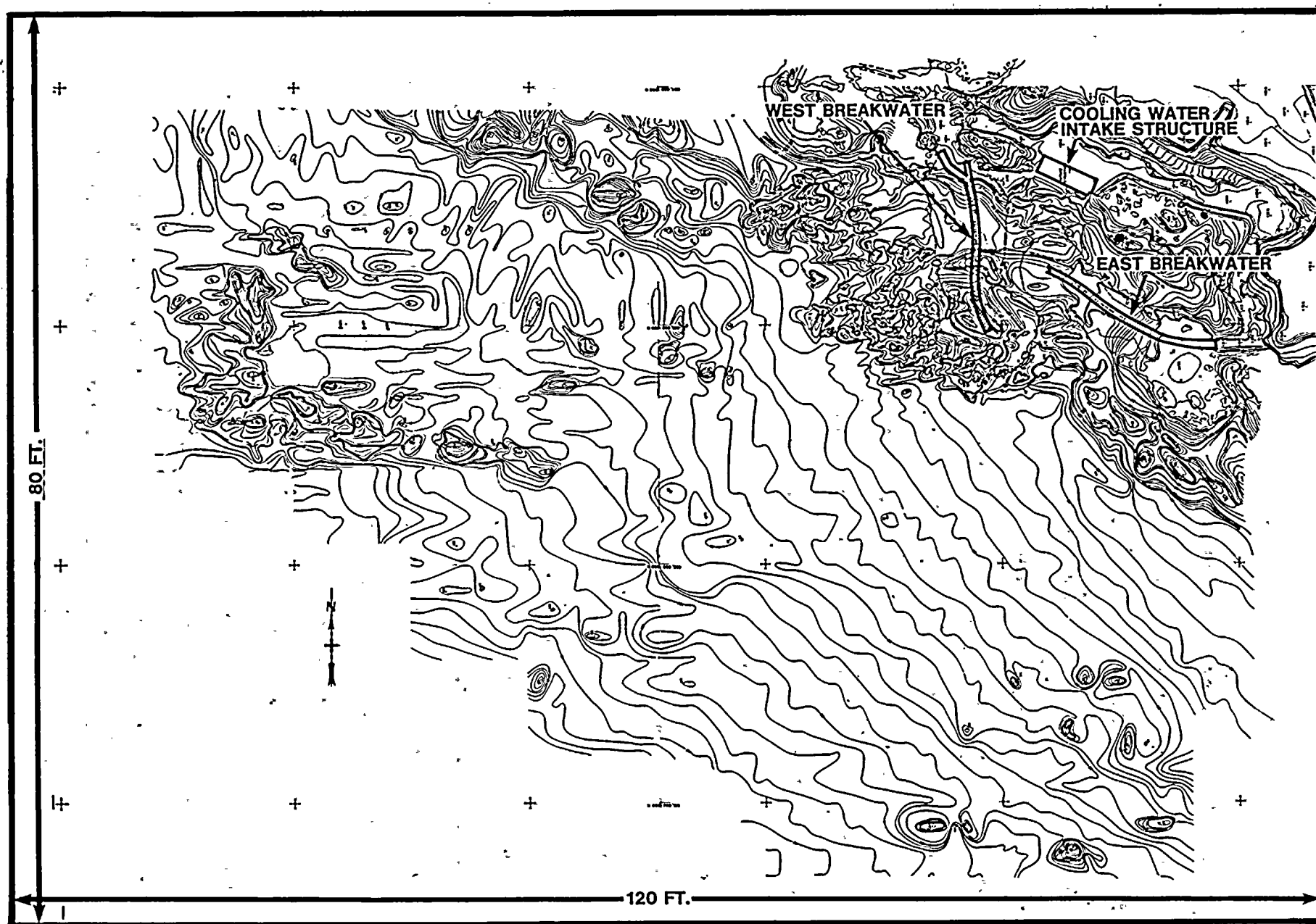


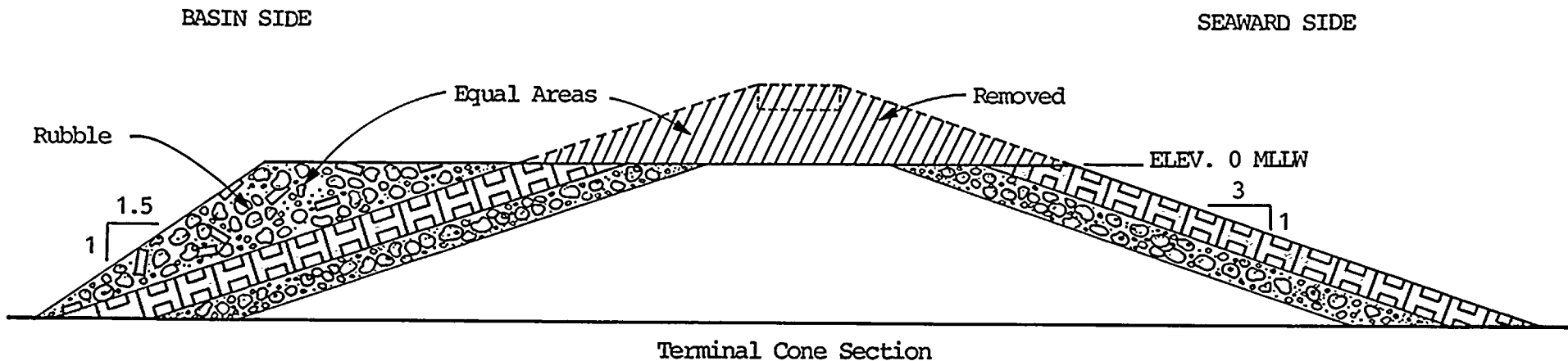
FIGURE 2 Basin Boundaries and Bathymetric Contours in Model
(after Lillevang, Raichlen, and Cox, 1982)

basin side widened by the volume of material which was transported from above MLLW. The slope on the basin side was inclined at 1.5 horizontal to 1 vertical. The breakwater materials, the core, the sub-armor rock, and the concrete tribars were modelled with regard to size and weight, and therefore a reasonable model of porosity and surface roughness was realized. The cross-section was stabilized in the model by means of netting which was held down by weights. Details of the degraded breakwater cross-section used in the model are shown in Figure 3.

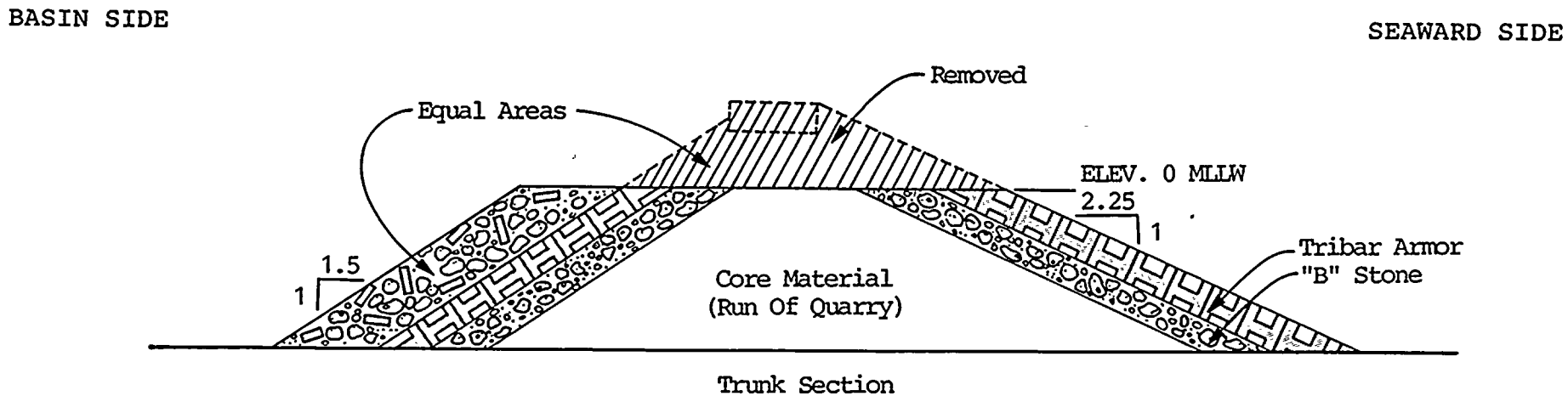
In Figures 4a, 4b, 4c, and 4d drawings are presented of the cooling water intake structure. Various elements of the structure are defined in these figures and this nomenclature will be used throughout this report. Comments regarding model details of the pump forebays will be presented in Section 2.5.

2.2 Wave Generators

Five wave generators were used, each 11 ft long; these could be arranged to provide long crested waves from south to west directions. The wave machines were of the pendulum type with the linkage designed to provide a piston motion for the generator plate with a minimum of rise of the plate from the floor, and were based on a design described by French (1969). (This rise was about one inch for the maximum stroke of 18 in.) Each wave plate was driven by a hydraulic piston with a common hydraulic power supply. The motion of the wave machine was monitored using a potentiometer which sensed location and provided input for feedback control. The voltage time history used to drive the wave machines was generated using the digital-to-analog system of computing facilities at the Offshore Technology Corporation.



Terminal Cone Section



Trunk Section

FIGURE 3 Typical Cross-Sections of Degraded Breakwaters in the Model (after Lillevang, Raichlen, and Cox, 1982)

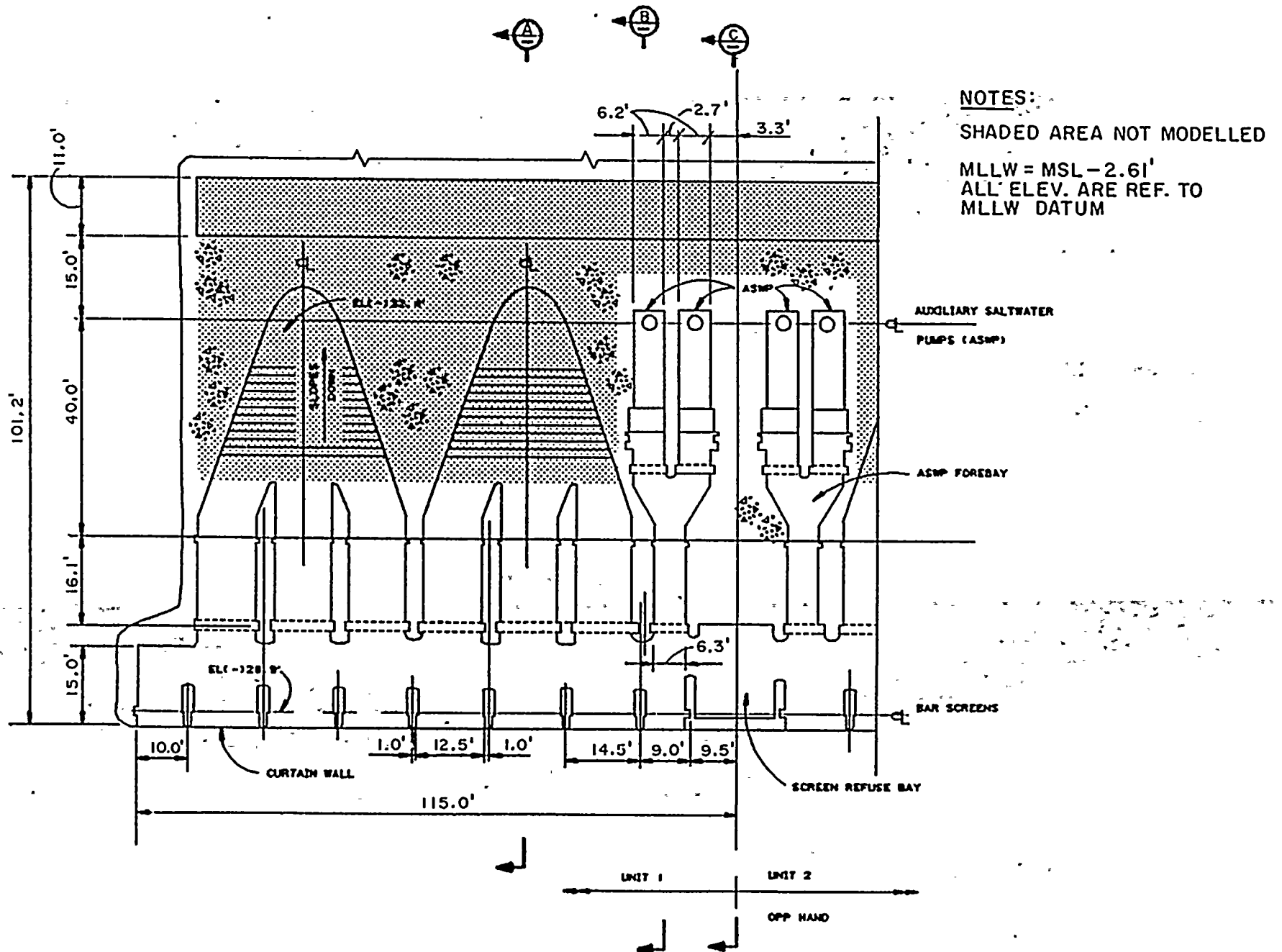
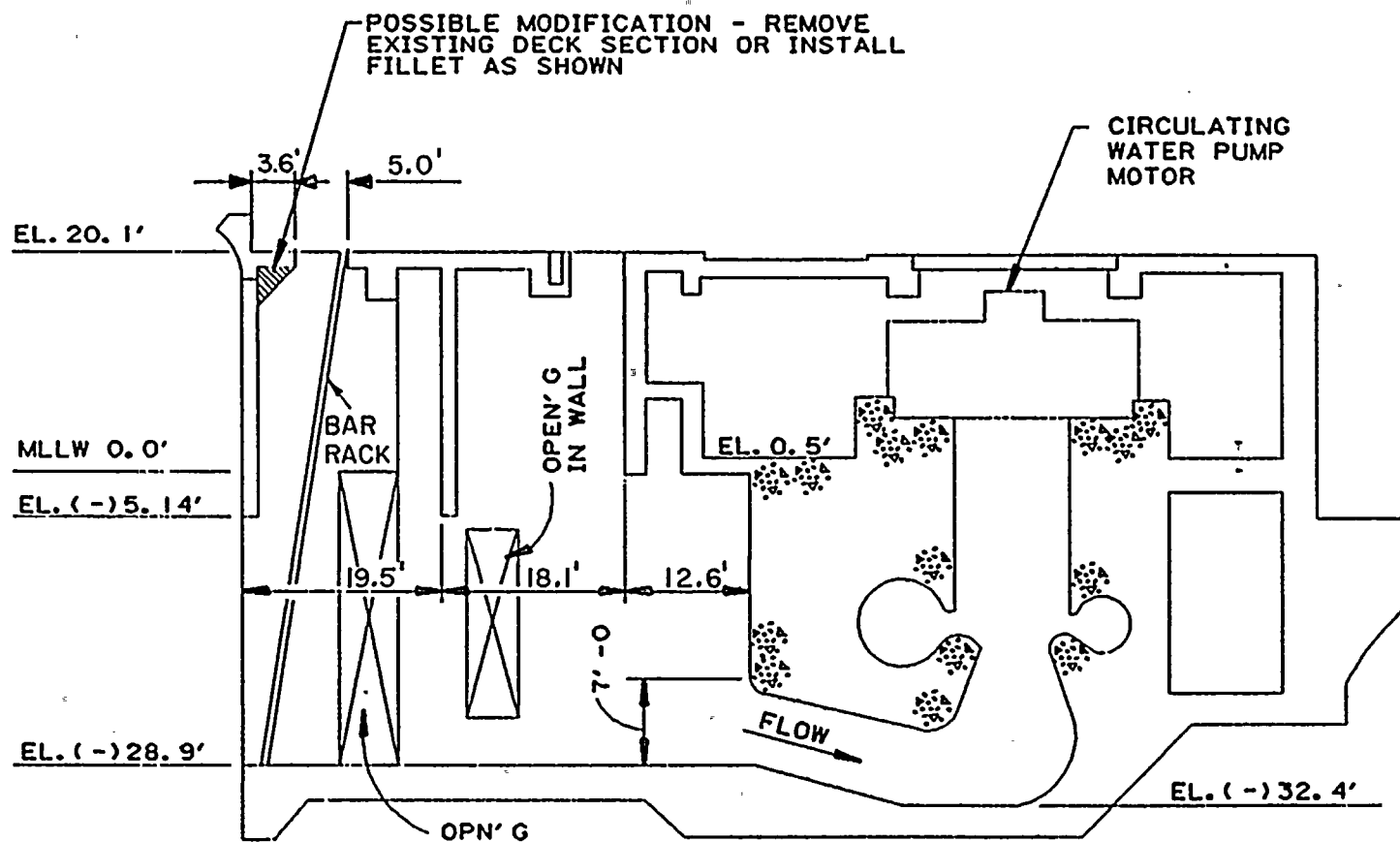


FIGURE 4a - Plan View of Cooling Water Intake Structure at Invert Elevation -28.9 ft MLLW

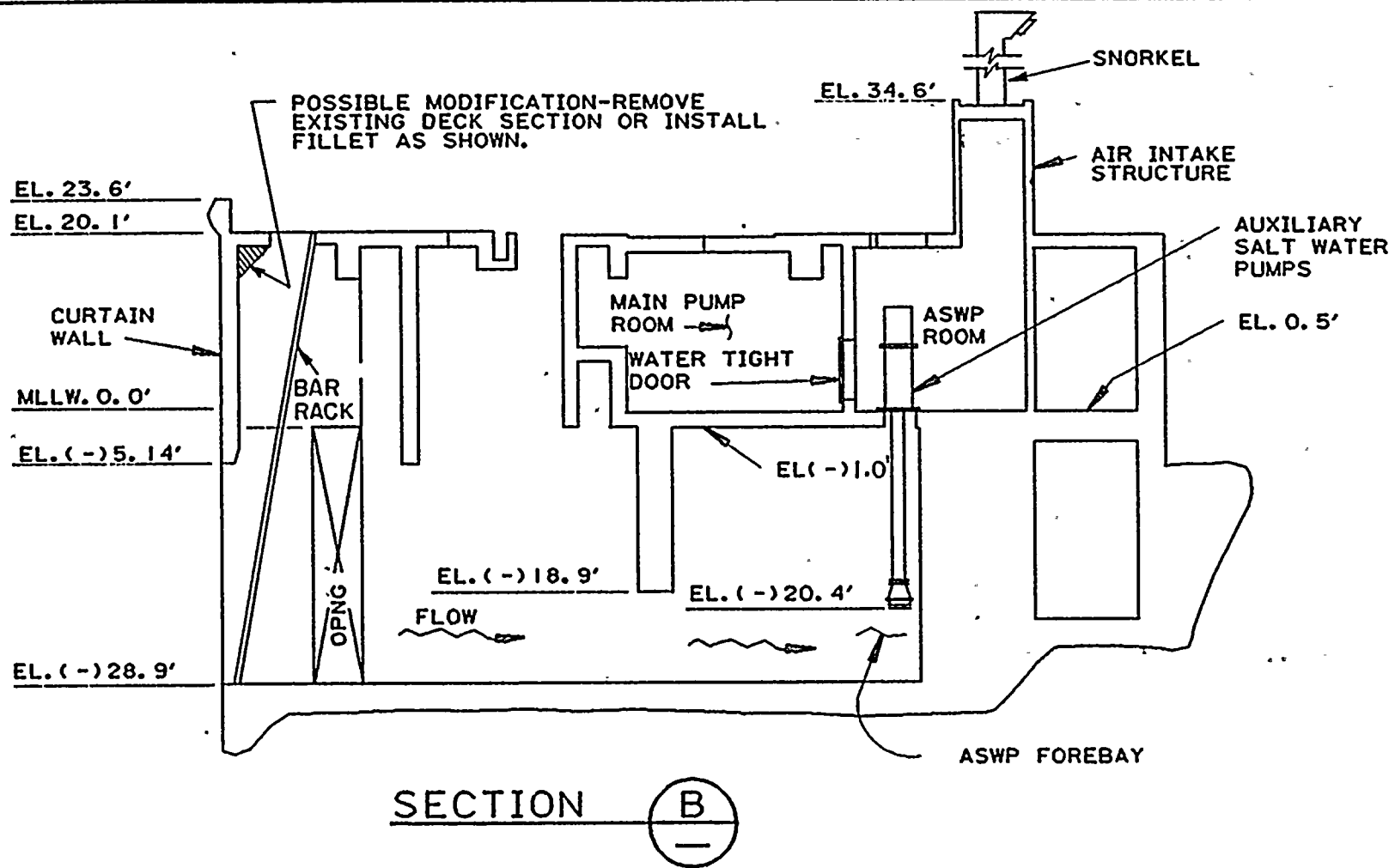


SECTION A
NTS

NOTES:

MLLW = MSL - 2.61'
ALL ELEV. ARE REF. TO MLLW DATUM

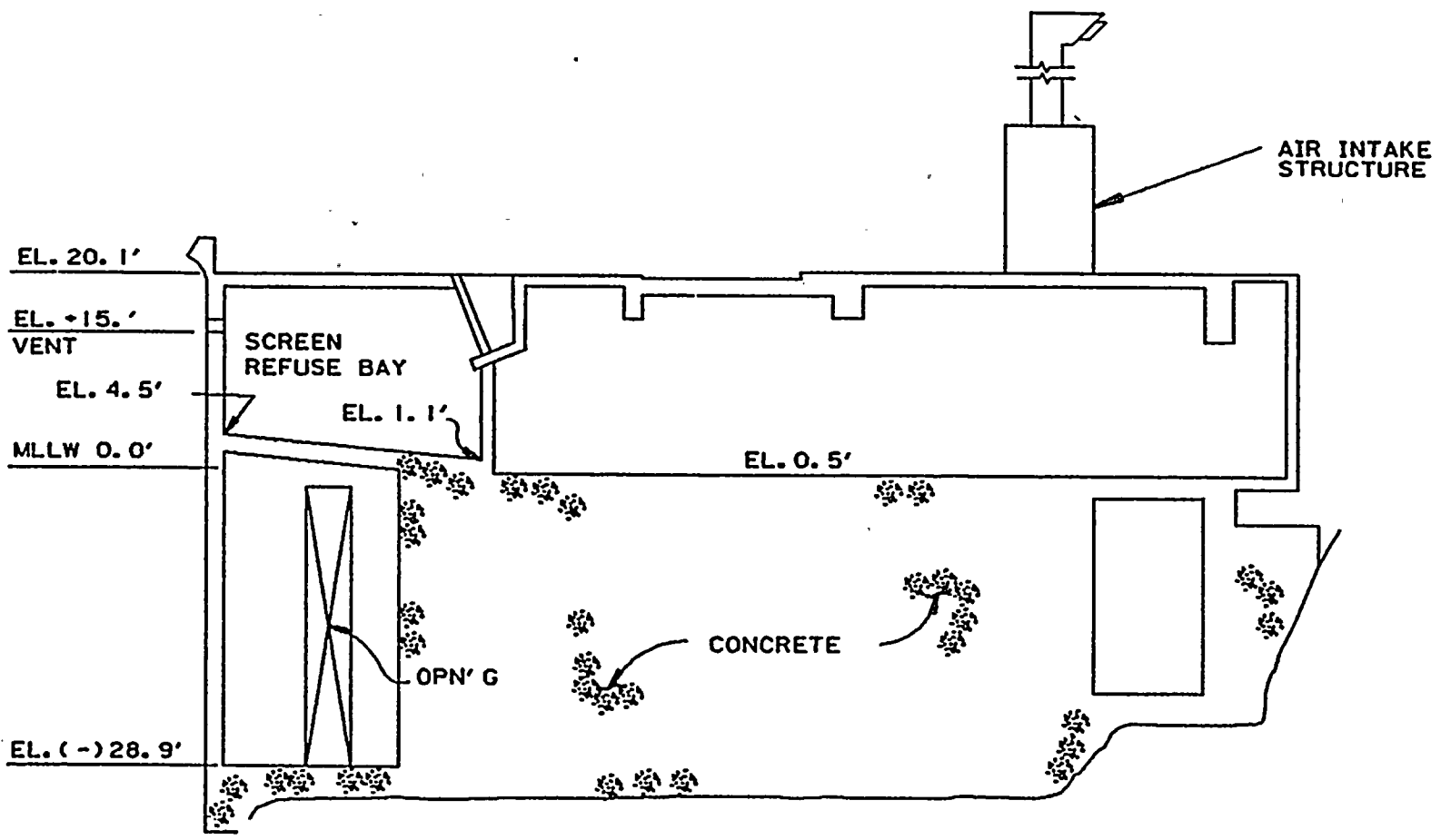
FIGURE 4b - Elevation of Cooling Water Intake Structure: Section A

**NOTES:**

MLLW = MSL - 2.61'

ALL ELEV. ARE REF. TO MLLW DATUM

FIGURE 4c - Elevation of Cooling Water Intake Structure: Section B



SECTION C
 NTS

NOTES:
 MLLW = MSL - 2.61'
 ALL ELEV. ARE REF. TO MLLW
 DATUM

FIGURE 4d - Elevation of Cooling Water Intake Structure: Section C

Storm waves were generated in the model using wave plate displacement time histories obtained from spectra related either to measured waves (for the January 28, 1981 storm) or to hindcast waves for other storms. A method proposed by Goda (1970) was used to define the water surface time history given a one-dimensional spectrum. In essence, this method uses a random number sequence to determine both frequencies and phase angles after initially specifying the limits of the frequency bands. This technique was used rather than the more direct inverse Fast Fourier Transform method to prevent harmonics from artificially being introduced into the wave record. In general, several different wave records were generated for each spectrum, and using a method proposed originally by Funke and Mansard (1980) the "groupiness" of the resultant signal was determined. The wave so synthesized with the maximum groupiness was used along with the response function of the wave machine to determine the voltage time history which must be used to actuate the wave plates. (See Section 3.1 for more discussion of the groupiness.)

To monitor the waves so generated, two wave gages were used spaced 2 ft apart and located on the centerline of the middle wave machine with the gage closest to the wave plate positioned 11.5 ft from the plate. Using the method of Goda (1976) water surface time histories obtained from these two wave gages were used to define the incident and the reflected waves and thus the incident and the reflected energy density spectra. If desired, the coefficients which define the wave machine trajectory for the various frequencies could be adjusted to provide a wave energy density spectrum more in agreement with the desired spectrum. Generally the procedure is trial and error to obtain

a given spectrum based on an initial estimate. However, in the experiments reported herein a spectrum which was more intense than that corresponding to the 1981 storm was used; this will be discussed more fully later.

For experiments with periodic waves the wave plate trajectory was adjusted to generate cnoidal waves using methods developed and reported by Goring and Raichlen (1980) and Goring (1979). For waves where the conditions were such that cnoidal waves were not necessary, a simple sinusoidal motion of the wave plate was used. In these periodic wave experiments only waves with prototype periods of 12 sec and 16 sec were used. The choice of these periods was based on the earlier results reported by Lillevang, Raichlen, and Cox (1982) and on the frequency of the peak of the energy spectra for the range of the important irregular storm wave events which were hindcast (see Section 3.1).

2.3 Wave Measurements

Capacitance wave gages were used at six locations in the model. Two wave gages located near the wave machine defined the incident and the reflected waves for irregular wave tests. Two wave gages located in the cooling water intake basin seaward of the cooling water intake structure measured the waves to which the cooling water intake structure was exposed. These were located at positions R and S (see Figure 5), and these are the same R and S positions used during the earlier study reported by Lillevang, Raichlen, and Cox (1982). The two locations are each approximately 100 ft seaward of the curtain wall of the cooling water intake structure and 150 ft apart. Two wave gages were used at the cooling water intake structure, one at the seaward face of

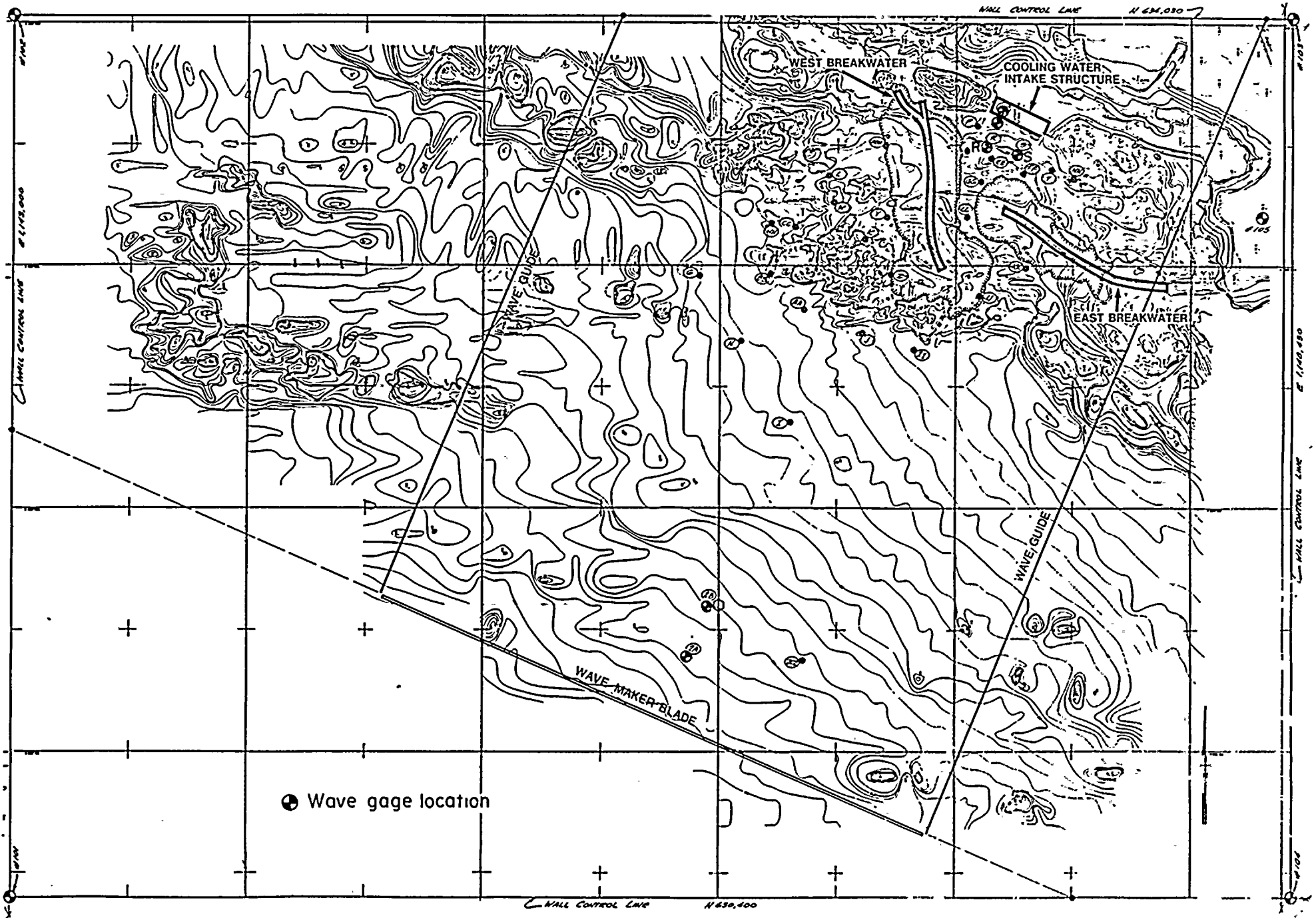


FIGURE 5 Locations of Wavemaker and Wave Gages for Waves from the South (203°) (after Lillevang, Raichlen, and Cox, 1982)

the curtain wall and one inserted through the opening in the deck as the bar screen (see Fig. 4b). These wave gages were used to define the instantaneous head difference across the curtain wall and the elevation of the free surface which occurred simultaneous with the maximum pressures on the curtain wall. All wave gages were calibrated before experiments, and it was found that there was little variation of calibration constants from day-to-day. For the range of wave heights measured, the calibrations were reasonably linear. An example of wave gage calibrations is presented in Figure 6 for two wave gages: one located at Station B near the wave machine and one located at the seaward face of the curtain wall.

2.4 Pressure Measurements

Pressure transducers using strain gages to measure diaphragm deflections were used to determine pressures at various locations in the intake structure. The transducers were 0.25 in. in diameter, manufactured by Micron Instruments, and they were mounted so that the sensitive diaphragm of the gage was flush with the surface in which it was mounted. The natural frequency of the gage in air was 10,000 hz and it was about 5000 hz in water, as determined from experiments.

This type of pressure gage has a temperature sensitivity (described earlier by French (1969)) which can affect their operation. If such a transducer with a diaphragm mounted strain gage is initially out of water, when water of the same temperature as the air comes in contact with the diaphragm the heat flux to the surrounding fluid results in a change in voltage output which can affect the interpretation of the measurements. Although this can be quite troublesome for gages which are alternately immersed and exposed, this effect is not present for transducers which

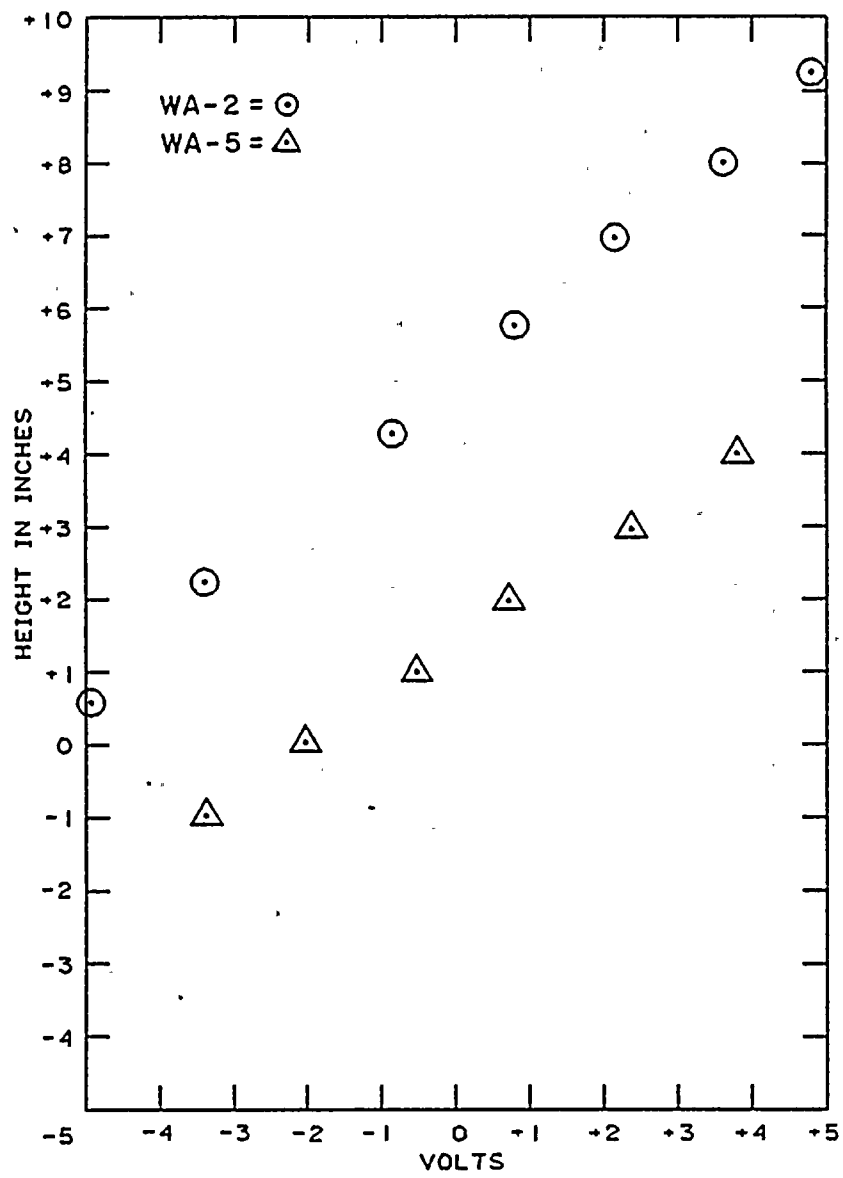


FIGURE 6 - Typical Wave Gage Calibration

are continuously submerged. From initial experiments it was determined that this temperature sensitivity primarily would affect slowly varying pressures, and the effect on impact pressure measurements would be negligible because the rise time associated with impacts would be short relative to the rise time of the voltage change related to the change in heat flux. A method was developed for analyzing the pressure time histories for gages which were initially exposed to air and then wetted; this will be described more fully in subsequent sections.

For the measurement of pressures on the curtain wall of the intake structure a false curtain wall about 1 in. thick was attached to the front of the existing curtain wall of the model to accommodate necessary instrumentation (see Fig. 7a). This had attached to it a parapet wall so that after installation it was equivalent to moving the intake structure 45 in. seaward in the prototype. It was the judgment of the investigators that this dissimilitude would not affect significantly the experimental results. The false wall was constructed to accept a pressure block of the same thickness into which seven pressure transducers had been mounted. A sketch of the vertical location of the transducers and a photograph of the pressure block are presented in Figures 7a and 7b, respectively. By modifying the false wall, the location of the pressure gages could be changed without significantly changing the existing model. The false wall was used only for the curtain wall pressure measurements; it was removed for other phases of the experimental program.

The pressure gages were calibrated in the following manner. For the curtain wall, and also for the pressure cells in the floor of the auxiliary saltwater pump chamber, the units were removed from the model

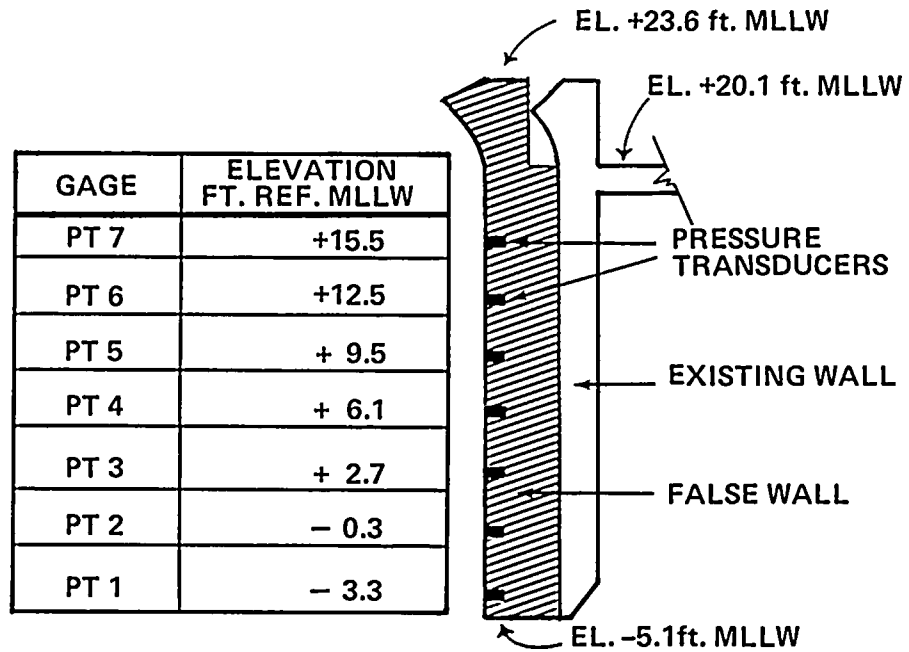


FIGURE 7a Vertical Location of Pressure Transducers in the Curtain Wall

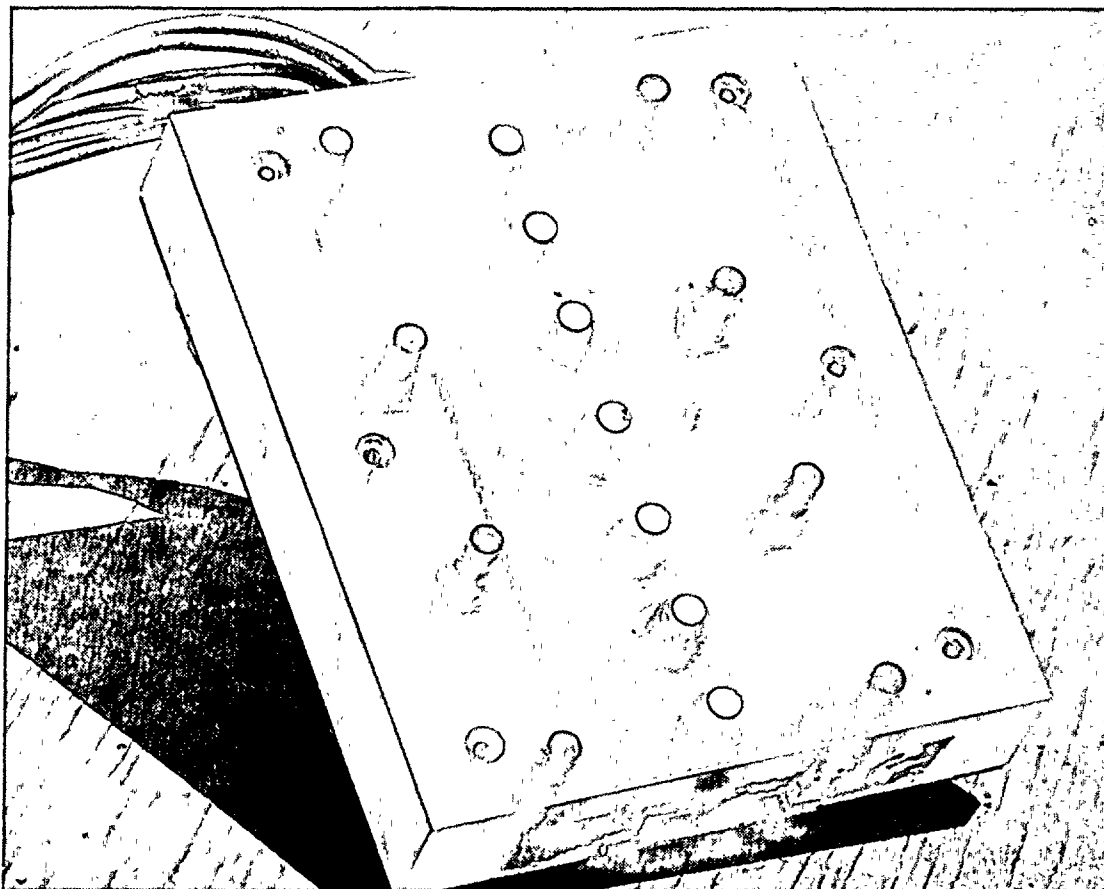


FIGURE 7b Pressure Transducers Mounted in the Pressure Block

and a calibration block was placed over the respective mounting blocks. Channels had been cut in the undersurface of the calibration block so all transducers were simultaneously in communication. This channel was connected to a compressed air source and by bleed-off valves and a manometer a calibration was obtained using air pressure. A photograph of the curtain wall pressure block connected to the calibration block is presented in Figure 8a. In addition, a second method of calibration was used to confirm the air method results with the pressure block immersed directly in water and lowered incrementally using an attached point gage. An example of these two calibrations is shown in Figure 8b indicating the relatively good agreement between the two methods. Individual pressure transducers which were subsequently mounted at different locations in the cooling water intake structure for other phases of the test program were calibrated in a similar manner.

2.5 Auxiliary Saltwater Pump Forebay Model

The model of the cooling water intake structure was modified from that used in the experiments reported by Lillevang, Raichlen, and Cox (1982) for the pressure measurements within the Auxiliary Saltwater Pump forebays. For these experiments the ASWP forebays were modelled out of lucite, and a photograph of the forebay unit before it was placed into the intake structure is presented in Figure 9a. The four auxiliary saltwater pump forebays can be seen to the left in this photograph along with the gasket material attached to the top walls of the structure to form an airtight seal between the walls and the ceiling. A lucite plate was bolted to these walls and pressure transducers could be mounted in different locations in this plate, i.e., in the ceiling of the ASWP

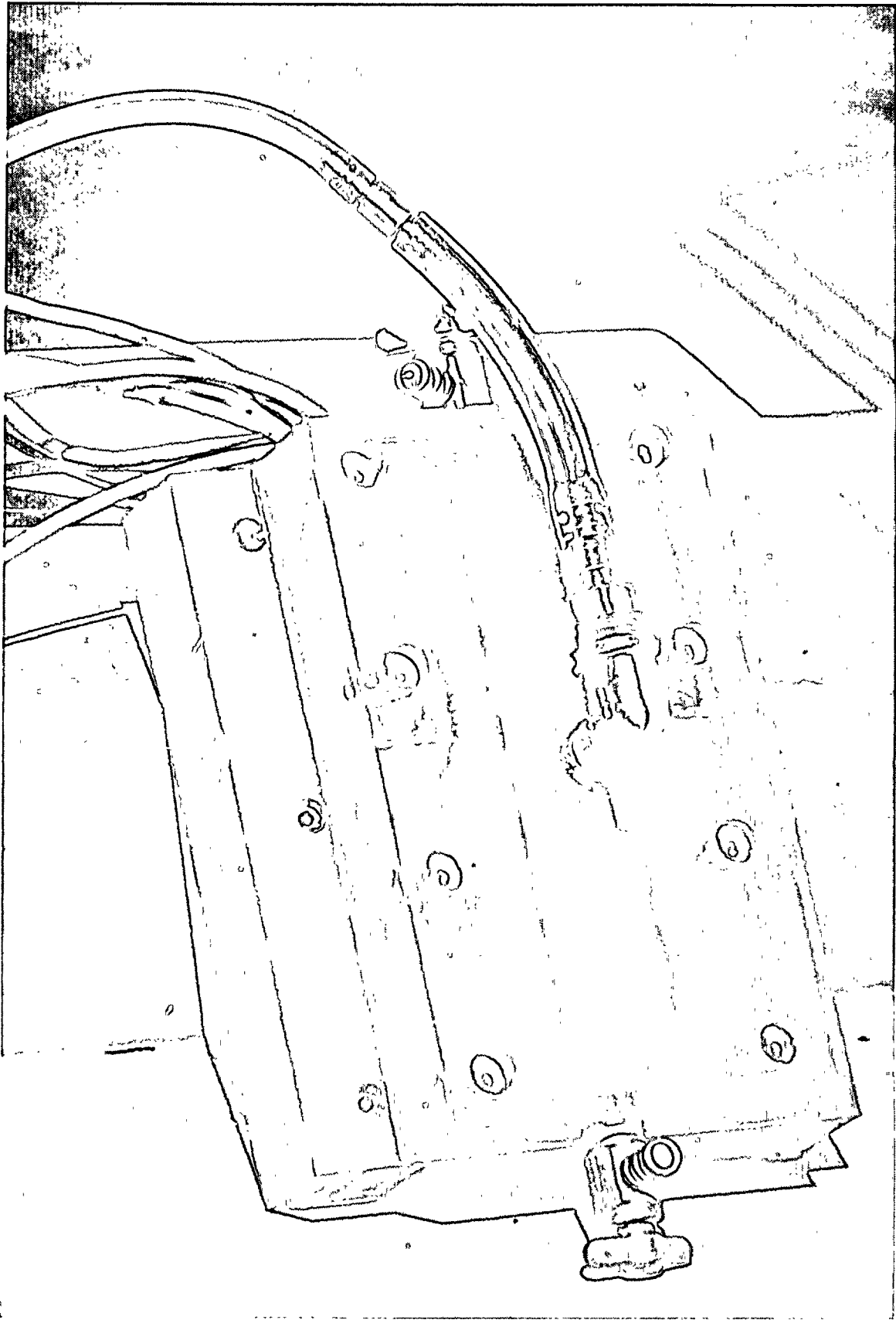


FIGURE 8a Curtain Wall Pressure Block and Calibration Block

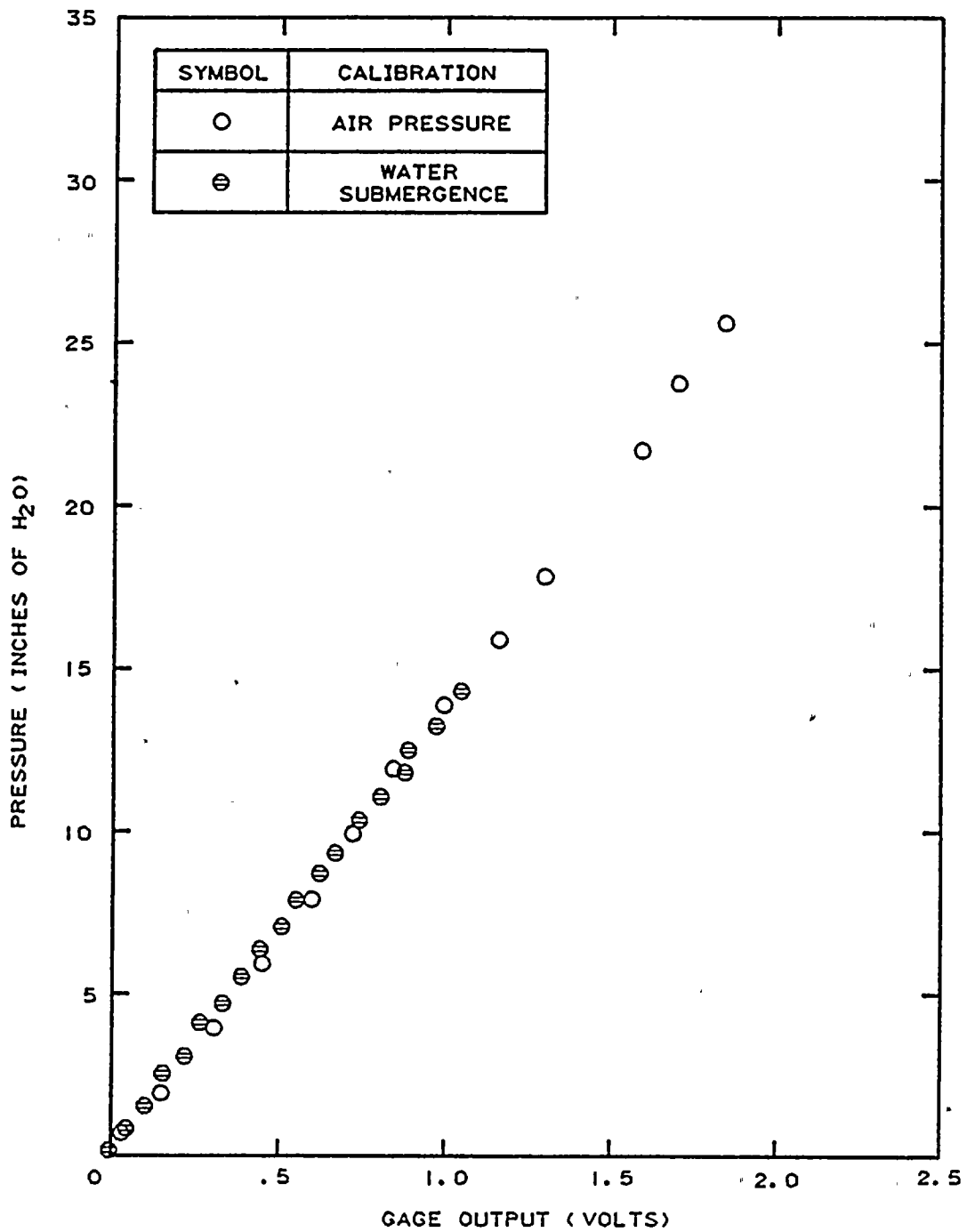


FIGURE 8b An Example of Pressure Cell Calibration Using (i) Air as the Pressure Media, (ii) Water Alone by Submergence of the Pressure Block

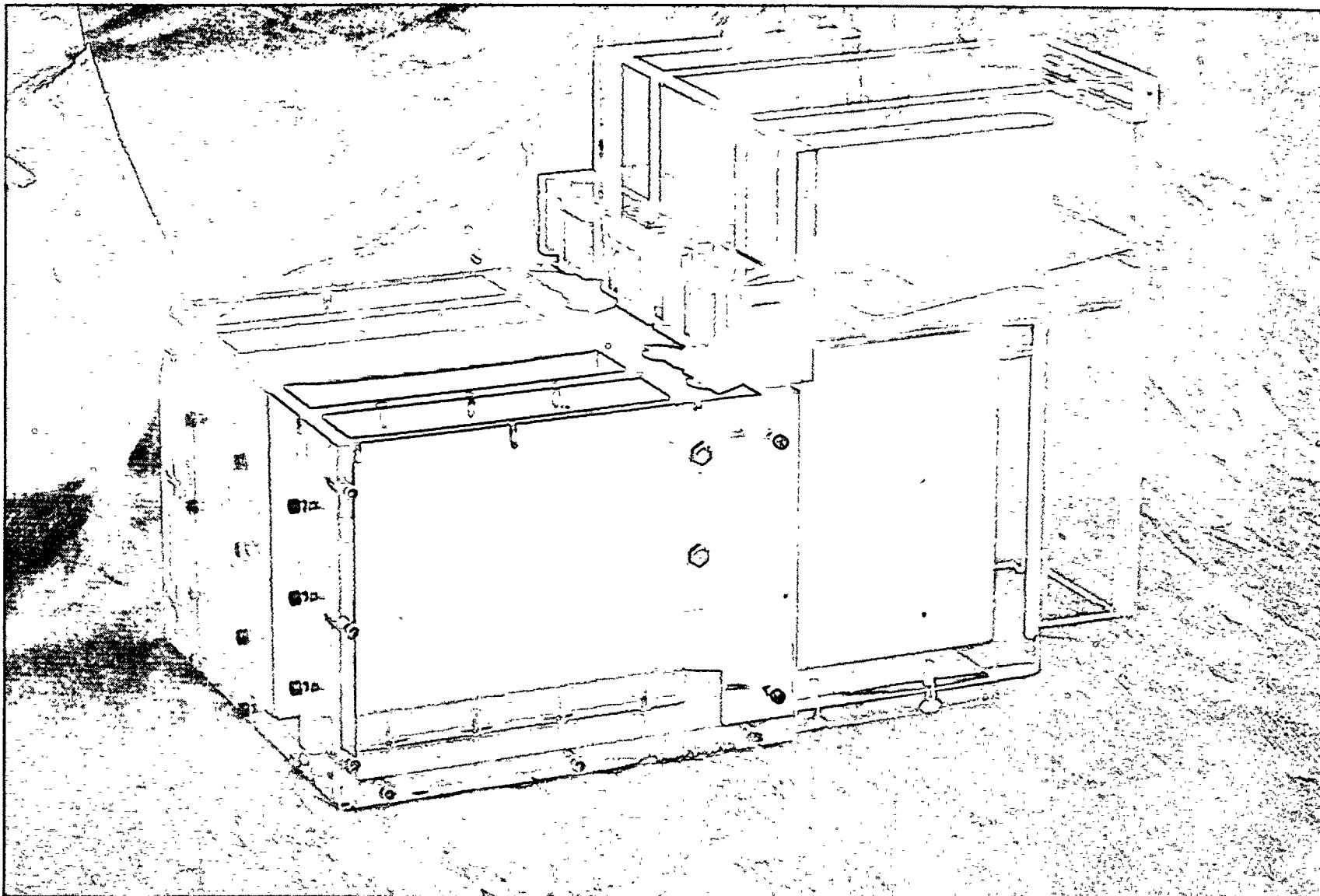


FIGURE 9a Model of the Auxiliary Saltwater Pump Forebays

forebay and in the floor of the main pump room (Fig. 4c). In each of the four forebays labelled as I, II, III, and IV (starting from the left-hand forebay when facing seaward) pressure cells could be located 5.2 ft (prototype) from the backwall of the pump chamber; these were denoted as locations a, b, c, and d respectively and can be seen in the schematic drawing presented in Figure 9b. (This location is 2.6 ft landward of the doorway of the ASWP.) In Forebay III two other pressure cells were located in the floor of the main cooling water pump room at a distance of 19.7 ft from the back of the ASWP forebay (location e) and at 25.1 ft from the back of this forebay (location f). This allowed for a more general survey of pressures on the ceiling of the ASWP forebay. The pressure transducers which had been used earlier in the curtain wall experiments were mounted in certain of these locations, but not all locations were surveyed simultaneously. The plate which represented the floor of the pump rooms could be removed and attached to a calibration plate so that the pressure transducers could be calibrated simultaneously in the same way as the curtain wall pressure transducers had been.

In Figure 10 a photograph is presented of the assembled cooling water intake model with the detailed forebay portion of the model shown. To either side of the forebay a wooden box can be seen in the photograph. In this box mirrors were mounted on the sides and in the rear of the forebay section with each inclined at 45°. This provided a means of obtaining a side view and a rear view of the forebay chambers from above for observations of the movement of dye injected into the forebay, and of plastic pellets introduced to assist in evaluating internal pump forebay current velocities induced by waves and their potential for the transport of material.

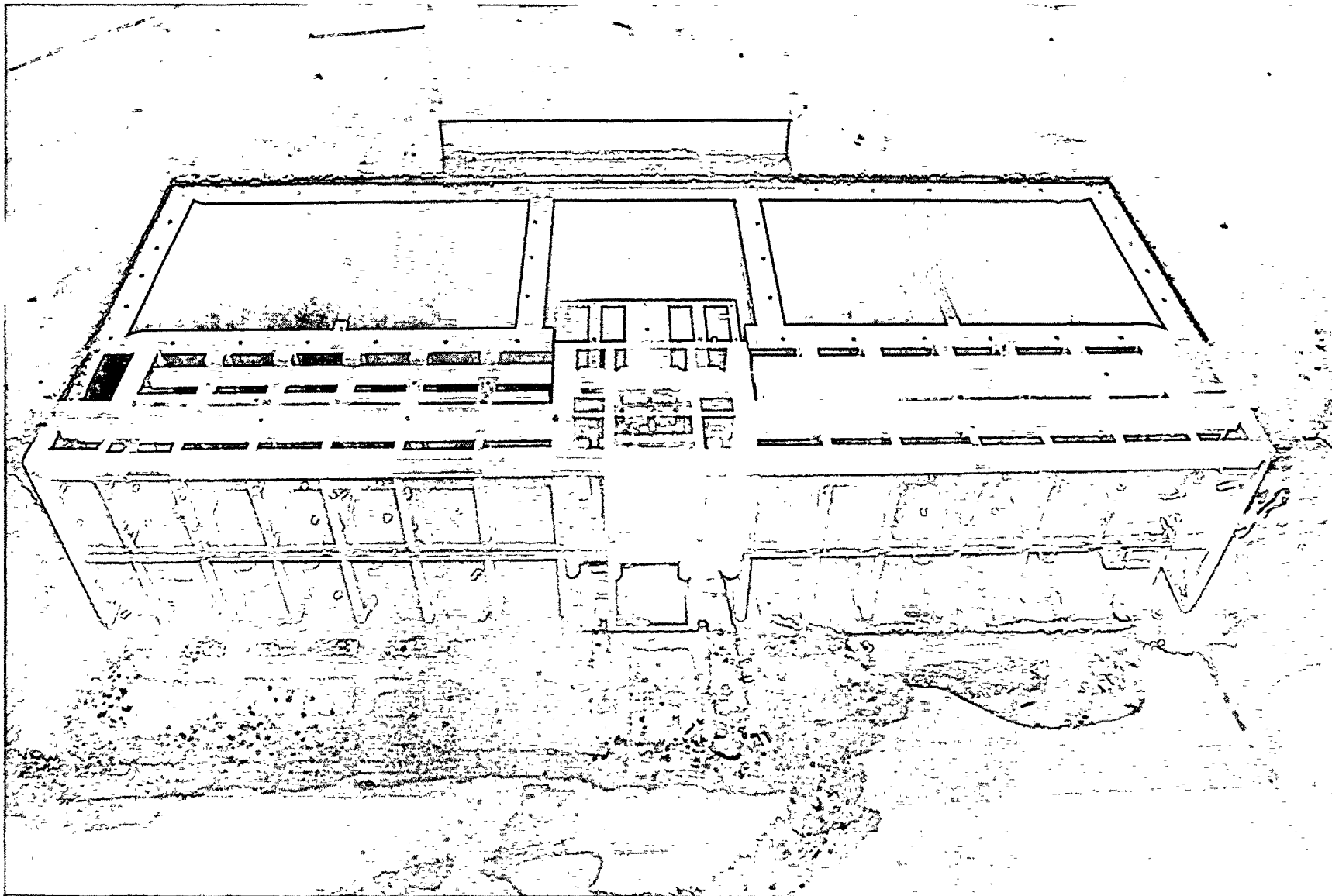


FIGURE 10 Model of the Cooling Water Intake Structure With the Forebay Section Attached

2.6 Velocity Measurements

For the investigation of the potential for water-borne missiles, velocities were measured near the gate opening to the ASWP forebays (see Figure 9b). Miniature propeller meters manufactured by Nixon Instrumentation Ltd. were used. These probes were about 10 mm in diameter and, according to the manufacturer, had a threshold velocity equivalent to about 0.7 fps prototype. It was noted in calibrations that for velocities less than 1.3 fps (prototype) a voltage output did not exist indicating perhaps the threshold is larger than that suggested by the manufacturer. Therefore, caution should be exercised in interpreting measured low velocities. With appropriate signal conditioning a continuous voltage-time history was obtained from which an estimate of the velocity could be made. It should be realized that these types of meters are insensitive to direction so that only the magnitude of the velocity can be obtained. A typical calibration curve of the current meter is presented in Figure 11.

2.7 Data Acquisition and Analysis

Three different data acquisition systems were used in conjunction with these experiments. The DEC PDP-11/23 sampled data at varying rates in the kilohertz range and provided a means to store these data in digital form. Both the DEC PDP-11/23 and a DEC PDP-11/44 were used for post-test analysis. Signal conditioning for all probes was provided by a system manufactured by NEFF Instrument Corporation which, in addition to the signal conditioning, provided analogue-to-digital conversion capability and programmable gain for all channels. The second digital data acquisition system was the Tektronix 4052 which had a much slower sample rate and, thus, was used primarily to acquire wave data. Both

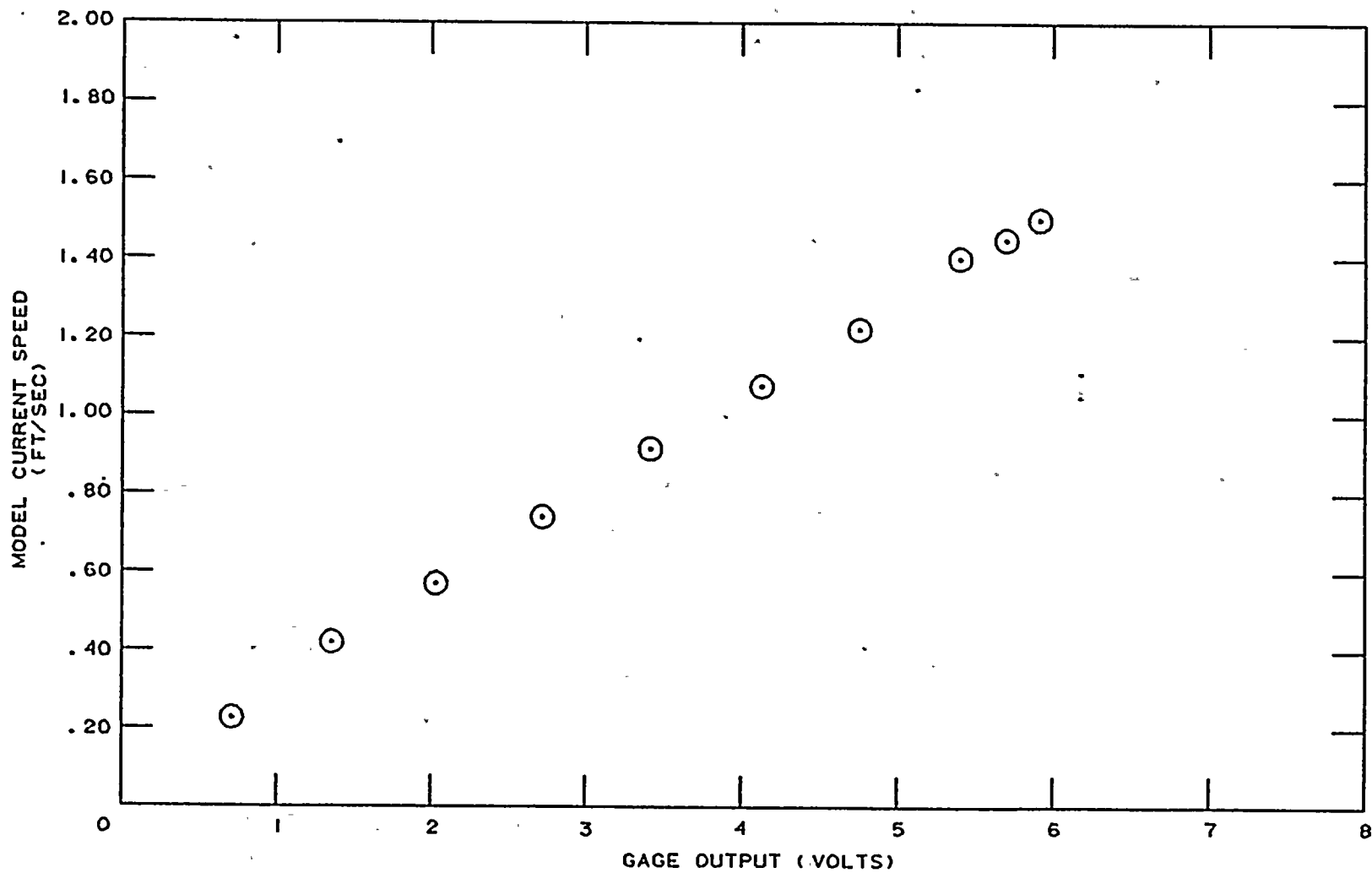


FIGURE 11 - Typical Miniature Current Meter Calibration

of these systems provided for rapid data analysis of experiments. The third system used for analogue signals was the Honeywell Visicorder (Model 1858) which was a light writing oscillograph with a reasonably flat response to 50,000 hz. This was especially useful in the exploratory phases of the experimental program where evidence of slam pressures on the curtain wall were investigated and the rise times of the pressures were not known beforehand.

As in any experimental program of this scope still photographs, high speed movies, and video tapes were obtained of selected aspects. These are on file and only a few examples of still photography will be presented herein.

2.8 Experimental Program

A wide range of conditions was used in the experimental program, and these will be discussed briefly in this section. In general, throughout the report experimental results will be presented in prototype units.

2.8.1 Wave-Induced Loads on the Curtain Wall

In the exploratory phase, the main interest was in determining whether slam pressures (high pressures of short duration) existed; therefore, the pressure gages on the curtain wall were not always calibrated in detail. For waves approaching from 203° the structure was first exposed to periodic 16 sec waves for water surface elevations varying from +13 ft MLLW to +17 ft MLLW in 2 ft increments. At certain elevations periodic waves of 12 sec were used and also irregular waves corresponding approximately to three different storms were imposed on the structure:

- (i) January 28, 1981 at 1800 hrs GMT
- (ii) January 25, 1914 at 2100 hrs GMT
- (iii) March 13, 1905 at 0300 hrs GMT

The manner in which the waves were determined from the spectra and certain characteristics of these are discussed in Section 3.1. The water level was reduced to a minimum of +4 ft MLLW in 3 ft. increments with periodic 12 sec and 16 sec waves used and irregular waves from the three storms described at various water levels. In certain experiments detailed calibration of the pressure gages were obtained before the experiments so that the results could be used to evaluate the pressures in the absence of impact loadings. For the exploratory pressure measurements the still water level was not lowered below +4 ft MLLW because the pressures on the curtain wall indicated decreasing pressures with decreasing depths without the occurrence of impacts.

The direction of the wave machines was changed for a wave approach from the southwest (225°) and exploratory experiments were continued with fully calibrated pressure transducers. Still water surface elevations of +17 ft MLLW and +7.5 ft MLLW were used with 12 sec and 16 sec periodic waves. Irregular waves approximating waves from the 1905, 1914, and 1981 storms were used.

2.8.2 Wave-Induced Loads on the Auxiliary Saltwater Pump Forebays

In this series of experiments, generally three configurations of the ASWP forebays were employed:

- (i) unvented, with the ceilings of the forebays airtight
- (ii) vented, with a 5.6 in. diameter opening in the ceiling of each forebay (denoted as moderately vented)
- (iii) vented, with a 17 in. diameter opening in the ceiling of each forebay (denoted as fully vented).

Pressure measurements were not conducted for all wave conditions for each of these configurations or in each possible gage location, since the experimental program was kept flexible and adjusted as results were acquired. In all cases the direction of wave approach was from the south (203° in 100 ft depth).

With the water surface at elevation +17 ft MLLW the structure was exposed to waves from the 1981⁺ storm for the unvented forebay and the two vented conditions described. Pressure measurements were made at various locations as shown in Figure 9b; these will be discussed in Section 3.2.1.

Experiments were conducted at two water surface elevations in addition to +17 ft MLLW. These were: +7.5 ft MLLW, and -2 ft MLLW. The latter was used only for these experiments because of the possibility of large pressures due to the presence of an air-water interface near the ceiling of the ASWP forebays. At the +7.5 ft MLLW still water level, pressures were measured for the unvented system and the moderate 5.6 in. vent for both 12 sec and 16 sec periodic waves, and waves due to the 1981⁺ storm. At an elevation of the still water surface of -2 ft MLLW experiments were conducted with 12 sec and 16 sec periodic waves for the unvented case and for the condition with moderate venting. For

16 sec waves and for maximum wave heights pressures in the fully vented forebays were measured. Exploratory tests were also performed for the -2 ft MLLW water level and the 1981⁺ storm.

2.8.3 Velocities at the Entrance to the Auxiliary Saltwater Pump Forebays

Velocities were measured at different elevations at the entrance to various forebays for conditions at still water surface elevations of: +17 ft MLLW, +7.5 ft MLLW, and -2 ft MLLW.

The direction of the waves was 203° at the wave generators.

At +17 ft MLLW the unvented condition was used with irregular waves corresponding to the 1981⁺ storm. For the still water level at +7.5 ft MLLW velocities were measured for periodic waves and the unvented ceiling condition. In the case of the water surface at -2 ft MLLW, velocities were measured for the unvented chamber for 12 sec and 16 sec periodic waves and for waves from the 1981⁺ storm. For the fully vented chamber, velocities were measured for 12 sec waves and for irregular waves from the 1981⁺ storm.

3. PRESENTATION AND DISCUSSION OF RESULTS

3.1 Wave-Induced Loads on the Curtain Wall

A review by a structural designer of the walls and slabs within the intake structure determined that the most vulnerable section of the curtain wall was the portion located on the centerline of the cooling water intake structure in front of the screen refuse bay. In addition, this section may be more vulnerable than other sections because if the trash refuse bin is free of water, hydrostatic plus dynamic pressures would be present on only the seaward side of the curtain wall. Hydrostatic pressure acts on both sides of the wall for the portion of the curtain wall east and west of the screen refuse bay. Therefore, the net loads would be less there than on the center section for the same applied dynamic pressures on the seaward side. However, slots in the center panel of the curtain wall which lead to the screen refuse bay suggest there would be water in the screen refuse bay particularly for high water levels. This would reduce the net load on the center panel of the curtain wall compared to the load predicted from combining measured dynamic pressures with hydrostatic pressures. Although the dynamic pressures on the center panel of the curtain wall were given the greatest attention in these experiments, selected measurements also were made of pressures near the west corner of the curtain wall, 110.6 ft west of the centerline. (For all experiments reported herein the crests of the east and the west breakwaters were kept at an elevation of mean lower low water defined earlier as the degraded breakwater condition.)

In Section 1 a discussion is presented relating to the importance of the southerly (203°) direction of wave approach which was used in

this study. As mentioned earlier herein, primarily this dealt with the approach of waves through the offshore terrain and through the breakwater gap and over both breakwaters which was easier for southerly waves than for waves from a more westerly direction. Another reason why the directions of wave approach which are more westerly than 203° are not more important than the direction of 203° is based on a phenomenon denoted as "ponding". As waves impinge upon a breakwater, whether degraded or full section, if the structure is overtopped, water is "injected" periodically into the breakwater protected basin. This "injected" water generates waves shoreward of the breakwaters, and due to the restricted opening between breakwaters there may be a general impounding (or storage) of a portion of this overtopping water inside the embayment leading to a superelevation of the water level. With an increase in the mean water level in this region waves run up and overtop the parapet wall easier. Ponding is defined as this increase in the mean water level above the still water level denoted herein as Δ . In these experiments the level of ponding was investigated at locations R and S which are about 100 ft seaward of the cooling water intake structure, and about 150 ft apart (see Figure 5).

In Figure 12 the ponding, Δ , is shown at locations R and S as a function of the wave height offshore at Station B for azimuthal wave directions at the wave machines of 203° , 225° , and 258° , for periodic 12 sec and 16 sec waves, and for the degraded breakwaters. (It should be noted that data corresponding to the 258° wave direction came from earlier studies conducted in connection with defining the forces on the ASWP air intakes.) It is seen in Figure 12 that the 16 sec waves generate a greater superelevation than 12 sec waves for the same

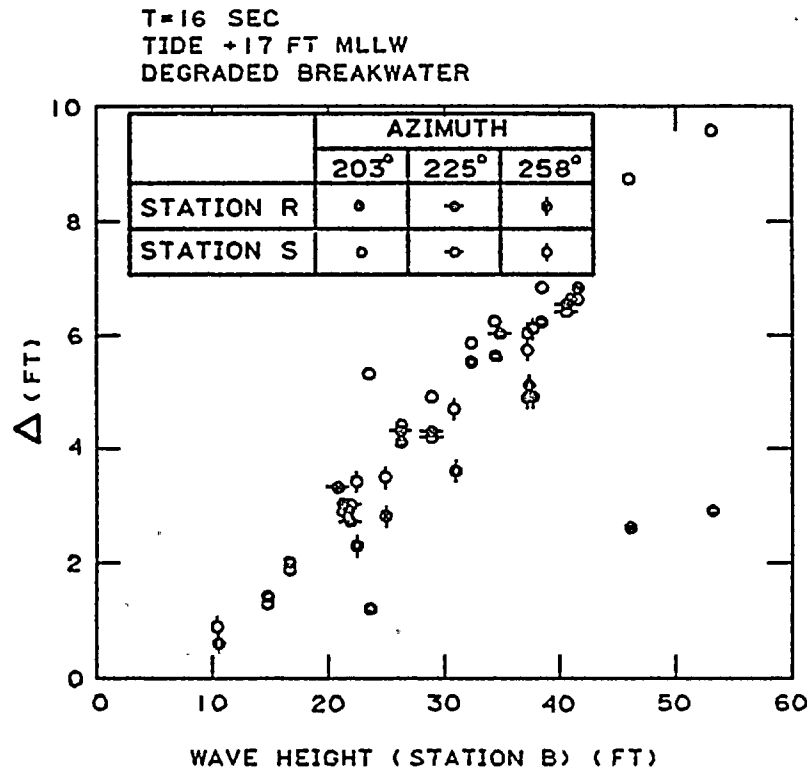
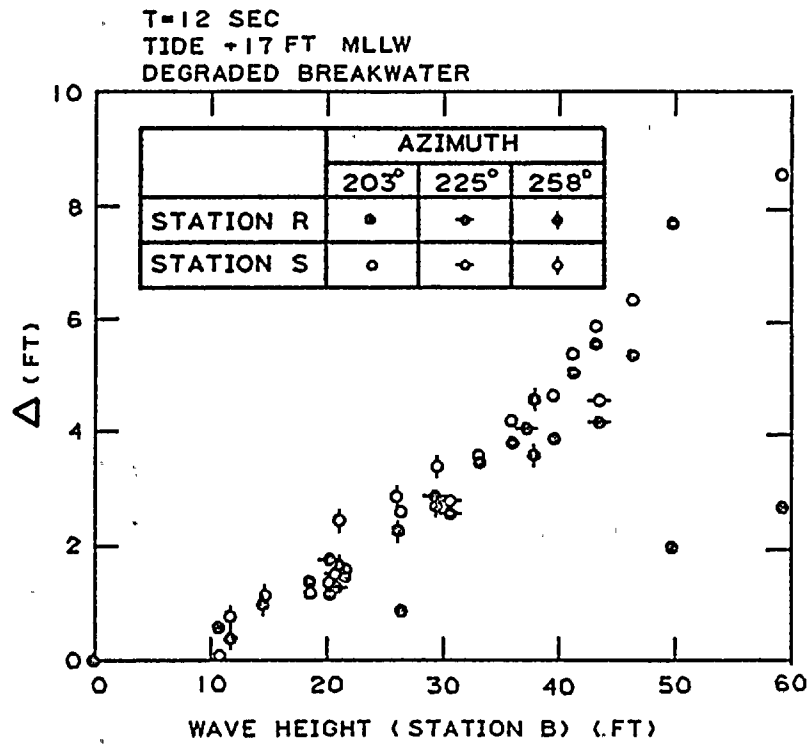


FIGURE 12 Ponding for Various Azimuth Directions and Offshore Wave Conditions as Measured at Locations R and S for Degraded Breakwater, +17 ft MLLW

offshore wave height. The effect of incident wave direction on ponding appears small for the degraded breakwaters; if anything, the ponding decreases somewhat as the azimuth of the incident wave increases. Nevertheless, there is not a significant difference in ponding with wave direction. This indicates that overtopping from more westerly waves is no more important than for waves from the south. Therefore, since certain variations in forces acting on the intake structure may be related to the ponding, one would not expect forces acting on the intake to increase with increase in azimuth of wave approach compared to those caused by southerly waves.

Before discussing in detail the results of the curtain wall pressure study certain general comments will be made. The most important is that for all measurements conducted at all water levels there were no impact pressures (a high pressure of short time duration) evident on the front face of the curtain wall. For a vertical wall this would be caused by local wave breaking against the structure. To investigate the possible occurrence of impact pressures the following procedure was used. With the wave propagating with an azimuth direction of 203° , at the wave generators, tests were conducted starting with the water level at +17 ft MLLW, and the depth was decreased in 2 ft increments to +13 ft MLLW and then in 3 ft increments to +4 ft MLLW with the breakwater in the degraded condition, i.e., reduced to a crest elevation of MLLW and held in place by netting. Periodic 12 sec and 16 sec waves with heights varying from about 20 ft to nearly 50 ft at the wave machine were generated at each of these water levels and pressure recordings were obtained using the oscillograph described in Section 2.7 which essentially had no frequency dependency relevant to this study.

Waves were imposed on the structure from a direction of 225° at the wave machine and exploratory tests were conducted for water levels of: +17 ft MLLW, +13 ft MLLW, and +7.5 ft MLLW. The pressure block was located on the centerline of the intake structure curtain wall and at the west corner for the periodic wave experiments with 12 sec and 16 sec waves.

In addition to these periodic waves, at most of the water levels, irregular waves from three different storms were imposed on the structure. The three storms were chosen from hindcasts of 47 major storms which were based on the review of available meteorological information from 1899 through 1981 by Strange (1982). These were taken as representative of a range in peak energies and frequencies of peak energies for the site. (Since the waves from one of the storms (1981) had been recorded by a NOAA data buoy, the recorded results were used in that case rather than the hindcast data.) Pertinent data for these three storms are presented in Table 1 with the hindcast or (in the case of the 1981 storm) measured significant wave height indicated for each storm along with the recurrence interval as given by Borgman (1982). As discussed previously, a numerical method proposed by Goda (1970) was used to obtain a corresponding water surface time history from the spectra, and from these the wave machine trajectories were defined.

In experiments conducted after the exploratory phase, waves simulating the spectrum from the storm of 1/28/81 were used, since this was a damaging storm with a predicted recurrence interval of about 15.6 years. The direction of the waves from this storm in deep water as determined from hindcast procedures was 262° (249° at a depth of about 100 ft). As

Table 1 Data on Irregular Storm Waves from Measurements and Hindcasts.

Date and Time	Peak Energy (ft ² sec)	Period of Peak Energy (sec)	H _{1/3} * (ft)	Return Period (years)
1/28/81-1800**	626.	15.6	21.8	15.6
1/25/14-2100	1328.	12.5	18.2	6.6
3/13/05-0300	2781.	14.7	30.8	91.1
*Refracted and shoaled significant height near breakwater tip. Note: these were not necessarily the significant wave heights used in the experimental program.				
**Spectrum measured by NOAA data buoy and refracted and shoaled to location near breakwater tip.				

a conservative procedure these waves were propagated from 203° and from 225° in the model, and the energy in the spectrum was increased and waves from the resulting spectrum denoted as 1981⁺ were used.

An example of the spectrum of the storm of 1/28/81 1800 hrs GMT as simulated in the model near the wave machine is presented in Figure 13 in prototype units for the direction of 203°. The ordinate is the energy density in ft² sec and the abscissa is the frequency in sec⁻¹. The spectrum was obtained using the two wave gages located near the center wave machine along with the procedure described by Goda (1976). Also presented in Figure 13 is the spectrum which was obtained from the oceanographic buoy after the various spectral components had been refracted and shoaled to a point near the breakwater. (The refraction coefficients used are based on a deep water direction of 262° which are somewhat larger than the corresponding frequency components of waves propagating from 180° in deep water.) It is noted that the spectrum measured at the wave generator in the model had a larger energy content than that from the storm refracted and shoaled

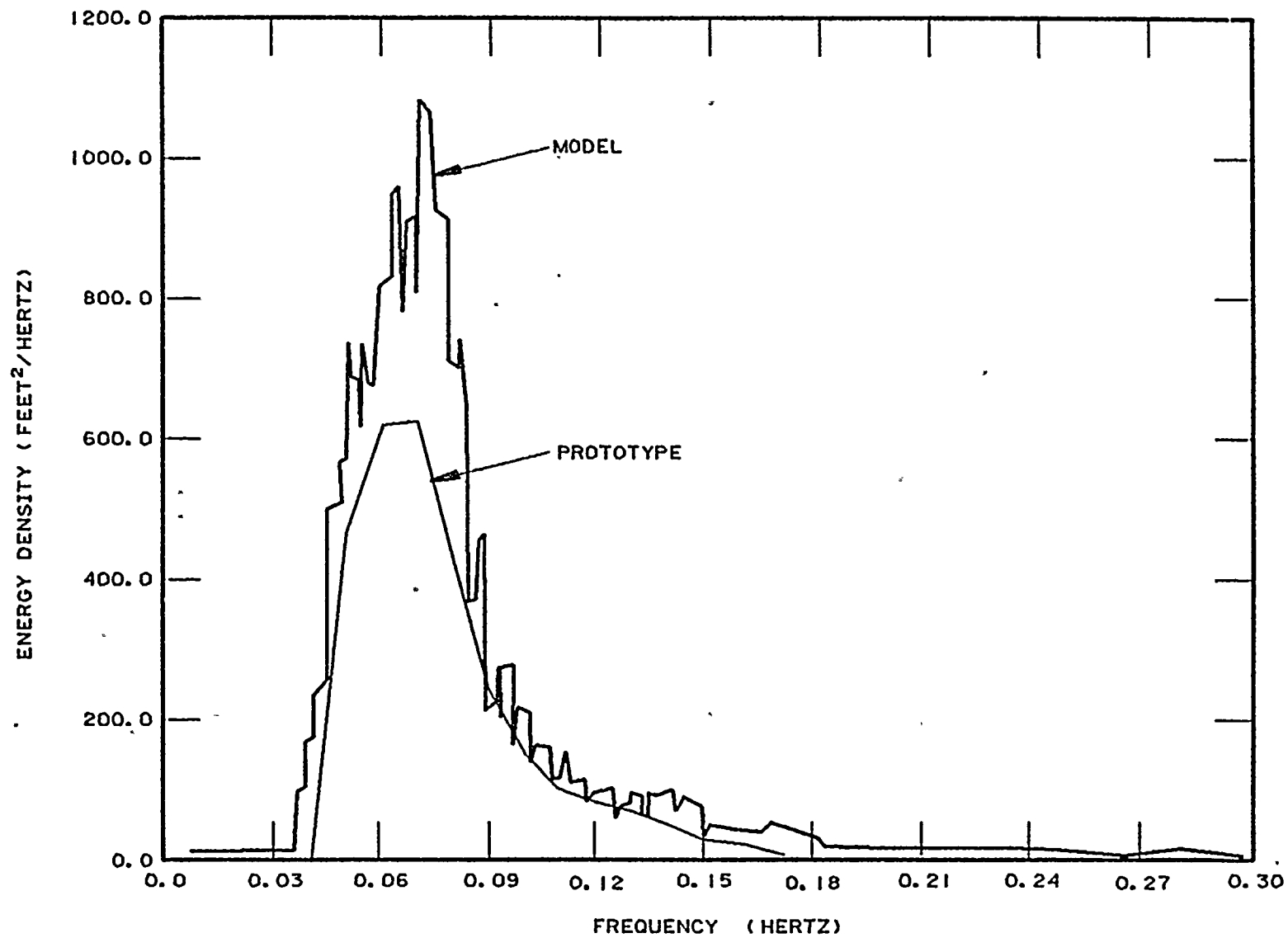


FIGURE 13 - Spectrum of Waves in Model Compared to Measured Spectrum
for Storm of 1/28/81 at 1800 hrs GMT

to the same location using a numerical procedure. The significant wave height obtained in the model for this storm was 26.8 ft compared to 21.8 ft inferred from the spectrum measured in the ocean and refracted and shoaled to a depth of about 100 ft. This was an additional conservative aspect of the experimental program which meant that the structure was exposed to irregular waves with a return interval which was greater than that predicted for the measured 1981 storm, but had the same relative energy distribution among frequencies. The return period of the model storm as predicted by the procedures of Borgman (1982) would be about 41 yrs compared to 15.6 yrs for the measured.

In Figure 14 a section of the water surface time history measured near the wave machines is presented. The "groupiness" of these waves, i.e., the packet-like appearance of the waves, is apparent. The groupiness was given some attention in developing the wave machine trajectories for irregular waves. Using the method of Goda (1970) a number of different irregular wave trains were obtained for each energy density spectrum. The wave trains were analyzed using a method proposed by Funke and Mansard (1980) to determine a "groupiness factor". The "groupiness factor" is defined by them as the ratio of the square root of the standard deviation of the smoothed instantaneous wave energy history about its mean to this mean. The magnitude of this groupiness factor perhaps is not as important as the relative magnitude when comparing one wave record to another. To define the wave machine trajectories used in these experiments wave records were used with groupiness factors of between 0.75 and 0.9, and the wave corresponding

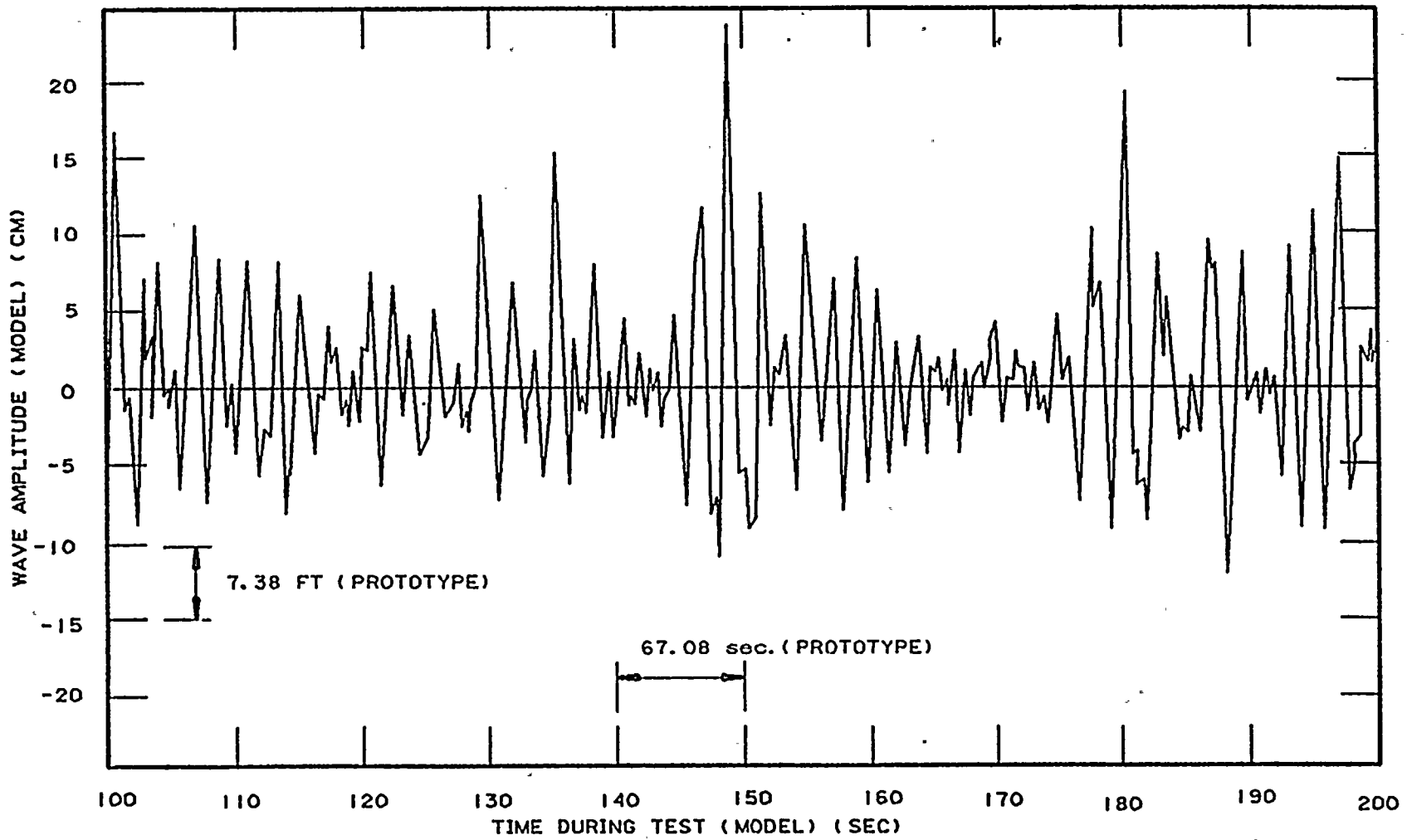


FIGURE 14 - Typical Time History of Waves at Wavemaker
During 1981⁺ Storm at +17 ft MLLW Water Level

to the maximum groupiness factor was used. Other investigators have found that the larger the groupiness factor the larger are wave-induced forces. Funke and Mansard (1980) state that "groupiness factors for prototype wave data so far observed at one location over a period of six months (Sea of Japan, N38°44'33", E139°39'48") fall in the range $0.46 \leq \text{Groupiness Factor} \leq 0.94$."

It is interesting to see the manner in which these waves impinge upon the front face of the intake structure. In Figure 15 a wave is shown as it strikes and overtops the parapet wall. The conditions for this test were irregular waves from the 1981⁺ storm at a water level of +17 ft MLLW and from the direction of 203°. The impression from Figure 15 is more of inundation than impact. In Figure 16 an example of 16 sec periodic waves with a height of 18 ft are shown for the condition of the water level at +7.5 ft MLLW showing the nature of the wave impingement at the lower still water level. In Figure 17 the lower (or receded) water surface is shown prior to wave impingement for the case of a periodic wave with a height of 36 ft and a period of 15 sec at a still water level of +7.5 ft MLLW. In Figure 17 it is easy to see the false wall installed in front of the curtain wall along with the wave gages which straddle this wall. The pressure block is just to the right of the wave gages in this photograph.

An example of measured pressure time histories is presented in Figure 18 taken from the oscillograph trace for the case of the 1981⁺ storm at a water level of +17 ft MLLW. The major time traces are one second apart. The upper two records are the water surface profiles: at the front face of the curtain wall and at the bar screen deck opening. These are displaced on the chart; hence, the difference in water surface

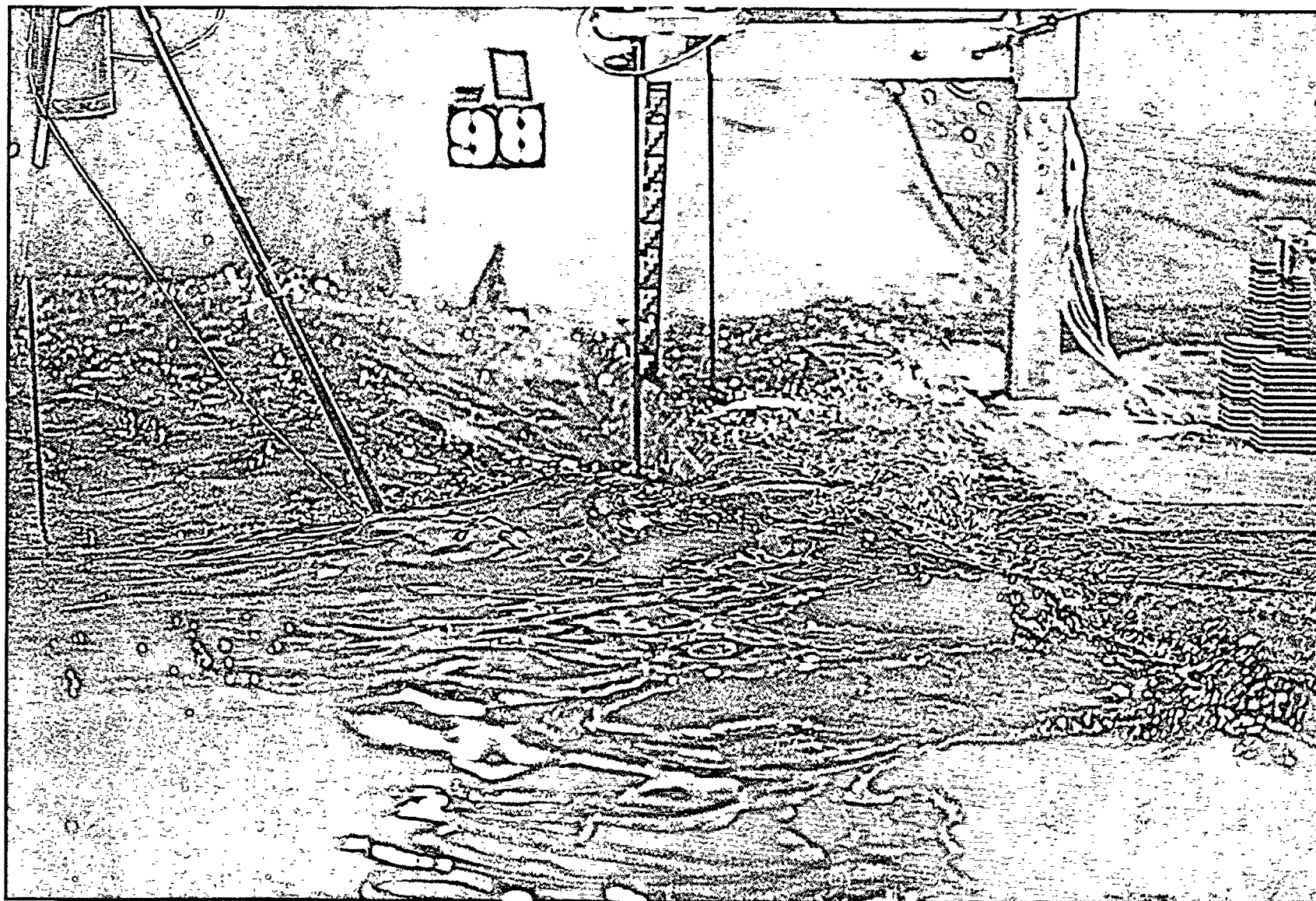


FIGURE 15 Waves from Storm (1981⁺), +17 ft MLLW, 203°Az

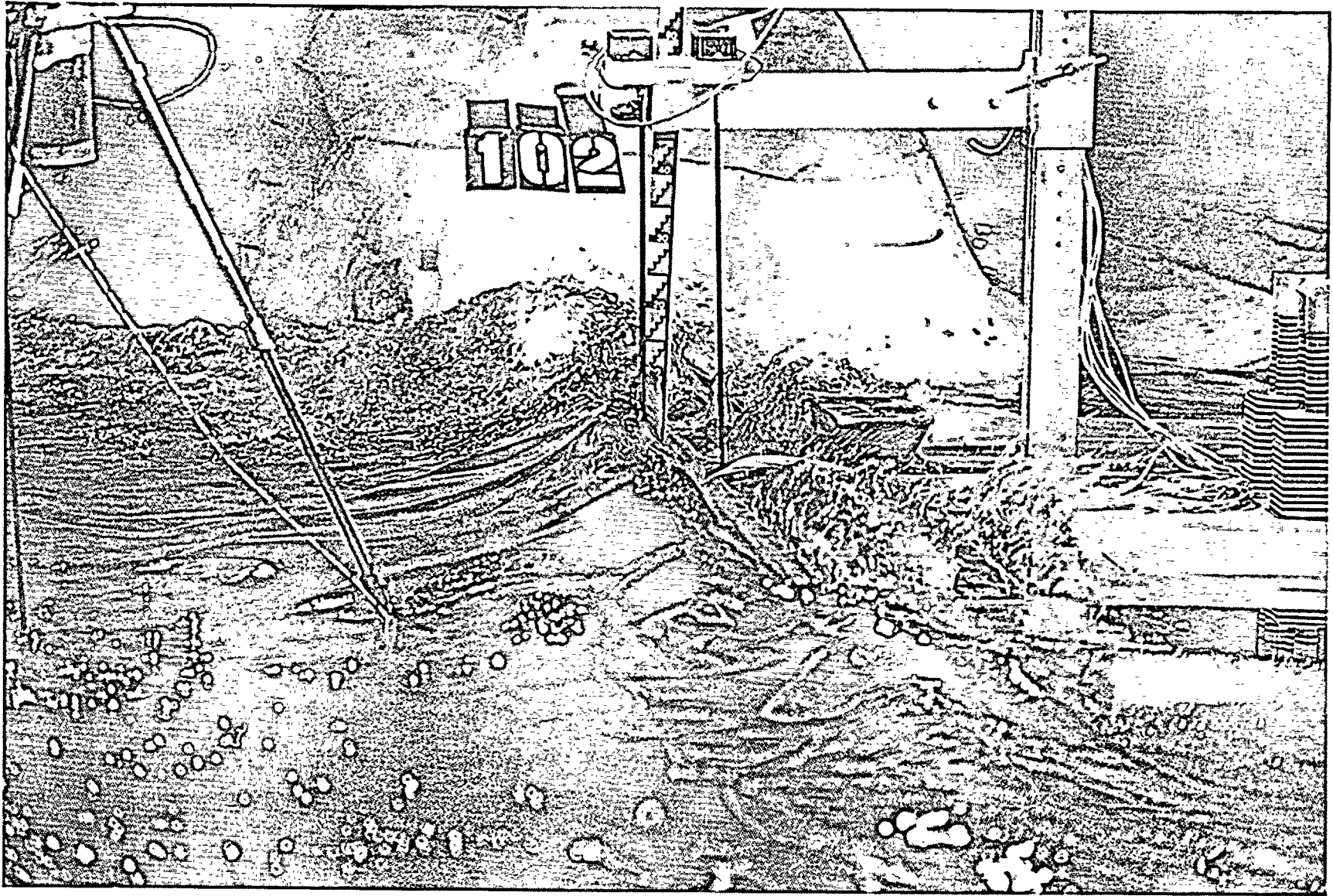


FIGURE 16 Waves for $T=16$ sec, $H_B=18$ ft, $+7.5$ ft MLLW, 203° Az

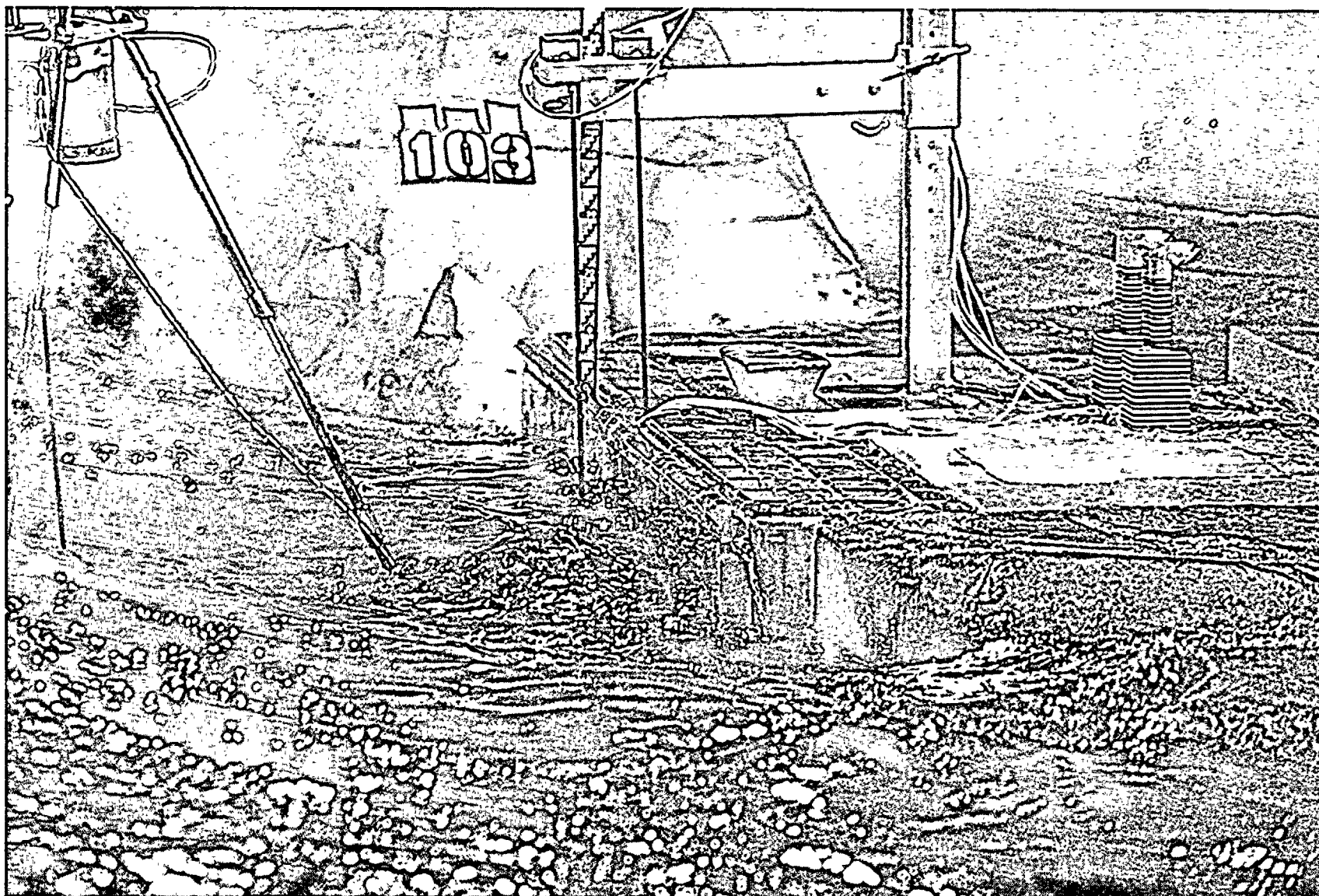


FIGURE 17 Waves for $T=16$ sec. $H_B=36$ ft, $+7.5$ ft MLLW, 203° Az

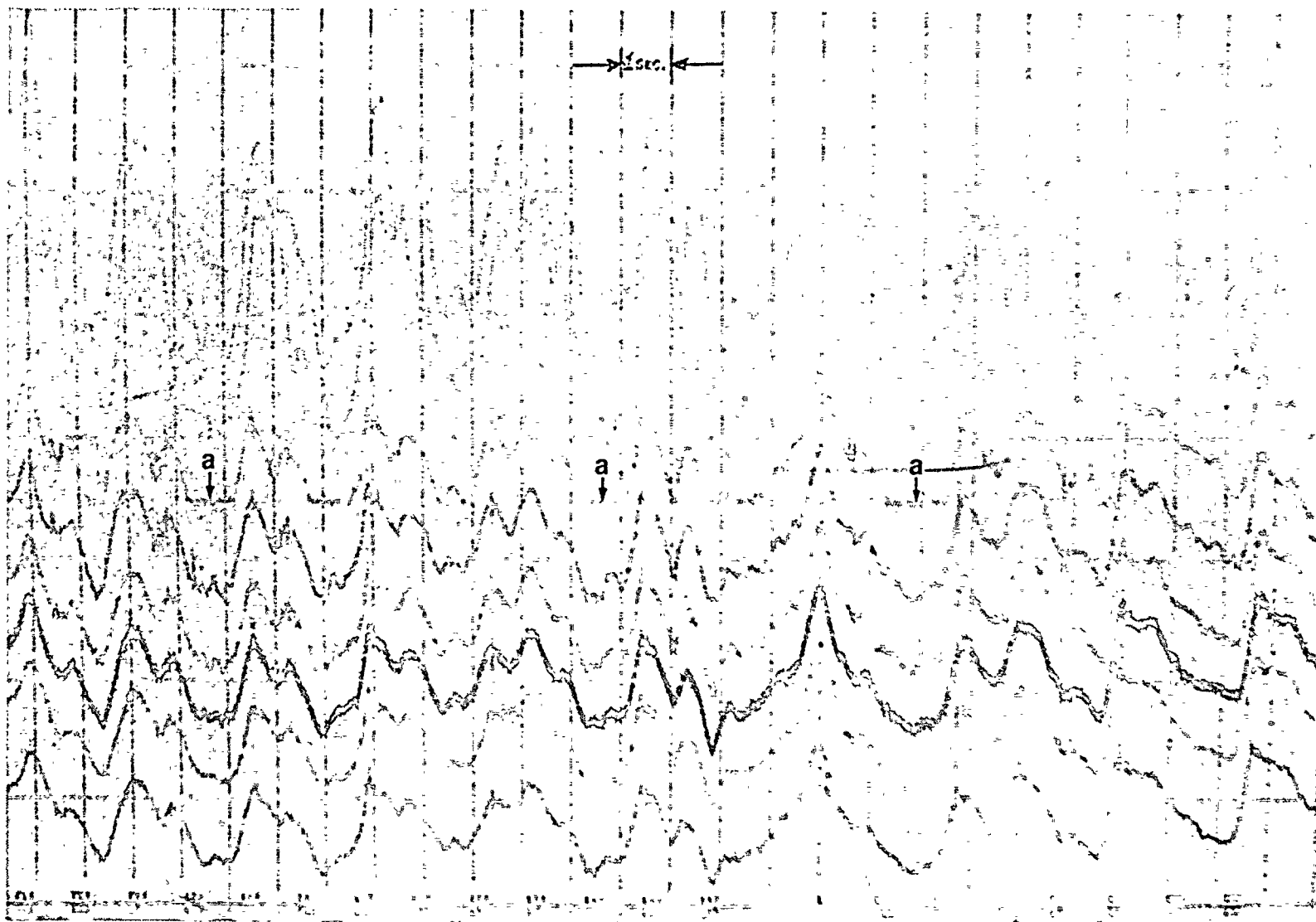


FIGURE 18 Section of Oscillograph Trace for Run 130: 1981⁺ Storm, +17 ft MLLW, 225^o Az, Center Panel Instrumented

elevation is not immediately apparent. The other traces are from six pressure cells arranged with the output from the lowest cell at the bottom of the figure and the traces corresponding sequentially to higher pressure gages lying above. In all cases in this report the pressures referred to are the values which correspond to the maxima with time from the recorded pressure-time histories. One major feature of the record is the similarity of the pressure traces which correspond to the lower five pressure cells. These are gages which are apparently completely immersed during the interval of time shown. The upper pressure record is from a pressure cell which is alternately immersed and exposed to air. The relatively "flat" portion of the trace between some peaks and labelled as "a" is evidence of the gages being exposed. Independent experiments which were conducted with the pressure block removed from the model indicated there would be uncertainties in the pressure readings for the gages which were alternately exposed and immersed. These experiments consisted of rapidly immersing and exposing the gage block with the block held horizontal and indicated that the transducers could give voltage outputs equivalent to from zero ft to 15 ft of water (prototype) in the direction opposite to the direction of positive pressure simply due to wetting of the gage face. The direct application of this measured shift due to changes in heat flux is open to question. Therefore, the pressure measurements associated with the upper transducers which come out of the water must be treated with caution due to the uncertainty which translates to an equivalent pressure head of from zero ft to 15 ft. However, there are certain differences between the experimental arrangement for the measurements which lead to this estimate and that for the actual pressure measurements. One of the most important differences is that to establish the heat flux

shift for all transducers simultaneously the gage block was horizontal when immersed whereas when measuring the curtain wall pressures it was mounted vertically. This may affect water collected behind the gages inside the gage block and thereby mitigate a shift due to heat flux when the gage block is in place in the curtain wall. This conclusion tends to be supported by the time histories shown in Figure 18. If there were a significant effect of heat flux occurring for each pressure peak measured, one would not expect to see zeroes between positive pressure maxima which represent the gage exposed being so "flat" indicating a rapid response to either exposure or wetting. Therefore, it is believed that the estimate of the uncertainty of up to 15 ft is too extreme, and a level considerably less than this would be more acceptable.

3.1.1 Pressures on curtain wall for the condition of:
tsunami, high tide, meteorological tide, and
1981⁺ storm; (+17 ft MLLW)

The results for this water level were obtained using the waves from a storm which is more intense than the 1981 storm to represent an extreme irregular wave occurrence. Two types of results will be presented: (i) certain details of the depthwise pressure distribution at the center of the front face of the curtain wall for waves from 203° and on the centerline and at the west corner of the intake structure for waves from 225°, and (ii) the cumulative frequency distributions of wave heights, pressures, and other pertinent quantities for these cases. Cumulative frequency distributions are typically used for presenting data for irregular waves. These experiments seek to determine the shape of the probability distribution which best defines the statistical nature of variables such as wave height, pressure, and etc. so that estimates can be made of the magnitude of extreme values of these variables. In all experiments reported herein the east and

west breakwaters were degraded to a crest elevation of MLLW.

The variation with depth of the pressure head (pressure divided by, γ , the specific weight of sea water, $\gamma = 64 \text{ lbs/ft}^3$) is presented in Figures 19, 20 and 21 for waves due to the 1981⁺ storm approaching from 203° and 225°. The pressure measurements were made on the centerline and at the west corner of the intake structure; each condition is defined in the figure. These distributions were obtained from the maximum pressure that was observed at any time during the complete pressure time histories recorded for each test condition at each pressure gage location. It is plotted along with the simultaneous water surface elevation as recorded on the wave gage mounted on the seaward face of the curtain wall.

Certain general comments are in order with regard to Figures 19, 20, and 21 before discussing them in detail. For these irregular waves it was found that when the maximum pressure occurred at a given elevation at a particular time during the experiment the pressures at all elevations simultaneously were a maximum at that time. Also, it was found that the water surface height recorded by the wave gage located just west of the pressure transducers usually was not a maximum when the pressures were a maximum.

As mentioned previously, due to a voltage shift caused by changing heat flux characteristics of a transducer when it was exposed to air compared to when it was wetted by a wave, it was necessary to interpret the record from the gages, so affected, differently from the trace from gages which were immersed all of the time. In the latter cases the pressures were interpreted by evaluating the trace on the oscillograph from a zero established before and after the run, i.e., the pressures were measured from the hydrostatic pressure level. For those transducers

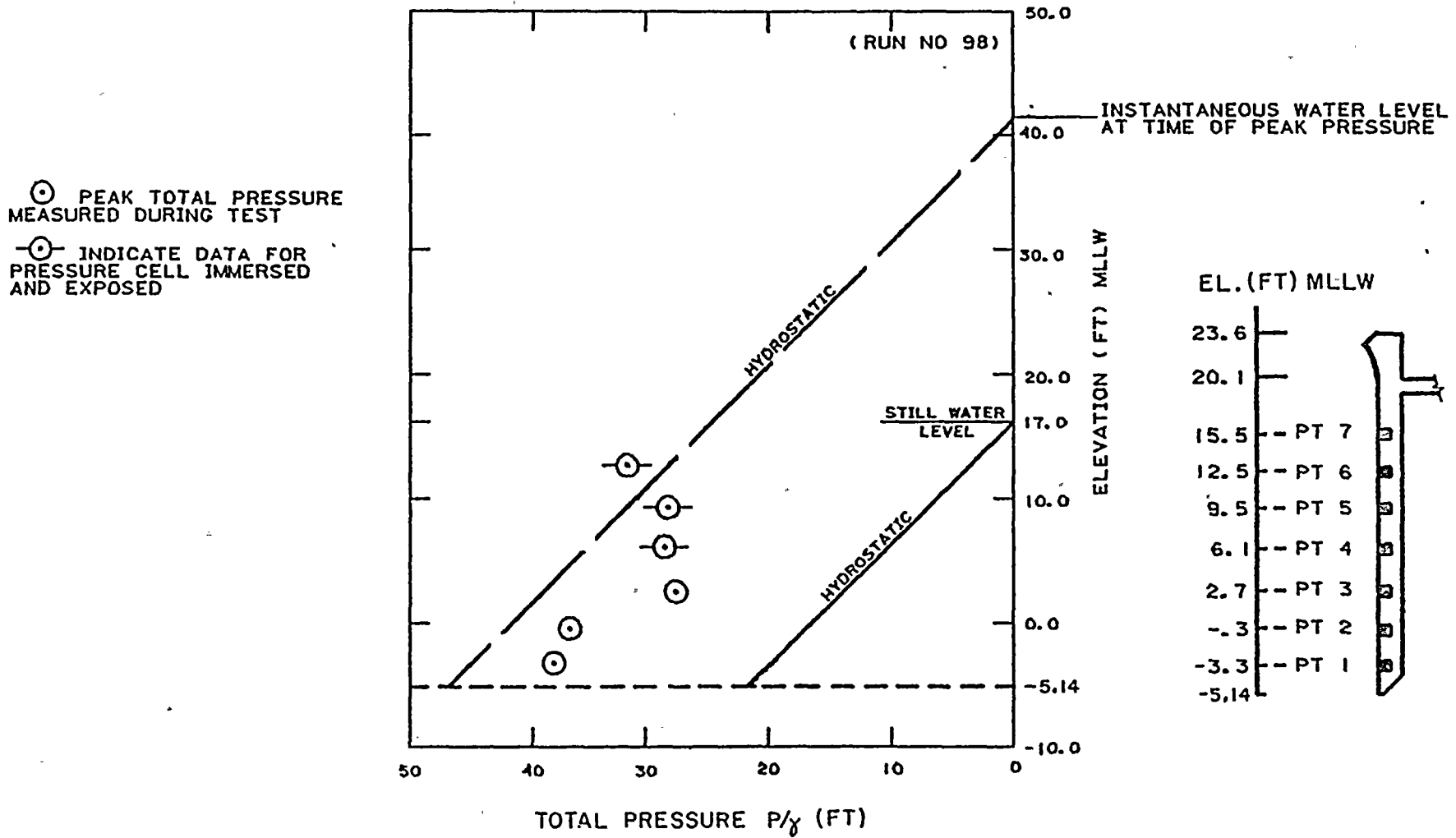


FIGURE 19 - Maximum Pressures Measured on Centerline During Storm of 1981⁺, +17 ft MLLW, 203⁰Az

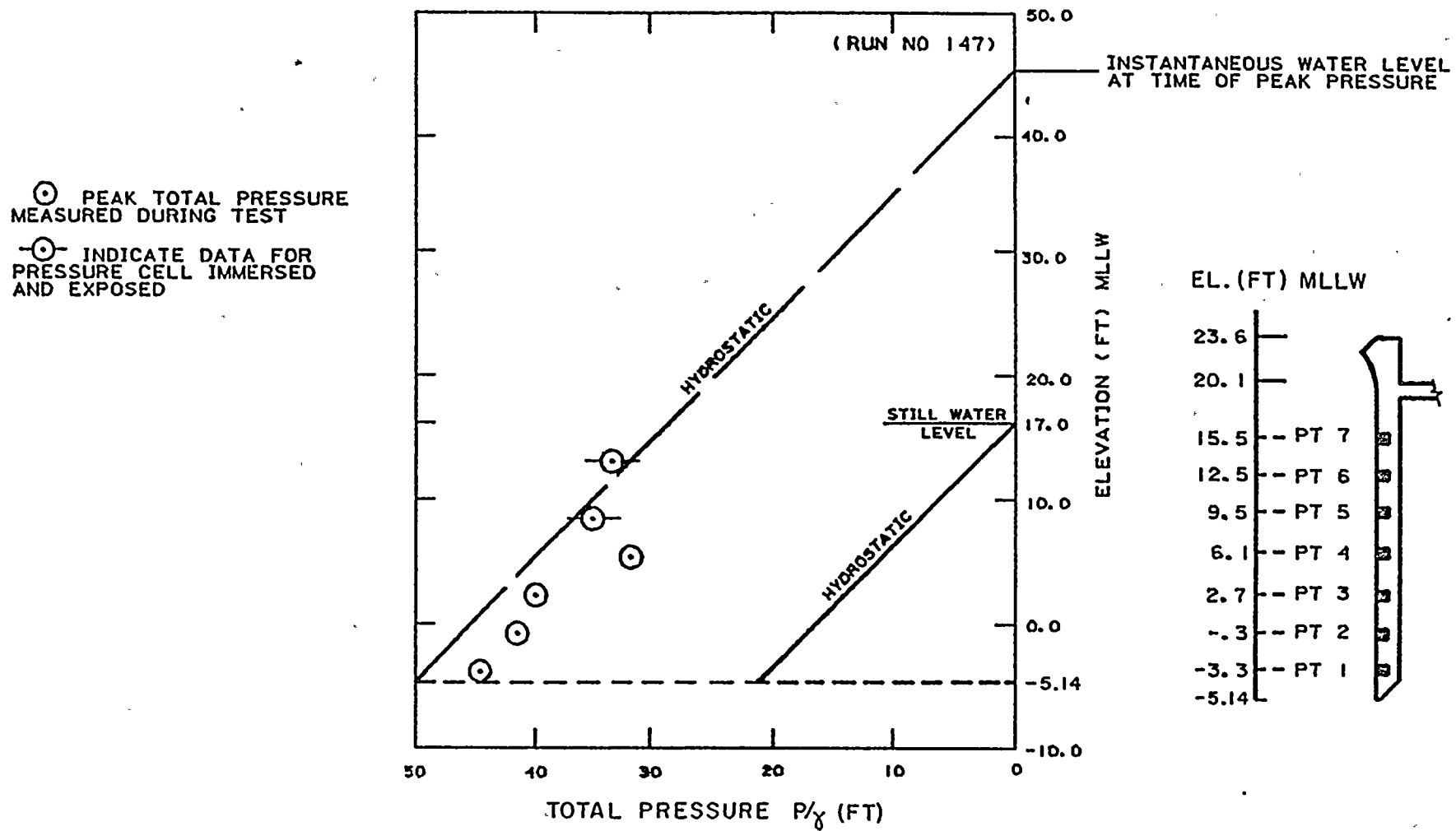


FIGURE 20 - Maximum Pressures Measured on Centerline During Storm of 1981⁺, +17 ft MLLW, 225°Az

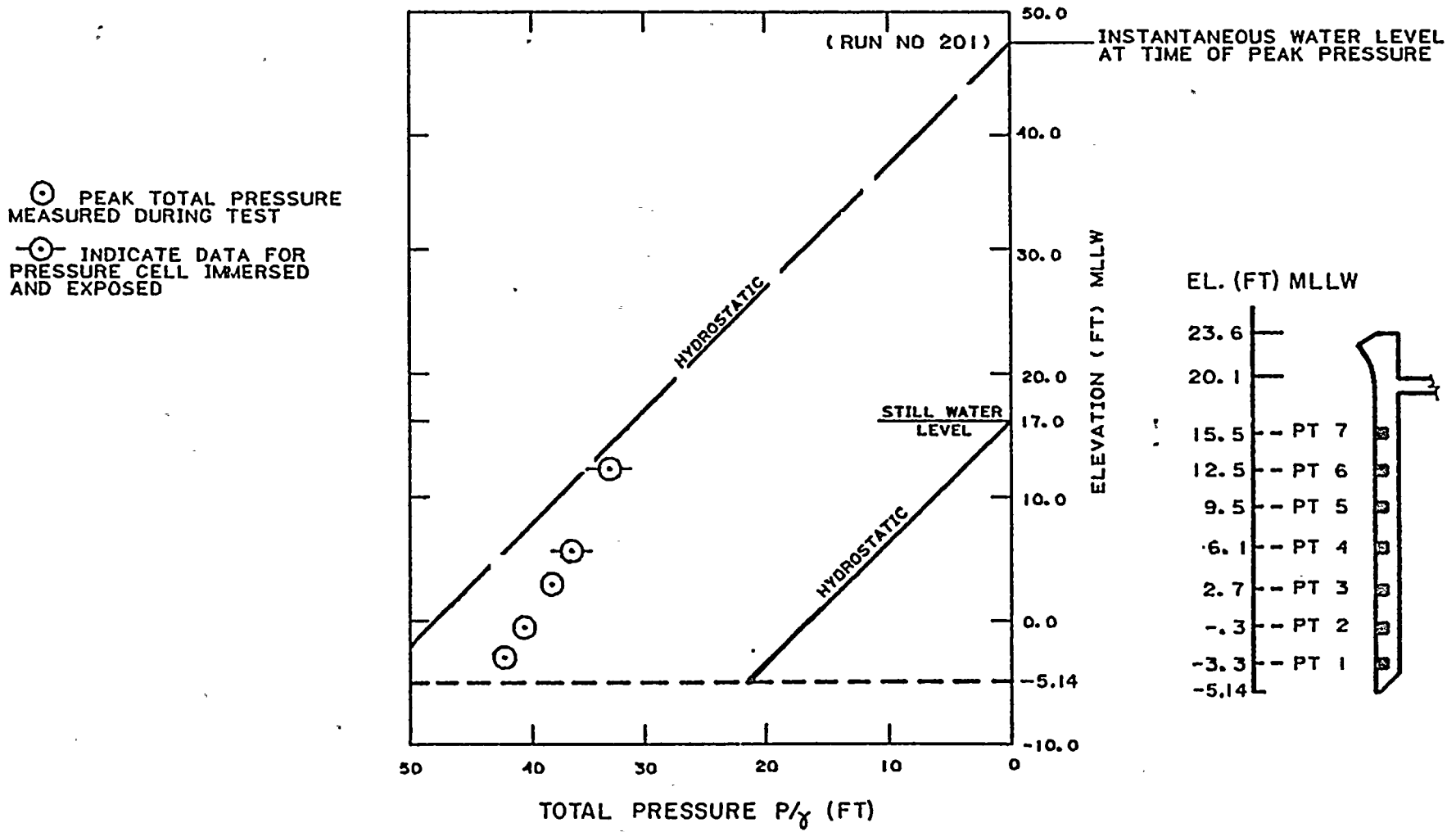


FIGURE 21 Maximum Pressures Measured at West Corner During Storm of 1981⁺, +17 ft MLLW, 225°Az

which were immersed and exposed during an experiment, a local zero was used to define the pressure. This is the zero which occurs adjacent to the maximum pressure caused by water receding from the face of the gage, see Figure 18. These upper transducer locations where the pressure sensitive face of the transducer was immersed and exposed are indicated by special symbols in Figures 19, 20, and 21. The pressure measurements shown for these gages has not been added to a hydrostatic pressure at the level of the gage, since the pressure is measured relative to a zero which occurred when the gage was out of the water. The uncertainty mentioned in Section 3.1 of at most 15 ft due to the heat flux characteristics of the gages makes the pressures indicated on the depthwise distribution for the alternately wetted and dried transducers relatively unreliable. Thus, the values shown should be used with some caution. However, as mentioned earlier this uncertainty is most probably unrealistically high. Indeed observations of the experiments coupled with the reasonably hydrostatic pressure distributions shown in Figures 19, 20, and 21 support this conclusion

It is seen in Figures 19, 20, and 21 if a line is extended from the instantaneous water surface elevation on the front face of the curtain wall, which occurred at the time of the maximum pressure, downward at a slope corresponding to hydrostatic pressure the observed pressures are generally less than this. This may be explained by the influence of horizontal and vertical accelerations. It can be seen that the pressure distributions are reasonably similar for the two different incident wave directions and for the centerline and the west corner of the structure for the same wave direction.

In Figures 22, 23, and 24 cumulative frequency distributions are

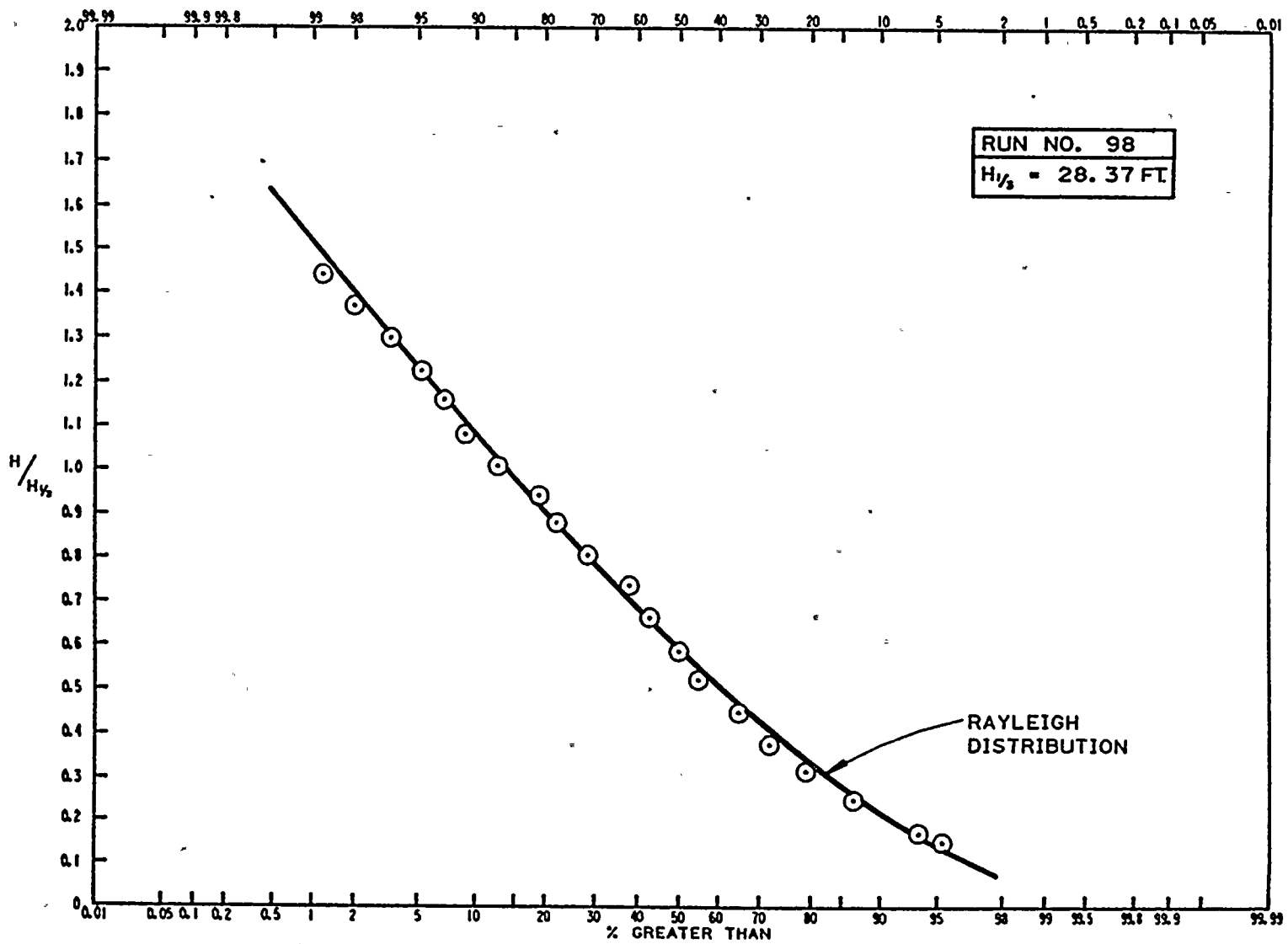


FIGURE 22 Normalized Wave Height Frequency Distribution: 1981+ storm, +17 ft MLLW, 203°Az

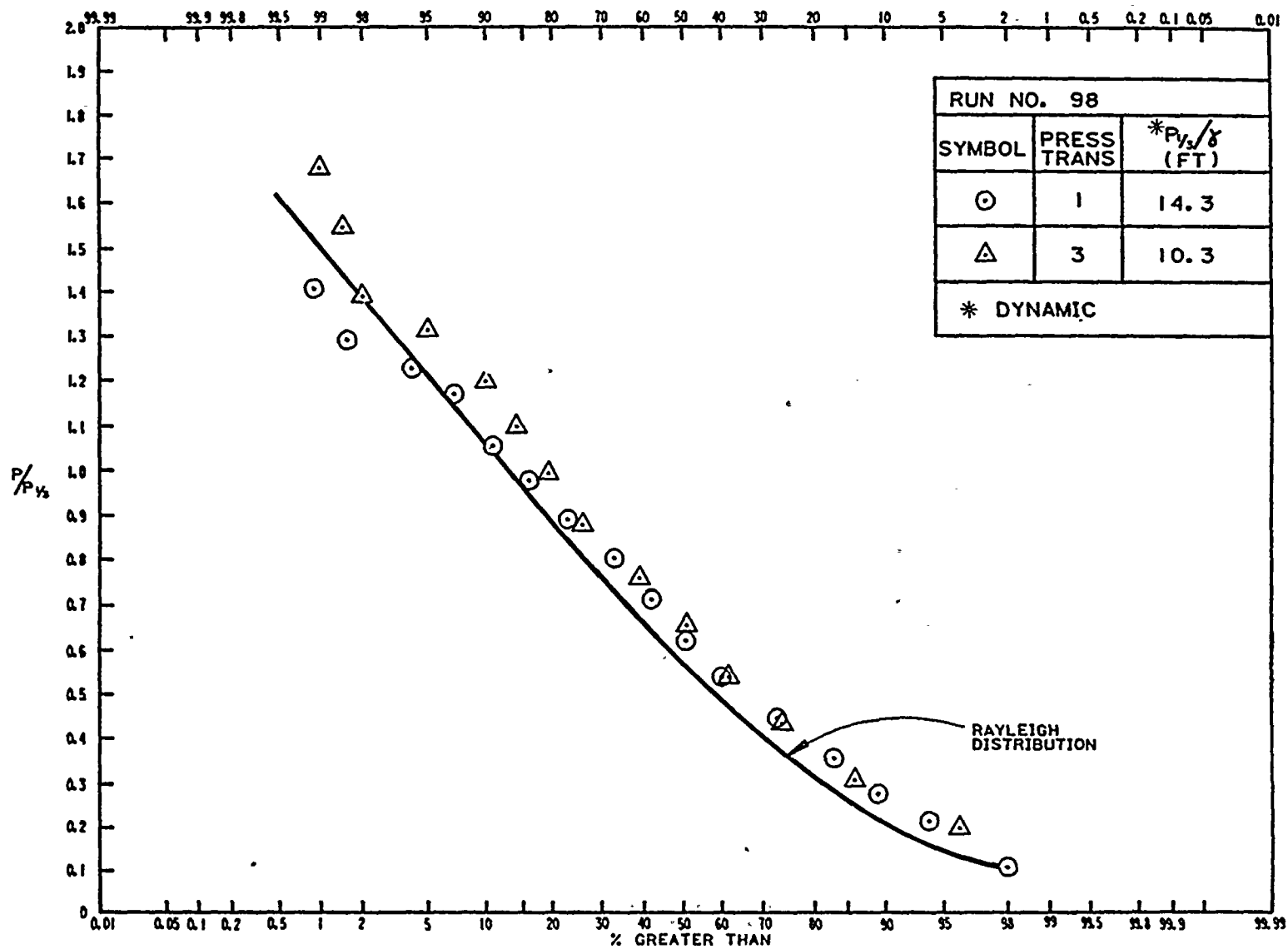


FIGURE 23 Normalized Pressure Frequency Distribution: 1981⁺ storm, +17 ft MLLW, 203°Az

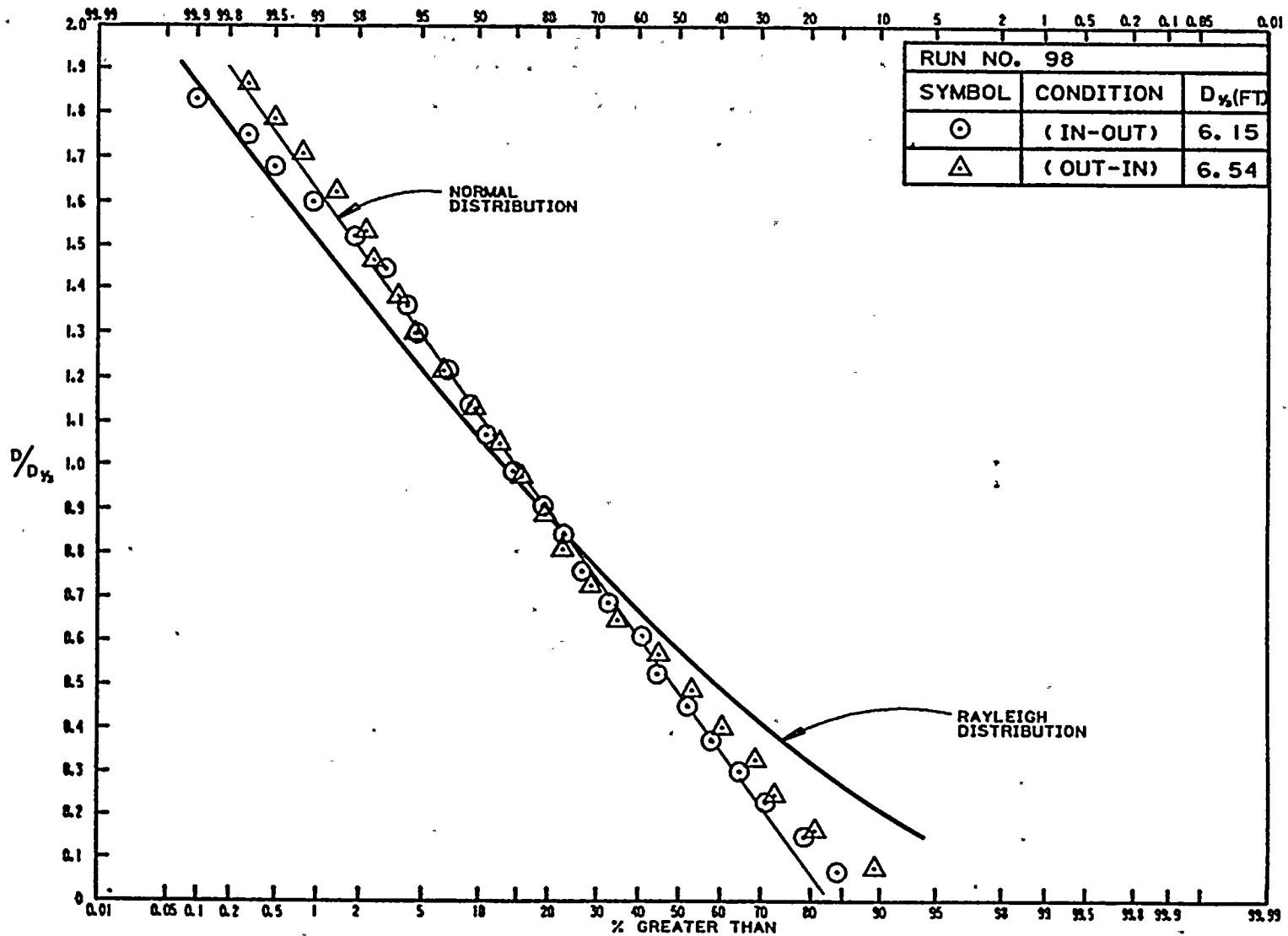


FIGURE 24 Normalized Head Difference Frequency Distribution: 1981⁺ storm, +17 ft MLLW, 203°Az

presented for wave height, dynamic pressures at two vertical locations, and the head difference across the curtain wall for the 1981⁺ storm impinging on the structure from the south (203°). (The number of the particular pressure transducer is shown in the inset in Figure 23, and its elevation can be determined from Figure 7a.) Similar curves are shown in Figures 25, 26, and 27 for pressure measurements made at the corner of the curtain wall for waves impinging from the southwest (225°). These data are plotted as the desired quantity normalized with respect to the "significant" value as the ordinate and the percent by number greater than the indicated ordinate value as the abscissa. (The "significant" value is defined as the average of the highest one-third of the values observed.) In Figure 28 similar results are plotted for waves impinging from 225° for the pressure measured on the centerline of the structure at two vertical locations, and in Figure 29 the head difference across the center region of the curtain wall is shown for the same direction.

In general, the wave heights and the pressures shown tend to follow a Rayleigh distribution which is shown on each figure. The cumulative frequency distributions of the head difference across the curtain wall (Figures 24, 27, and 29) appear to deviate from the Rayleigh distribution and agree better with a normal distribution. Two different symbols are indicated on the head difference plots: circles indicating the difference obtained from the peak water surface elevation outside subtracted from that simultaneously occurring inside, and triangles indicating the difference between the peak occurring inside and the simultaneously occurring water surface elevation outside.

Longuet-Higgins (1952) and Ochi (1973) each have given attention to the question of the probable maximum wave (or other quantity) when the

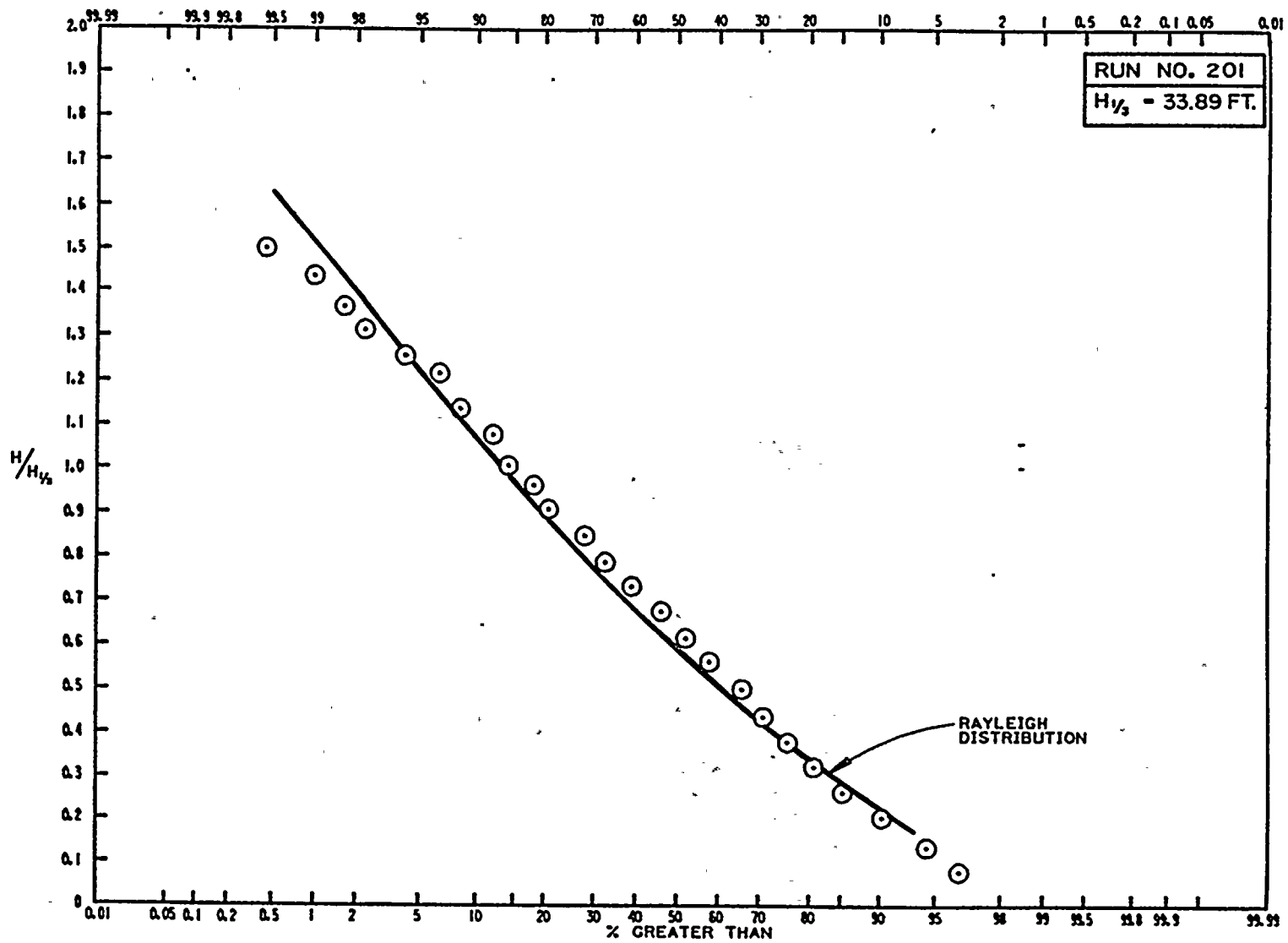


FIGURE 25 Normalized Wave Height Frequency Distribution: 1981⁺ storm, +17 ft MLLW, 225°Az, West Corner

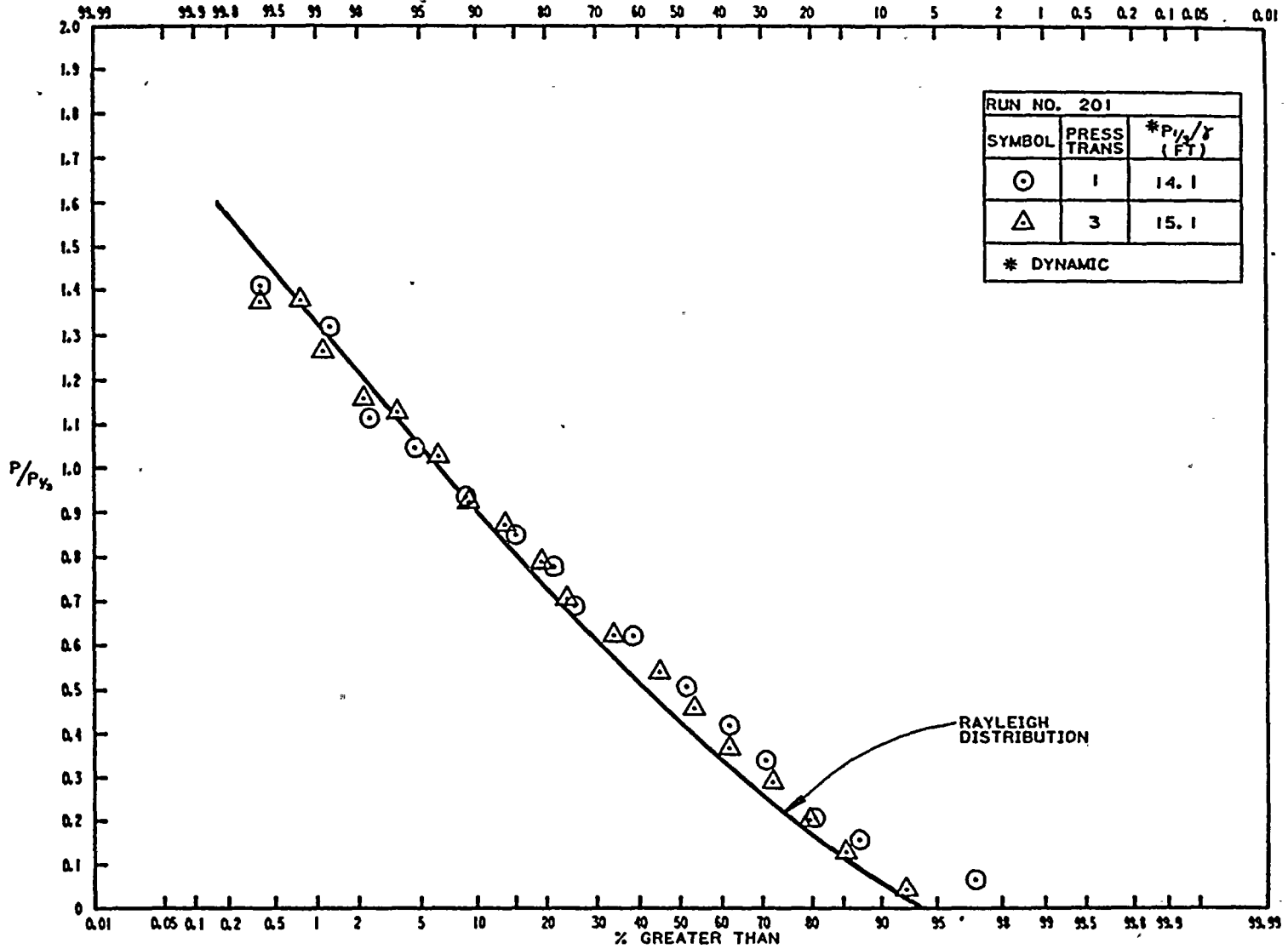


FIGURE 26 Normalized Pressure Frequency Distribution: 1981⁺ storm, +17 ft MLLW, 225°Az, West Corner

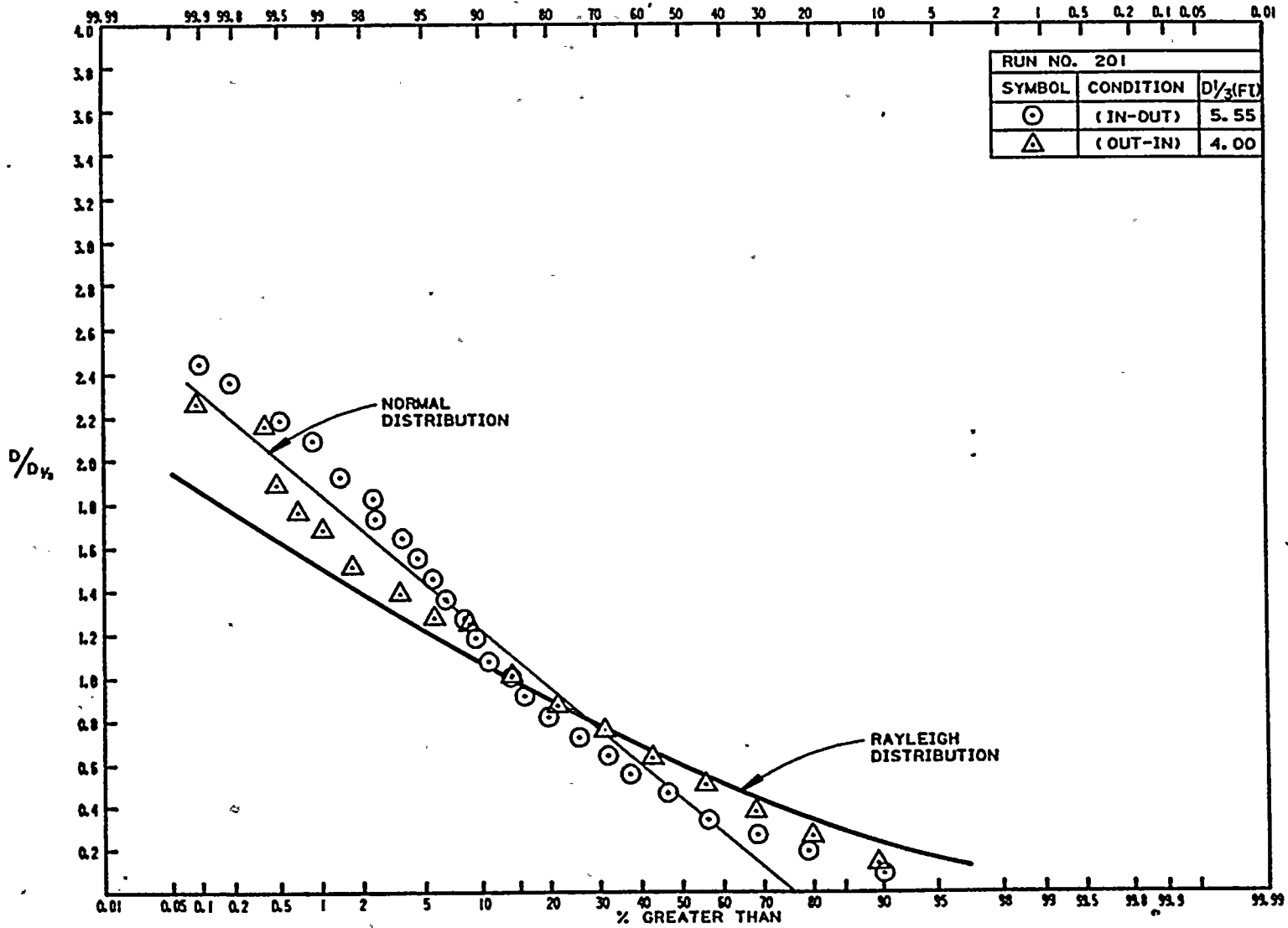


FIGURE 27 Normalized Head Difference Frequency Distribution: 1981+ storm, +17 ft MLLW, 225°Az, West Corner

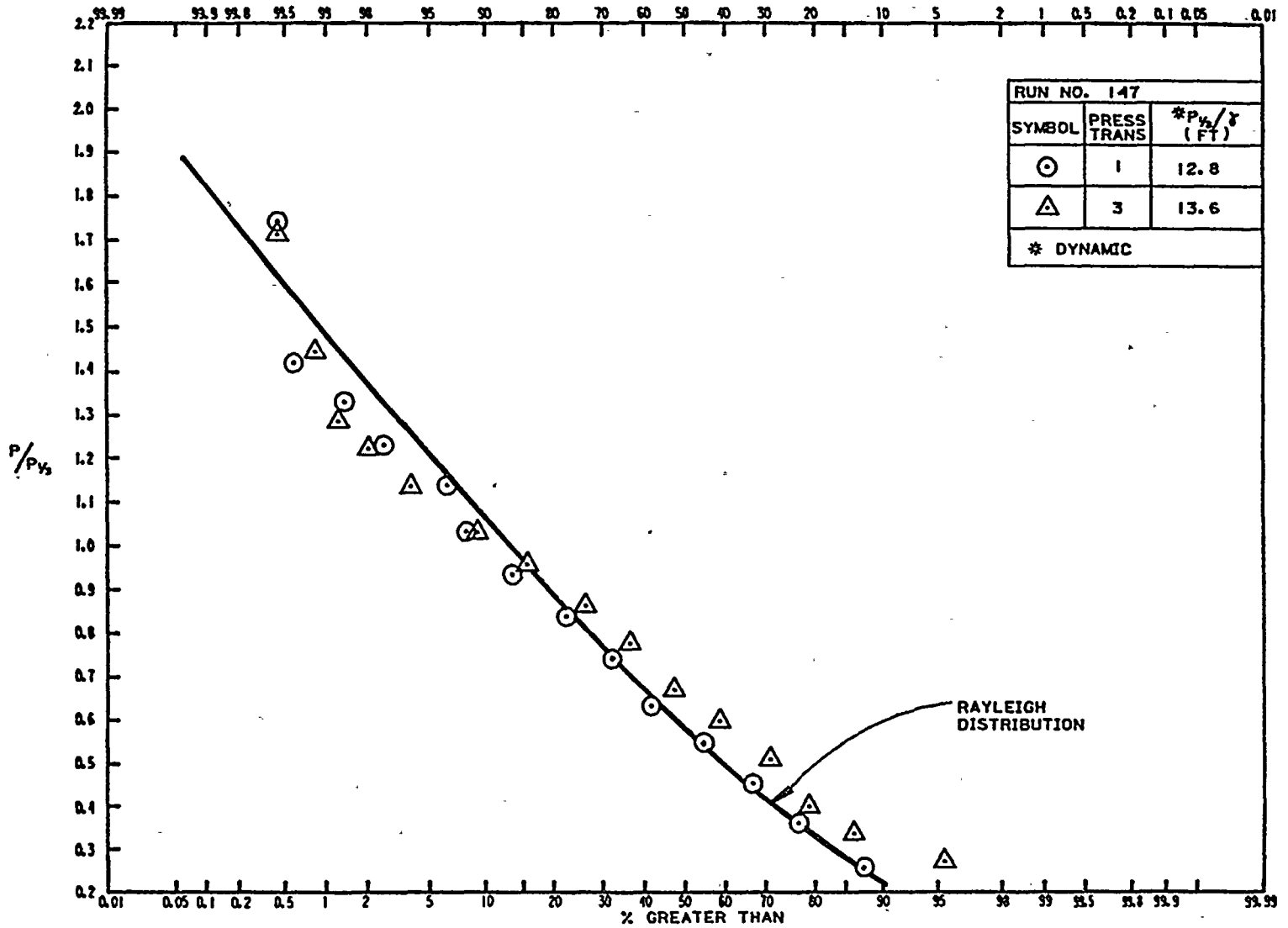


FIGURE 28 Normalized Pressure Frequency Distribution: 1981⁺ storm, +17 ft MLLW, 225°Az, Center

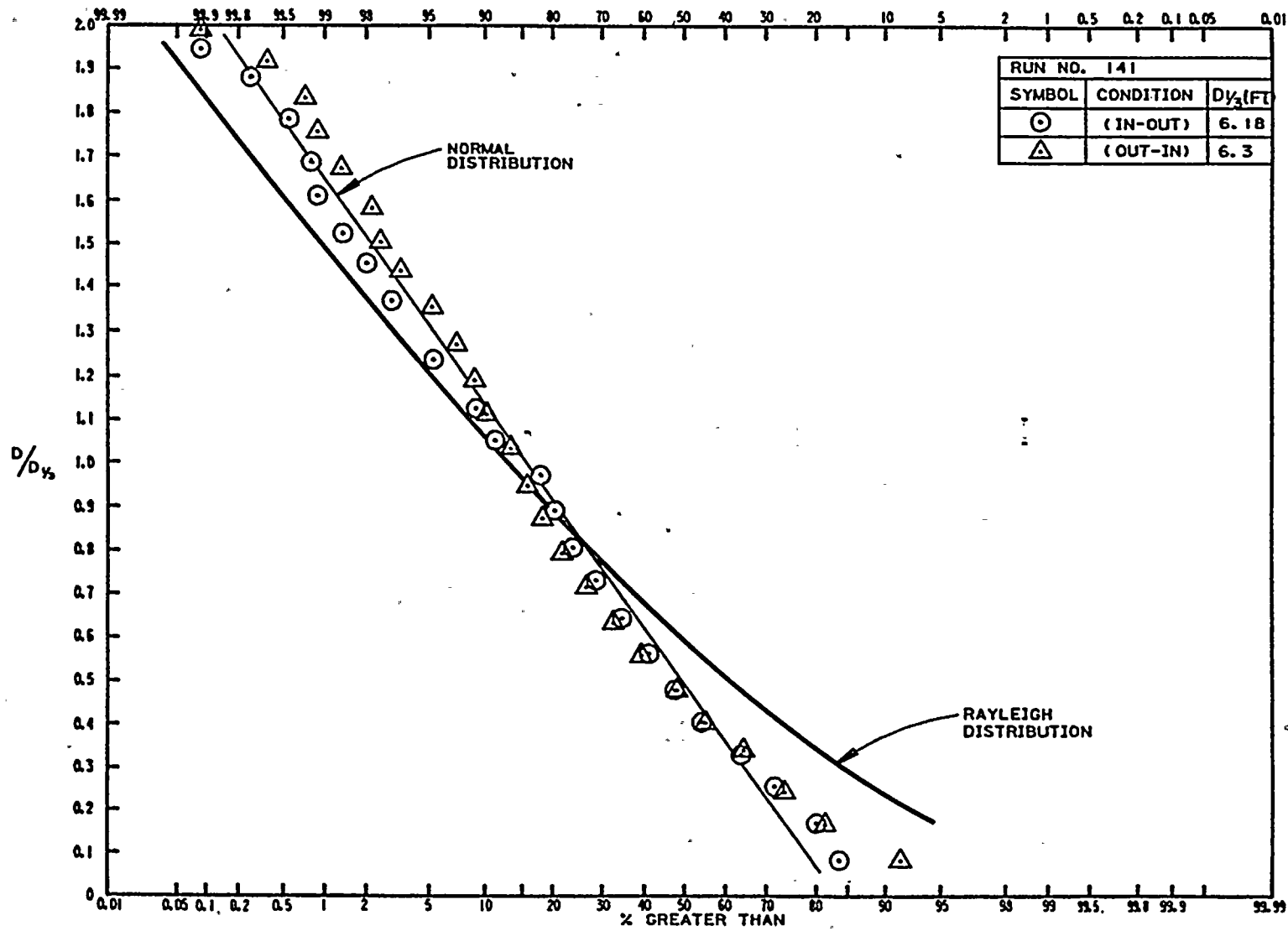


FIGURE 29 Normalized Head Difference Frequency Distribution: 1981⁺ storm, +17 ft MLLW, 225°Az, Center

distribution is defined by a Rayleigh distribution; this is based on a given number of events. In practical applications this probable maximum event is an estimate of the largest event that may occur over a given duration. Equivalently, as done by Ochi (1973) it may be obtained from the probability distribution of largest events that occurs in samples of N events. Taking the maximum duration for the most intense portion of the 1981⁺ storm, i.e., 1800 hrs GMT, as about 10 hrs and for average wave periods of 15 sec, there are about 2400 waves during that interval. These two approaches yield values of the ratio of the probable maximum wave height (or other quantity) to the significant wave height (or other quantity) from 2 to 2.5. The latter value is proposed by Ochi (1973) for a probability of 1% that the maximum in 2400 events would be exceeded. In other words, for storms with identical statistics (or different portions of the same storm), the probability of exceeding the probable maximum parameter, e.g., wave height, pressure, etc., is 1%.

The probable maximum dynamic pressure for these cases using this definition was between 26 ft of water and 37 ft of water. Adding hydrostatic pressure to this, probable maximum total pressures of between 48 ft and 59 ft were estimated, as compared to a maximum measured pressure of 44 ft. In addition, the probability of occurrence of the maximum wave during the time of +17 ft MLLW water level is much reduced since this water level occurs only for about 2 min to 3 min due to the period of the tsunami. Thus, the probability of the pressures exceeding these maximum total pressures would no doubt be extremely remote. This section of the curtain wall is even safer than these pressures imply because for a still water level of +17 ft MLLW there will almost always be water in the refuse bin since the invert level of the port in the curtain wall is about +15 ft MLLW. Hence, a hydrostatic pressure will be present on

the back of the center section of the curtain wall. This would lead to a maximum net pressure on this section which would be closer to the maximum dynamic pressure reported, i.e., 37 ft, rather than to the sum of the dynamic and the hydrostatic pressures (59 ft).

For the region away from the center of the curtain wall there is water on both sides of the curtain wall due to the bar screen chamber, e.g., see Figures 4b and 4c. Since Figures 19, 20, and 21 have indicated that the dynamic plus the static pressure on the front face of the curtain wall is generally less than the hydrostatic pressure distribution defined by the water level on the front face of the curtain wall at the time of maximum dynamic pressure, the net water surface elevation difference across the curtain wall defines the wave-induced loads for that part of the structure. In Figures 24, 27, and 29 the cumulative frequency distributions of the net head difference across the curtain wall as measured by the two wave gages shown in Figure 16 are presented, and the significant head difference is indicated in each figure. Assuming a Rayleigh distribution the maximum probable head difference appears to be less than about 17 ft of water. Curves which correspond to a normal distribution also are shown on these figures. The corresponding value of the normalized probable maximum value for a normal distribution as determined by Ochi (1973) is 3.7 compared to 2.5 for the Rayleigh distribution. If such a distribution is assumed, the probable maximum head difference would be about 24 ft of water, which is less than the pressures measured on the center panel.

During the study it was observed that there were slam pressures on the underside of the deck of the cooling water intake structure caused by water rushing up through the trash rack and impinging on that surface before exiting through the openings in the deck. To investigate whether

these pressures might be transmitted acoustically down the inside of the curtain wall thus resulting in high interior pressures, pressure measurements were made on an inside wall next to a region of high deck pressure. These measurements showed that the pressure decreases with increasing vertical distance below the deck similar to an acoustic pressure emanating from a point source. Due to scaling problems associated with unknown air entrainment in the fluid and structural elasticity of the model, accurate prototype pressures cannot be inferred from the model measurements. However, for purposes of comparison the scaling of these pressures has been done in a Froudian manner, i.e., the pressure head in the model is multiplied by the length scale to give the prototype value. This is considered to be conservative. The measurements were made at the following three distances below the underside of the deck: 1.9 ft, 6.6 ft, and 11.3 ft. The model was exposed to waves from 203° for the 1981⁺ storm at a water level of +17 ft MLLW and the maximum pressure measured which occurred in the pressure time history which was recorded 11.3 ft below the underside of the deck was 54.7 ft. (The cumulative frequency distribution for these pressures indicate an exceedance for the maxima reported of 0.2% to 0.4%.) The pressures are larger closer to the underside of the deck. The maximum pressure (including hydrostatic) observed in the pressure time history 6.6 ft below the deck was 59.4 ft and 1.9 ft below the deck the maximum measured pressure was 364 ft.

It was decided to explore means to reduce the potential for slam pressures on the deck between the bar rack opening in the deck and the parapet wall. One solution is to remove that section of the deck. This would allow water to rise vertically with no horizontal surfaces to impede the flow and to create high pressures. Measurements in the model at the

location of the lowest transducer without this deck section for the wave and tide conditions mentioned indicated a reduction of pressure to about 31.8 ft. At a distance of 6.6 ft below the deck the total pressure was reduced to 32 ft by this modification. (Due to a transducer malfunction a corresponding value at the upper location is not available.)

Another remedial measure tested was the addition of wedge-shaped fillets fitted under this section of the deck to eliminate the horizontal surface which causes wave impact. Two alternate wedge shapes were tested and denoted as 45° and 30° (meaning the angle between the curtain wall and the face of the wedge). The maximum total pressure measured 11.3 ft below the underside of the deck was 38.1 ft for the 45° wedge and 39.7 ft for the 30° wedge. There is a 30% reduction in interior pressures compared to those measured at the same elevation with the original deck configuration.

The pressure distributions on the face of the wedge-shaped fillets were not measured, but they can be inferred easily from the results of investigations of pressures on wedges which impact the free surface of a fluid. As a wedge of fixed width penetrates the surface a pressure distribution is developed with the peak pressure on the face of the wedge located at a distance from the apex of the wedge. This distance increases with increasing immersion, and this condition is denoted as partial immersion. When the top of the wedge reaches the free surface the maximum pressure occurs at the apex of the wedge; this will be referred to as full immersion. The results of Smiley (1952) have been used to define the peak pressure in these two cases.

For the partially immersed case the maximum pressure on the front face of the wedge is a function of the wedge angle. It can be expressed as the ratio of the peak pressure to a stagnation pressure defined as: $\frac{\rho}{2} V_n^2$ where V_n is the normal velocity of the apex of the wedge or for a fixed wedge the

normal velocity of the free surface relative to the wedge. For the 45° wedge this ratio is about 2.5 and for the 30° wedge it decreases to about 0.8. If the pressure measured 11.3 ft below the underside of the deck is used as the stagnation pressure, i.e., about 30 ft, the maximum pressure on the face of the wedge for a condition of partial immersion would be estimated to be between about 24 ft and 75 ft. For the condition of full immersion the maximum pressure would be estimated to be approximately 30 ft.

Based on the results of these tests, it appears that removing the deck sections or installing the 30° or 45° wedge fillets reduces the interior pressures compared to those measured with the deck section in place. Thus, considering the conservative scaling from model to prototype for these measurements and the effect on the interior pressures of the suggested modifications the front curtain wall pressure measurements and the measurements of head differences across the curtain wall are sufficient to define the maximum loads on the curtain wall.

3.1.2 Pressures on the curtain wall for the condition of: maximum tide and limit waves (+7.5 ft MLLW)

As discussed earlier, the condition of a "maximum credible wave" event is treated using the limiting wave concept proposed by Lillevang, Raichlen, and Cox (1982). In that study periodic waves were imposed upon the structure at a tide level of +7.5 ft MLLW and it was demonstrated that these waves reached a limiting height in the cooling water intake basin. In all experiments reported herein both breakwaters were modelled with the crest elevation at MLLW.

A typical pressure distribution for periodic waves is presented in Figure 30 for 16 sec waves with a height of 41 ft approaching from the

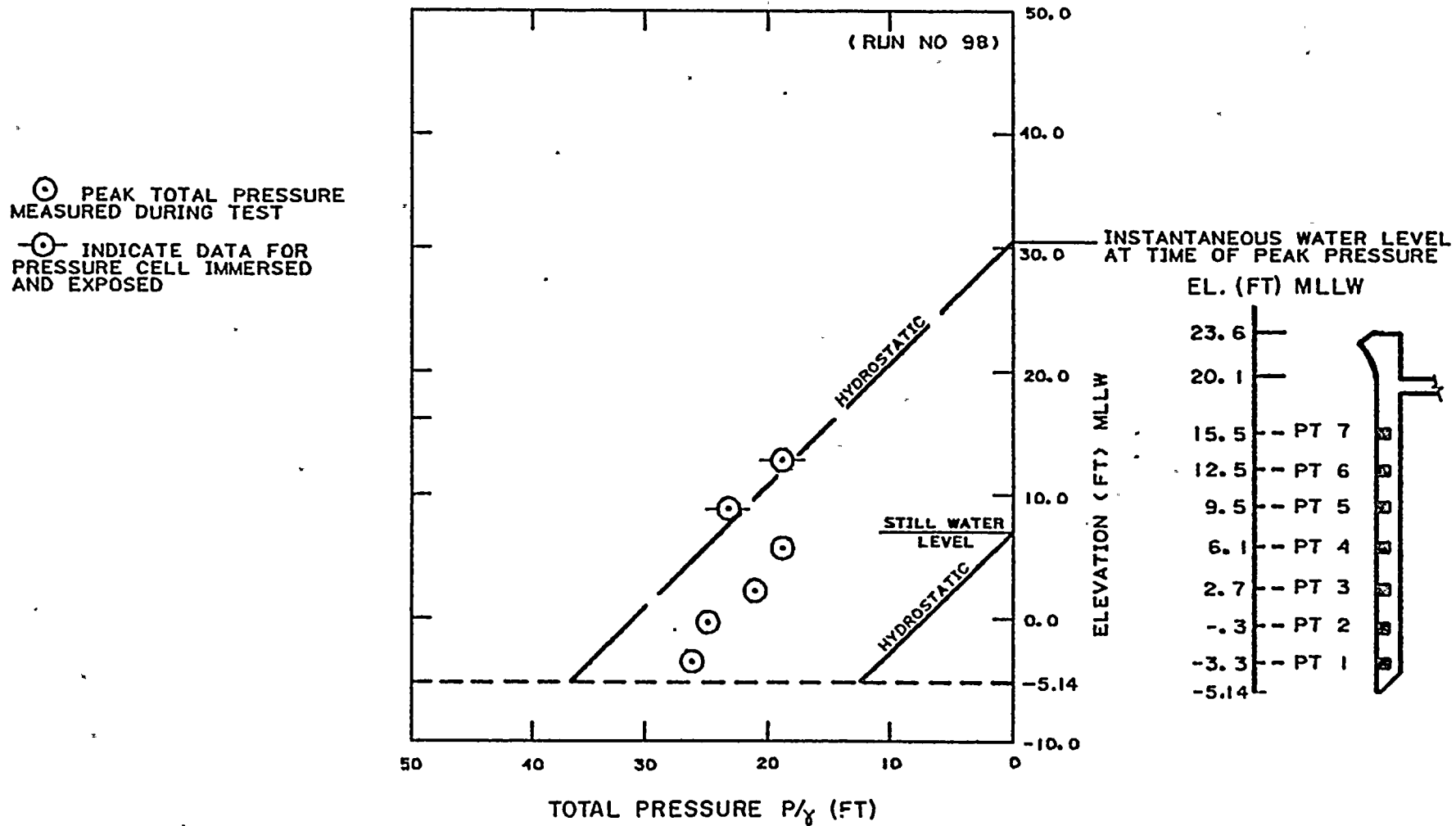


FIGURE 30 Maximum Pressure Measured on Centerline for Periodic Waves: +7.5 ft. MLLW, $T=16$ sec, $H_p=41$ ft., $225^\circ Az$

southwest (225°). The pressures plotted are the maximum that occur in a group of regular waves and the instantaneous water level measured at the front face of the curtain wall is shown also. Upper pressure transducers were exposed during these experiments also.

In general, the pressures are less than hydrostatic relative to the simultaneously occurring water level on the front of the curtain wall except for the two upper locations which, as discussed previously, could be in error due to the effects of heat flux. In all cases where pressure distributions were obtained the variation with depth was similar to that shown in Figure 30.

The maximum total pressures (dynamic plus hydrostatic) at the three lowest elevations are presented as a function of the offshore wave height in Figures 31 through 36. (These elevations are: -3.3 ft MLLW (PT-1), -0.3 ft MLLW (PT-2), and +2.7 ft MLLW (PT-3.) At these elevations these transducers are continuously immersed. The ordinate in these figures is the sum of the maximum dynamic pressure observed and the hydrostatic pressure, and the abscissa is the wave height at Location B (see Figure 5). These results are presented for 12 sec and 16 sec waves approaching from the south (203°) and from the southwest (225°) and impinging upon the center panel and for waves from the southwest (225°) impinging upon the transducers located near the west corner of the intake structure; the former are labelled "centerline", the latter are labelled "corner". On each figure the maximum, minimum, and average pressures are indicated for given wave heights as observed from records of six to nine waves. Since the waves at Station B are periodic and reasonably uniform and the variation of the pressures at each vertical location is significantly less than those presented in the cumulative frequency distributions, this simple form of data presentation is used.

	PT-1	PT-2	PT-3
MAX.	⊖	⊠	△
AVG.	⊙	⊡	▲
MIN.	⊕	⊞	▽

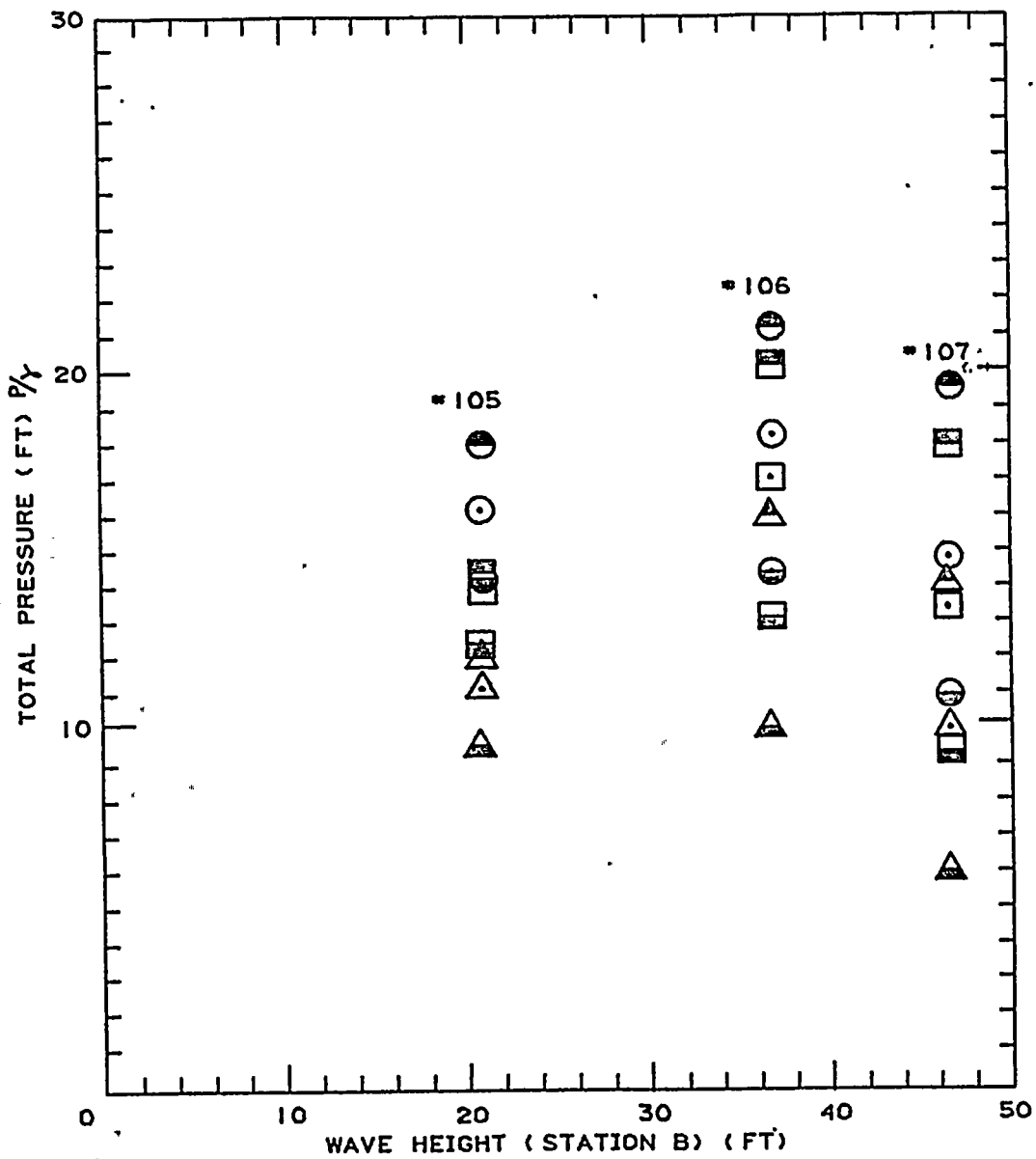


FIGURE 31 Variation of Total Pressure With Offshore Wave Height: +7.5 ft.
MLLW, T=12 sec, 203°Az, Centerline

	PT-1	PT-2	PT-3
MAX.	⊖	■	△
AVG.	○	□	△
MIN.	⊕	⊗	△

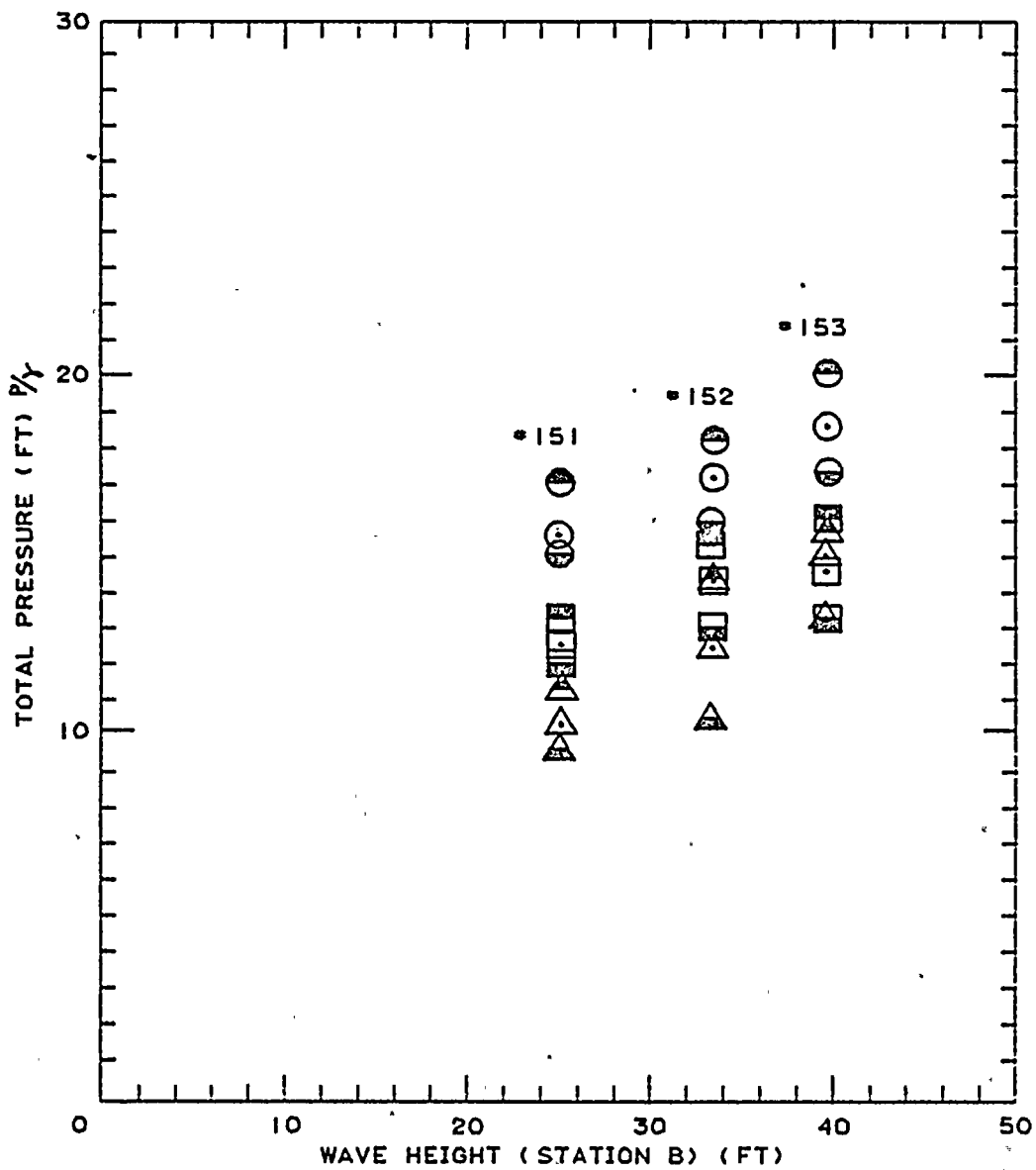


FIGURE 32 Variation of Total Pressure With Offshore Wave Height: +7.5 ft. MLLW, T=12 sec, 225°Az, Centerline

	PT-1	PT-2	PT-3
MAX.	◐	◑	◒
AVG.	○	◻	△
MIN.	◑	◒	◓

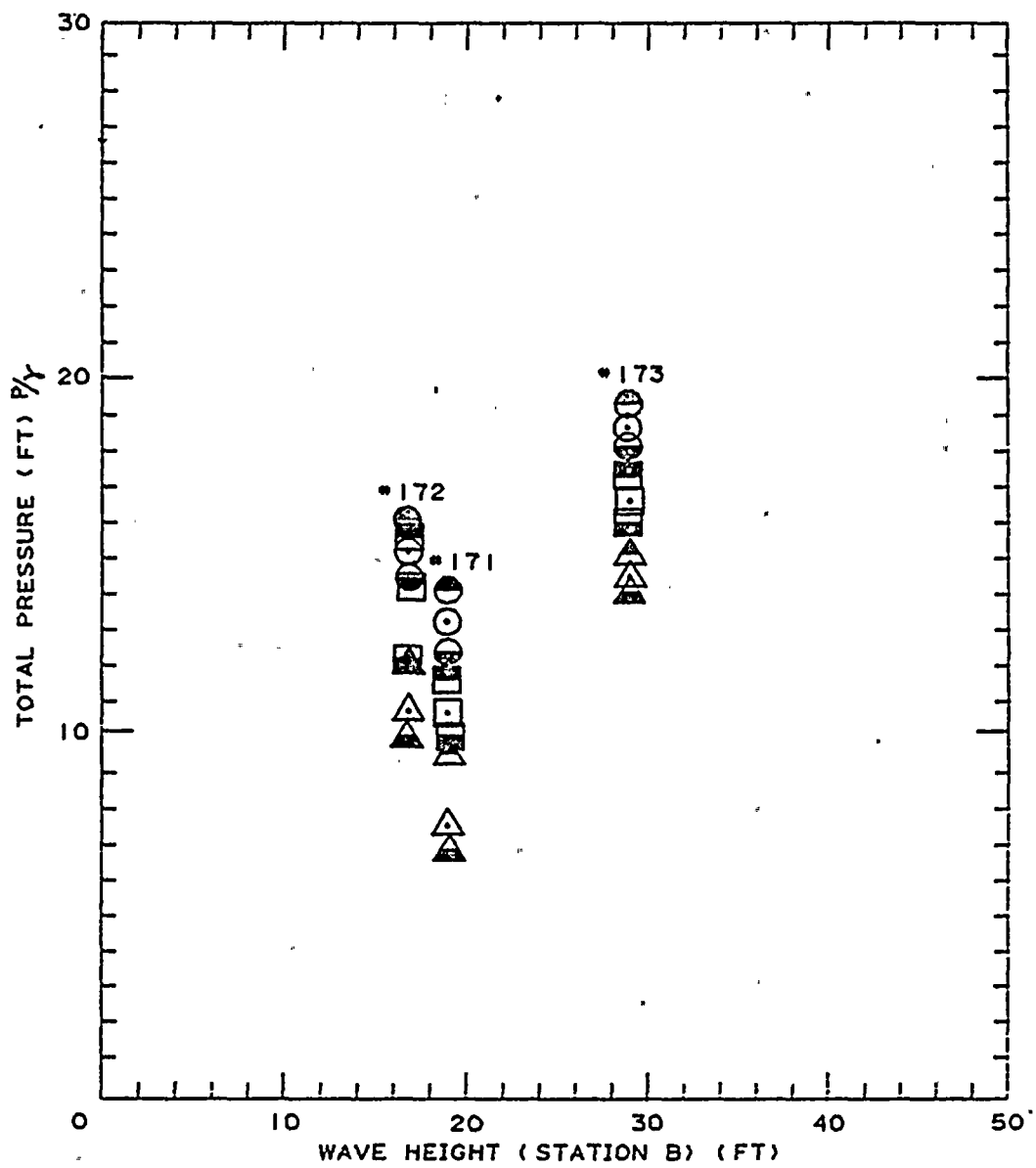


FIGURE 33 - Variation of Total Pressure with Offshore Wave Height:
+7.5 ft MLLW, T=12 sec, 225°Az, Corner

	PT-1	PT-2	PT-3
MAX.	●	■	▲
AVG.	○	□	△
MIN.	◐	◑	◒

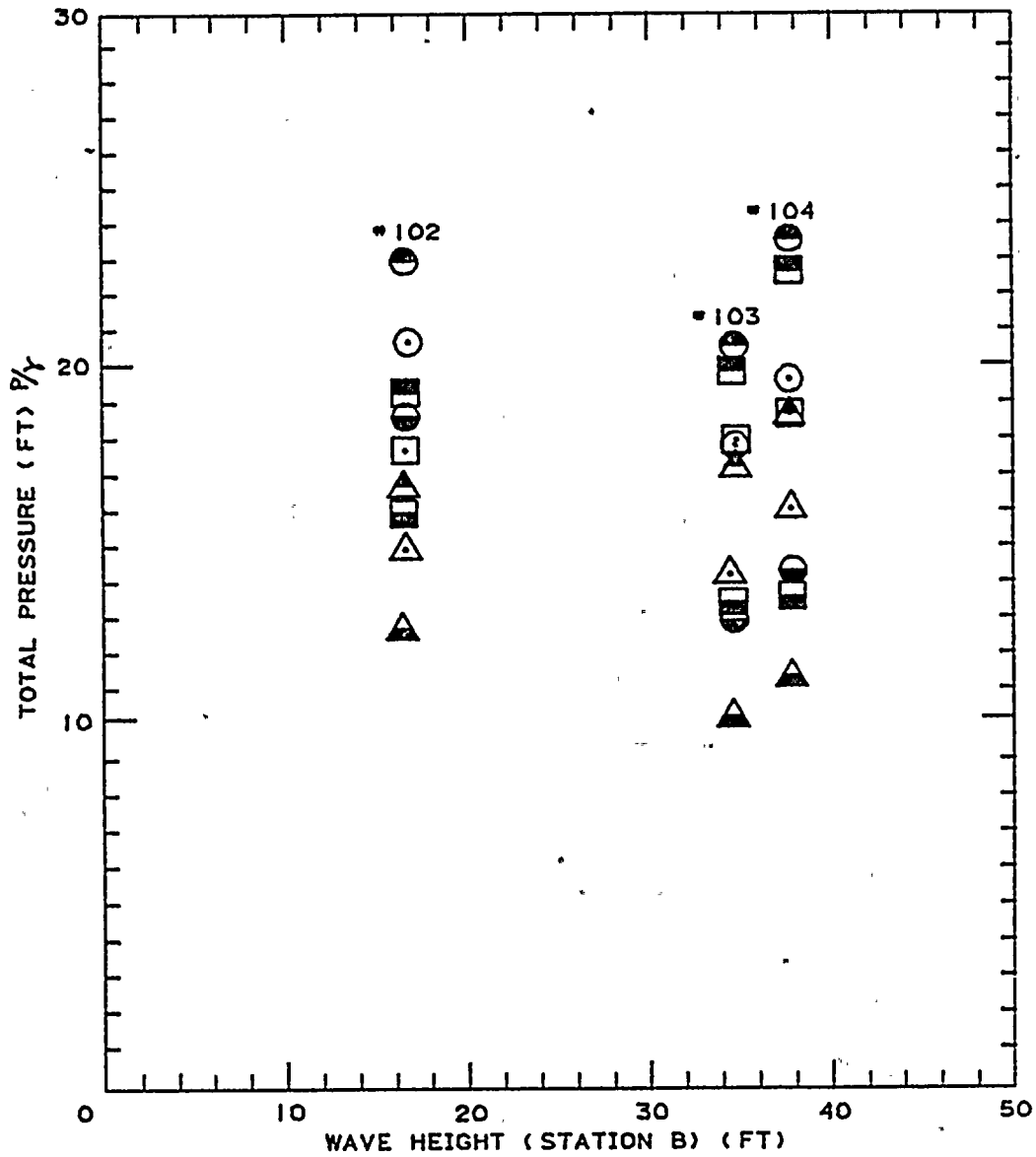


FIGURE 34 - Variation of Total Pressure with Offshore Wave Height:
+7.5 ft MLLW, T=16 sec, 203°Az, Centerline

	PT-1	PT-2	PT-3
MAX.	⊗	⊠	△
AVG.	○	□	△
MIN.	⊙	⊡	△

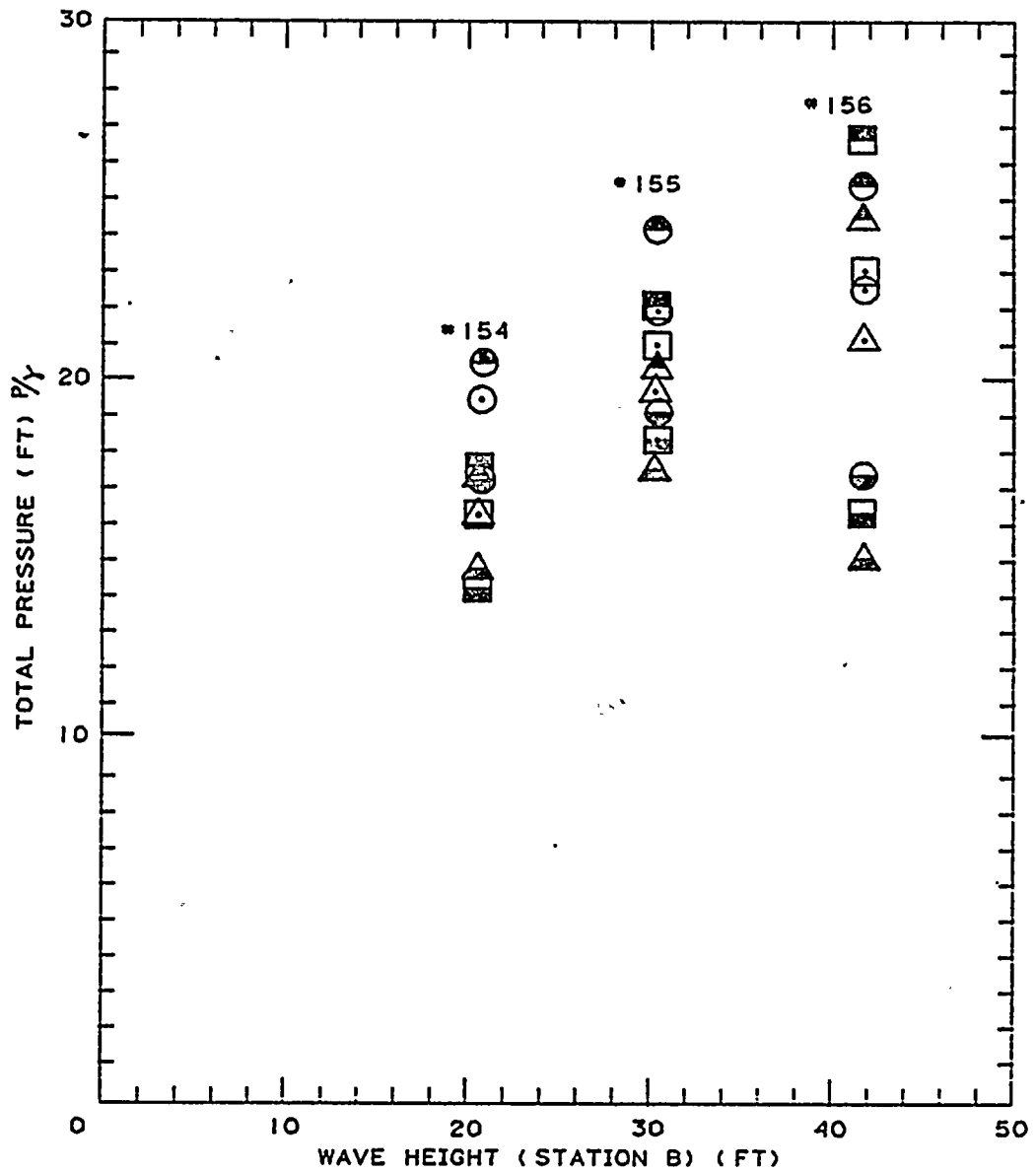


FIGURE 35 - Variation of Total Pressure With Offshore Wave Height:
+7.5 ft MLLW, T=16 sec, 225° Az, Centerline

	PT-1	PT-2	PT-3
MAX.	●	■	▲
AVG.	○	□	△
MIN.	◐	◑	◒

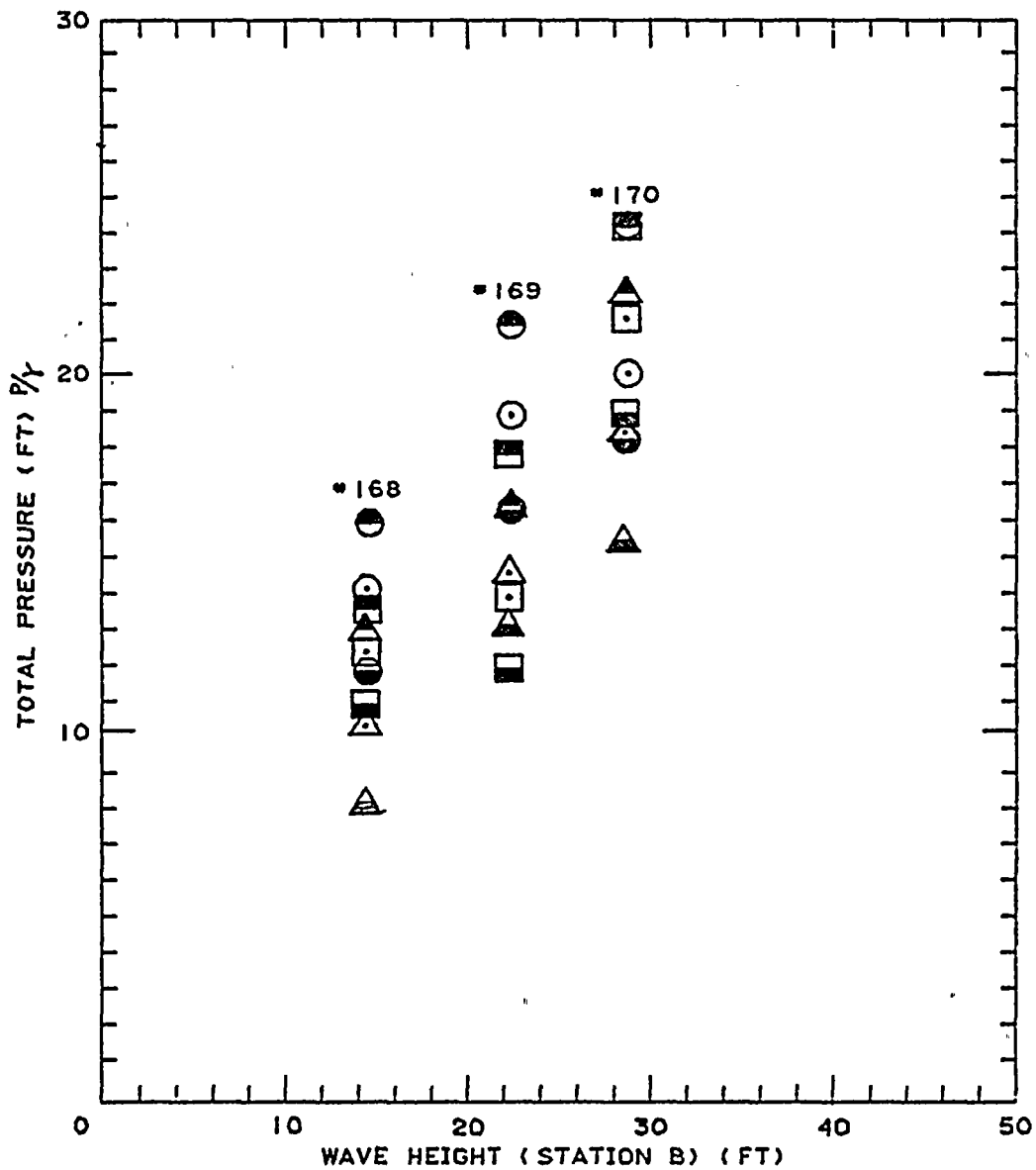


FIGURE 36 - Variation of Total Pressure With Offshore Wave Height:
+7.5 ft MLLW, T=16 sec, 225°Az, West Corner

In all cases shown in Figures 31 through 36 the maximum total pressures are relatively independent of direction and location, and the longer period waves result in somewhat greater pressures. The maximum total pressure measured was 27 ft which is considerably less than the maximum pressure measured at the same elevation with a still water level of +17 ft MLLW. Exploratory experiments conducted with irregular waves at this reduced still water level (+7.5 ft MLLW) generated dynamic pressures which when combined with the hydrostatic pressures also were less than those measured at a water level of +17 ft MLLW and reported in Section 3.1.1.

3.2 Wave-Induced Loads on the Auxiliary Saltwater Pump Forebays

As discussed in Section 2, the intake model used earlier was rebuilt to accurately model the forebays of the four auxiliary saltwater pumps (see Figures 9a and 10). The pressure cells which were used in the curtain wall experiments were mounted in the ceilings of the pump forebays to measure pressures during various still water levels and wave conditions. In certain experiments, which will be defined, pressures were measured only on the floors of the Auxiliary Saltwater Pump rooms, while in others, pressures were measured simultaneously on the floors of the ASWP and the Main Cooling Water pump rooms.

The conditions used for testing essentially were the same as for the curtain wall pressures, i.e., water levels of +17 ft MLLW and +7.5 ft MLLW, with the additional water level of -2 ft MLLW corresponding to an extreme low tide also tested. The -2 ft MLLW tide level was investigated because it permits an air space between the water surface and the ceiling of the ASWP forebay (at -1 ft MLLW) which increases the potential for high pressures associated with wave impacts. The east and west breakwaters were modelled as degraded to a crest elevation of MLLW for these experiments.

There were three different conditions that were investigated during this phase of the study. The first condition, which is denoted as "unvented", refers to the fact that the forebay is airtight with no possibility of flow upwards through openings in the floor of the Main Cooling Water Pump room or the ASWP room. However, manholes are located in the floor of this portion of the chamber, so it was considered that leakage possibility could take place. Therefore, a series of exploratory experiments were conducted to represent the case of full ventilation. In the model vertical standpipes of 3/8 in. diameter were mounted to the floor of the main cooling water pump room and extended up through the top of the deck of the cooling water intake structure. This represents an opening in the prototype with a diameter of about 17 in., and is defined herein as "fully" vented. The exploratory experiments showed that high pressures could exist during certain water surface elevation-wave condition combinations. For this reason, it was determined that corrective measures would be necessary in the prototype to eliminate the possibility of the "fully vented" condition and therefore that leakage through a more modest gap should be considered in further experiments. Hence, a series of experiments were conducted with a third configuration which is denoted here as "moderately" vented. In the model each of the 3/8 in. diameter standpipes was capped by an orifice plate with a hole of 1/8 in. diameter which corresponds to an opening in the prototype of 5.6 in. diameter. The area represented by this hole (about 25 sq. in.) was considered to represent a conservative upper limit of leakage in the prototype.

Unless otherwise specified, the "vented" case refers to the moderately vented condition.

3.2.1 Pressures on the ceiling of the ASWP forebays for the condition of: tsunami, high tide, meteorological tide, and 1981⁺ storm; (+17 ft MLLW)

The 1981⁺ storm approaching from the south (203°) was used with a water surface elevation of +17 ft MLLW, i.e., the same experimental conditions were used as were used for the investigation of curtain wall pressures, with the crests of the east and the west breakwaters degraded to MLLW. Cumulative frequency distributions of the dynamic pressure are presented in Figures 37 and 38 for the unvented and the vented cases, respectively. The ordinate is the ratio of the pressure to the significant pressure (defined, as before, as the average of the highest one-third of the pressures measured.) The pressures presented were measured at Positions c and either e or f in Forebay III; these locations are shown in Figure 9b.

In both cases, if it is reasoned that the frequency distribution approximately follows a Rayleigh distribution, the range of the probable maximum pressure, including hydrostatic pressure, would be between 65 ft (vented moderate) and 71 ft (unvented) of water based on a ratio of maximum probable pressure to significant pressure of 2.5. If, on the other hand, the pressures are considered to be more closely defined by a normal distribution, the ratio of the probable maximum pressure to the significant pressure is about 3.7 (see Ochi, 1973). The measured significant pressures yield a range of probable maximum total pressure (probable maximum dynamic pressure plus hydrostatic) for a postulated normal distribution of between 88 ft of sea water and 97 ft of sea water.

These frequency distributions indicate that the pressure process may be somewhat different for the forebays compared to that for the curtain wall. For the curtain wall, since the frequency distribution of pressures

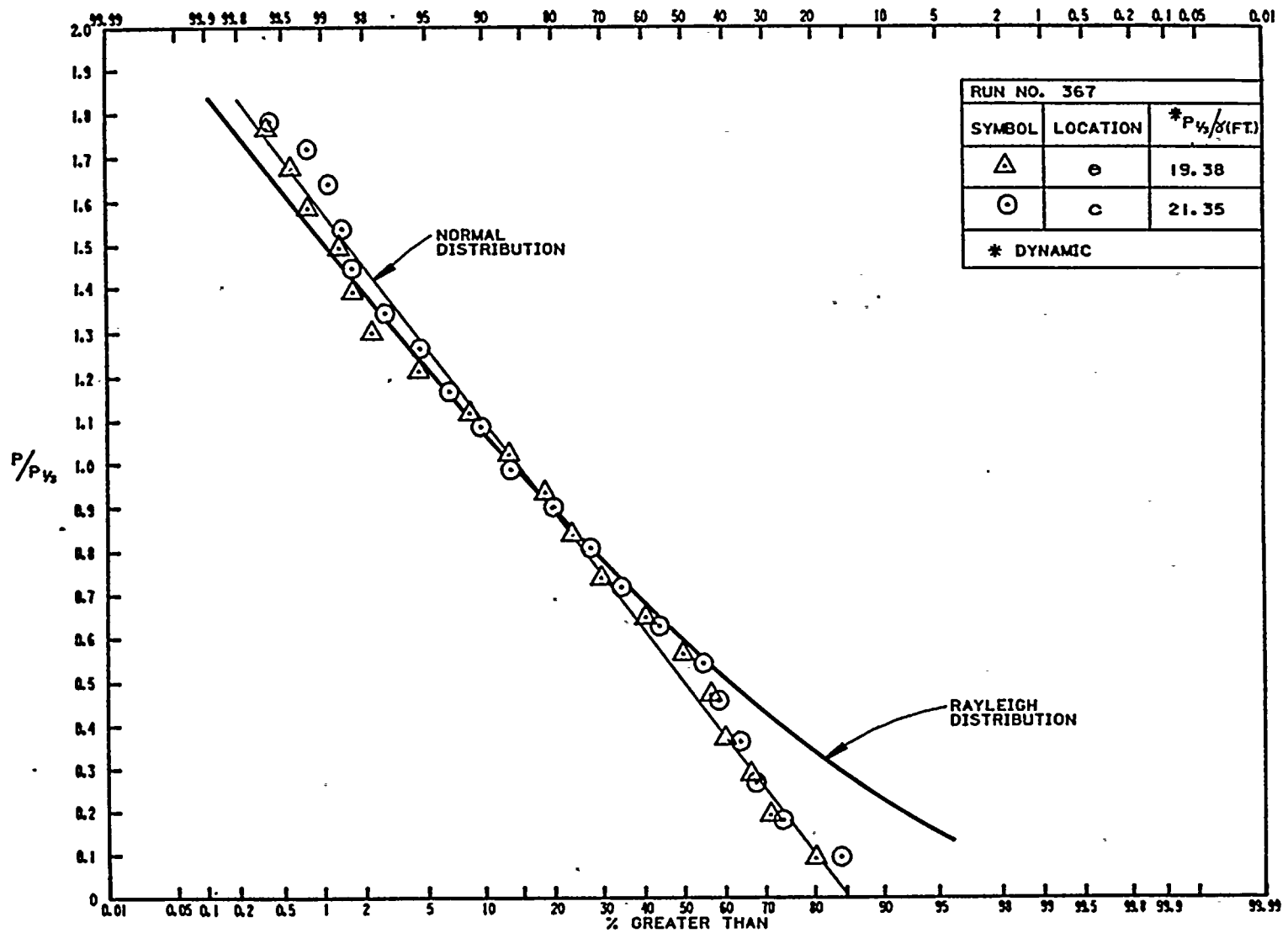


FIGURE 37 Normalized Pressure Frequency Distribution on Forebay Ceiling:
1981⁺ storm, +17 ft. MLLW, 203°Az, unvented

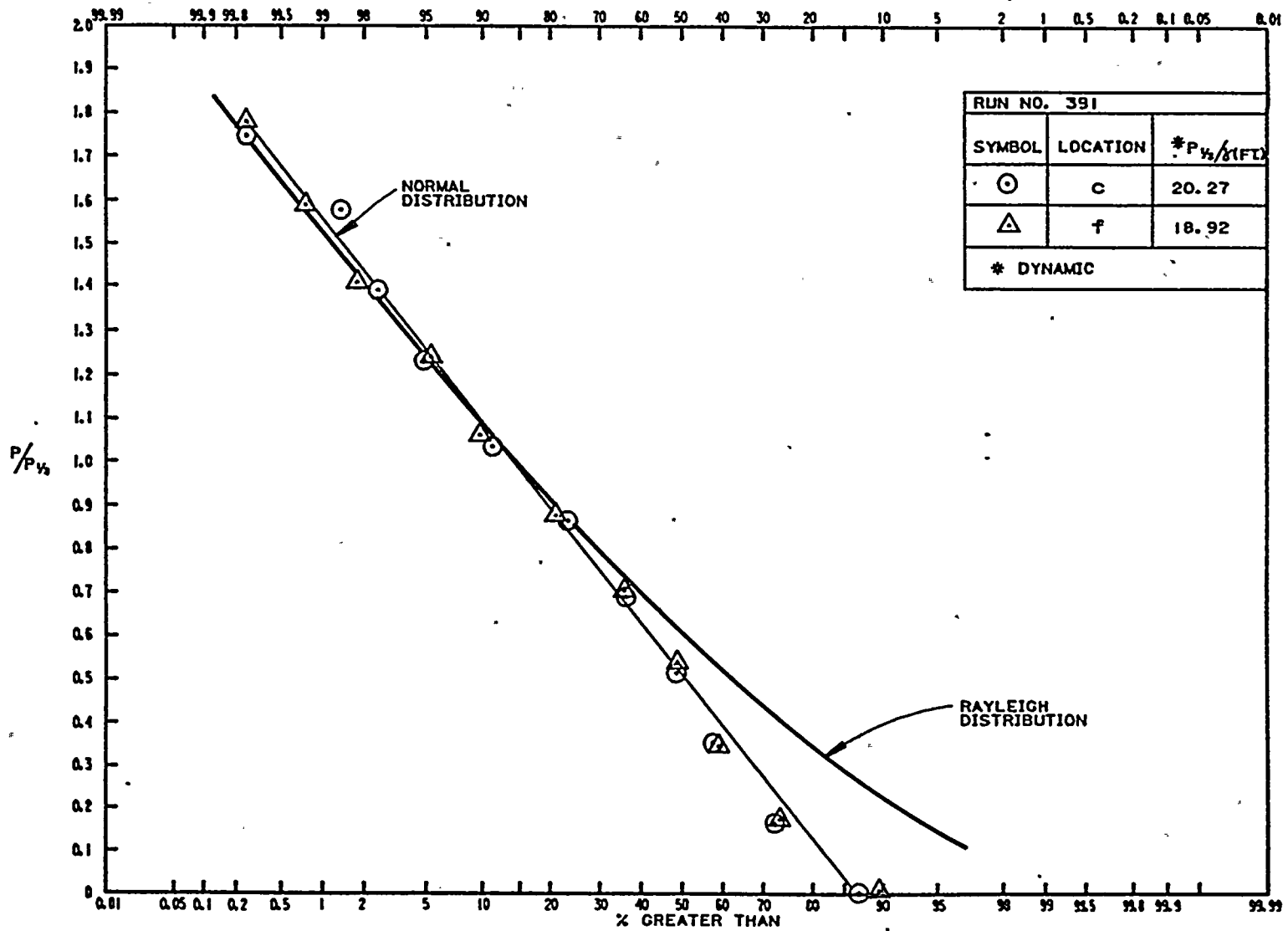


FIGURE 38 Normalized Pressure Frequency Distribution on Forebay Ceiling:
1981⁺ storm, +17 ft. MLLW, 203°Az, vented (Moderate)

tends to follow a Rayleigh distribution, the spectrum of pressures would be more narrow-banded, i.e., similar to that of the waves. However, for the interior pressures the spectrum appears to embody more frequencies, i.e., a broader band spectrum, because the frequency distribution is more similar to a normal distribution. (The interested reader is directed to Sarpkaya and Isaacson (1981) for a discussion of this.) This may be due to the effect on the interior pressures of splash-up and the overtopping of the intake structure. It will be shown in the next section that the pressures in different forebays are approximately the same.

3.2.2 Pressures on the ceiling of the ASWP forebays for the condition of: maximum tide and limit waves (+7.5 ft MLLW)

In this section the results of pressure measurements on the ceiling of the ASWP forebays for the case of a water surface elevation of +7.5 ft MLLW are presented. As before, the testing procedure was to use regular waves with periods of 12 sec and 16 sec approaching from the south (203°); these periods bracket the periods of the peak energy of extreme storms which have been hindcast for the region and were defined in Table 1; the limit wave concept was used to define the wave heights (see Lillevang, Raichlen, and Cox, 1982), and the east and west breakwaters were degraded to crest elevations of MLLW. In Figures 39 to 42 data are presented for the variation of the total pressure, i.e., the dynamic plus the hydrostatic pressure normalized by the specific weight of sea water, existing at several positions on the ceiling of the forebay as a function of the offshore wave height at Station B which is located near the wave generator. Experimental results from both unvented and

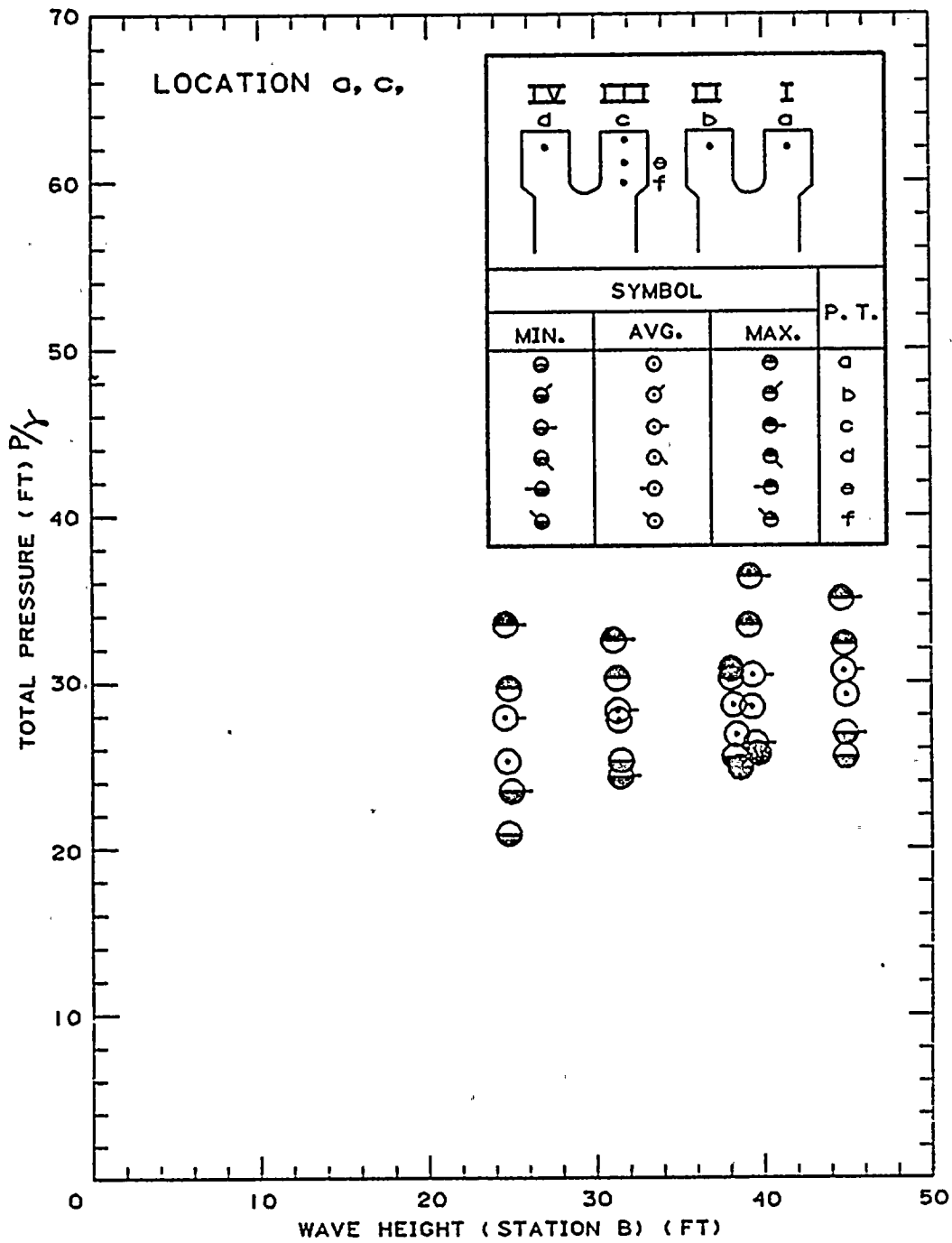


FIGURE 39 Total Pressure on Forebay Ceiling vs. Wave Height: +7.5 ft MLLW, T=12 sec, 203°Az, Unvented

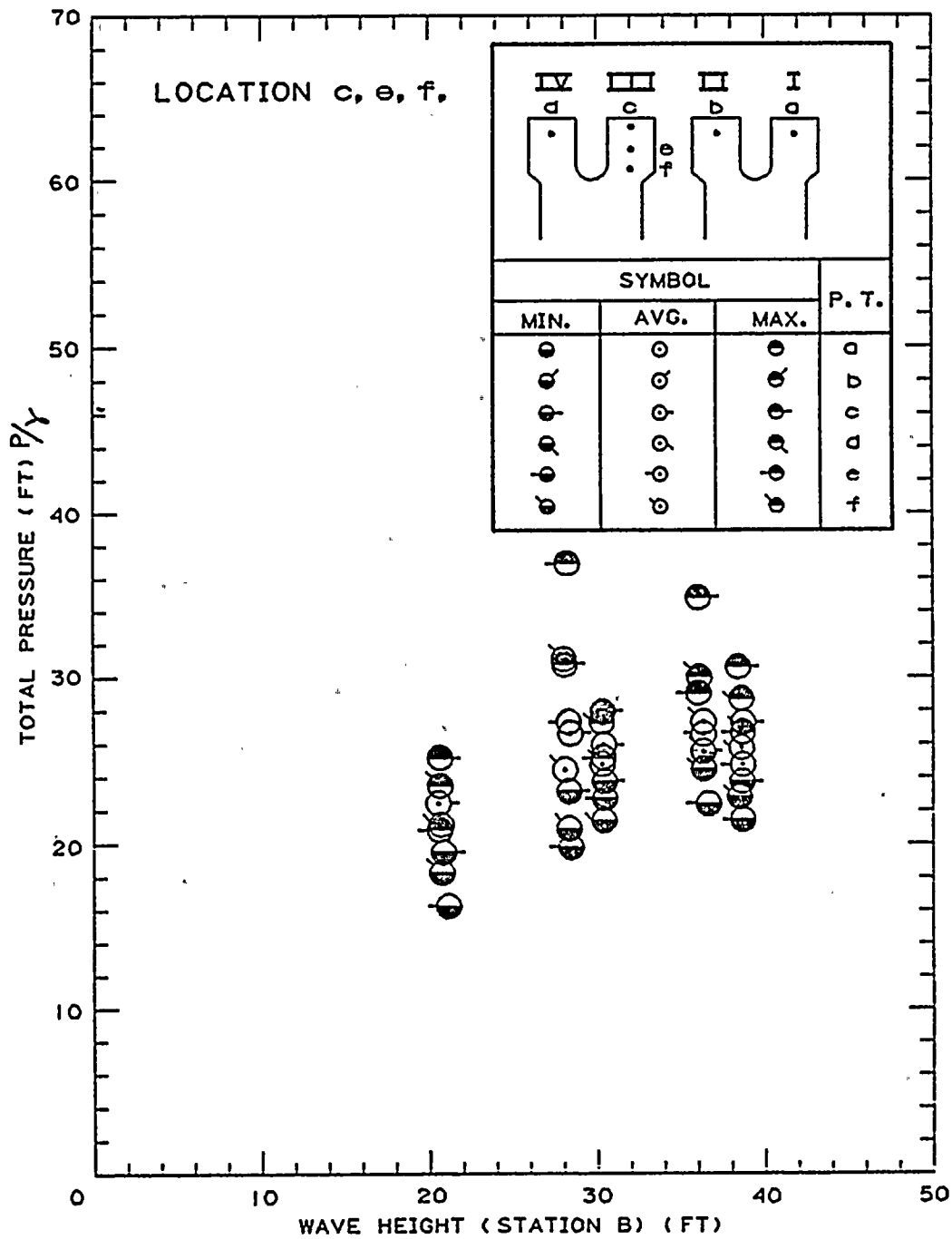


FIGURE 40 Total Pressure on Forebay Ceiling vs. Wave Height: +7.5 ft. MLLW, T=12 sec, 203°Az, Vented (Moderate)

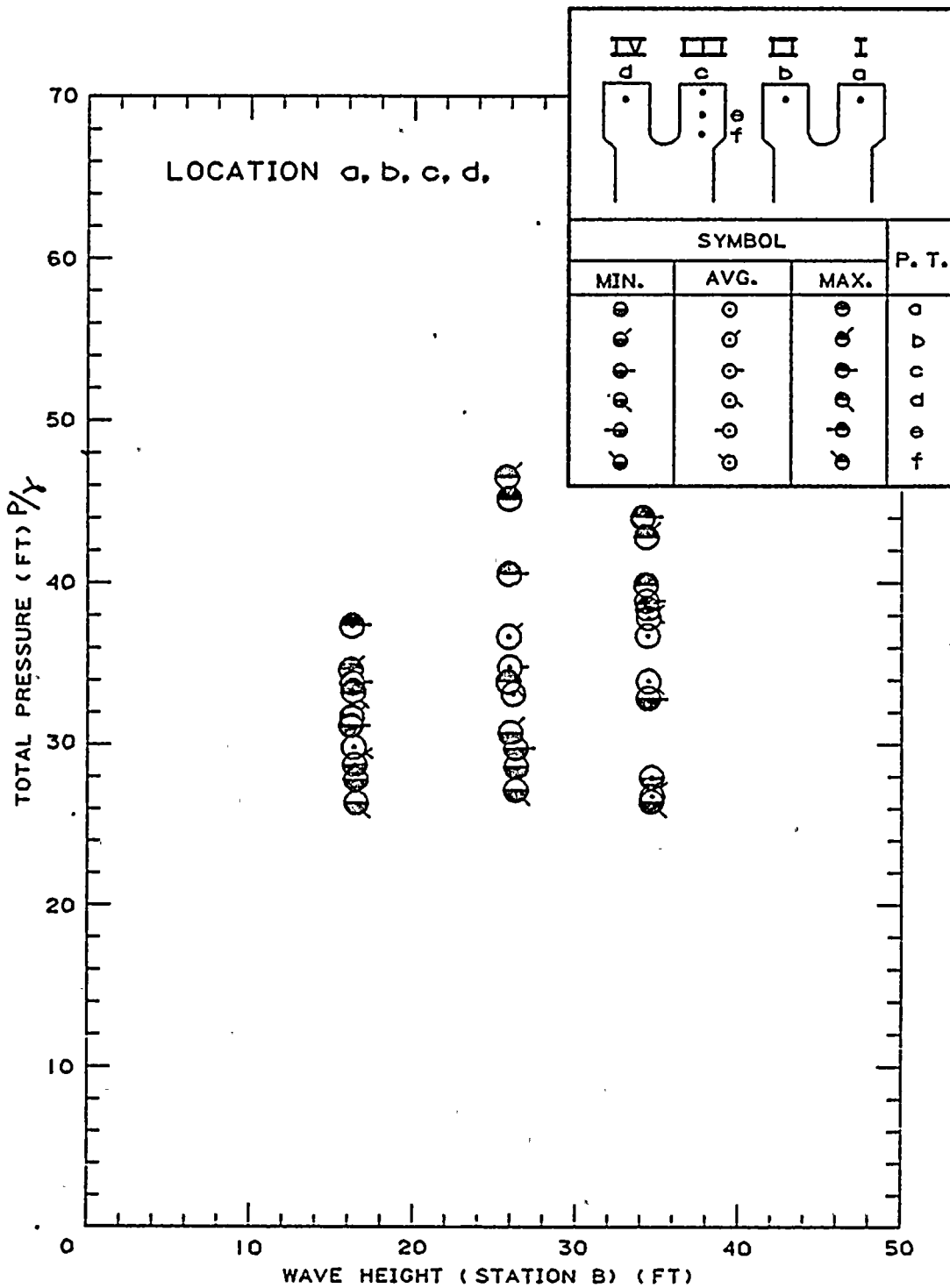


FIGURE 41 Total Pressure on Forebay Ceiling vs. Wave Height: +7.5 ft MLLW, T=16 sec, 203°Az, Unvented

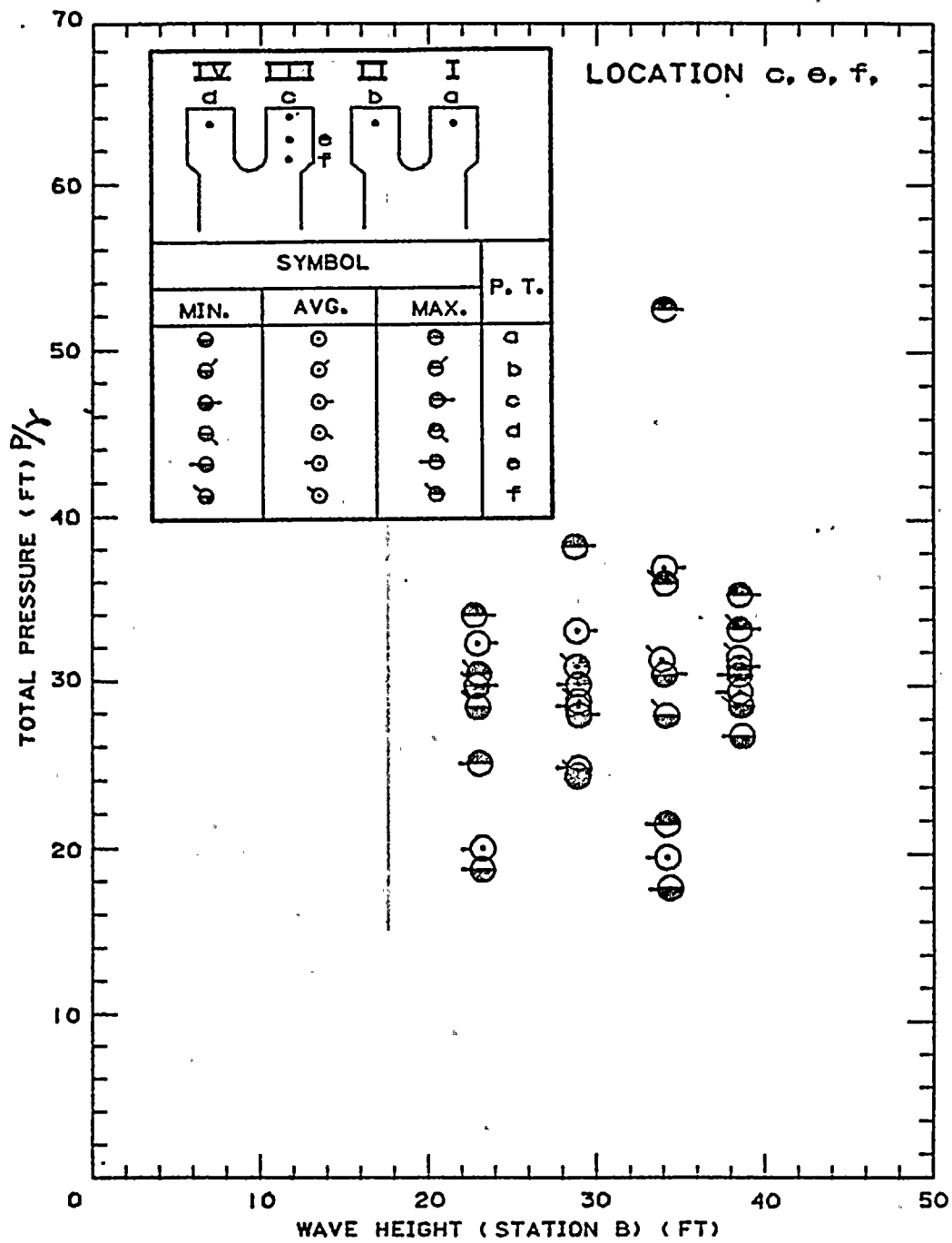


FIGURE 42 Total Pressure on Forebay Ceiling vs. Wave Height: +7.5 ft MLLW, T=16 sec, 203°Az, Vented (Moderate)

moderately vented forebays are presented. Shown are the maximum and minimum pressures measured and the average of pressures occurring for six to nine waves.

Pressures measured at locations a and c which are near the backwall of the Forebay I and III for the unvented chamber for $T=12$ sec and presented in Figure 39 generally depict the type of conditions that were seen in all experiments. These conditions are that the pressures are slightly greater in Forebay III than they are in I, probably due to the three-dimensional nature of the waves acting on the front face of the structure, but in both locations the total pressures are less than about 36 ft of water. The difference in maximum pressures between Location a and c is between 9% and 14% so the pressures in Forebays I and II appear quite similar. For the vented case, pressures are shown in Figure 40 measured in Forebay III at three locations along the ceiling: locations c, e and f. Comparing the pressures measured in the unvented case to those measured in the vented case, it is seen that at location c the pressures in the former are slightly greater than those in the latter. At locations e and f the pressures are essentially the same as those at location c.

The variations of pressures with offshore wave height for the 16 sec waves are presented in Figures 41 and 42. In Figure 41, for the unvented case, the variation with incident wave height of pressures at the back of each of the four forebays is shown, and the pressures are essentially the same for each chamber and slightly greater than the pressures measured for the 12 sec waves. This is consistent with other pressure measurements which indicate that pressures are somewhat larger for the waves with larger periods. With respect to the shorter waves, as shown

in Figure 42 for the vented case, the pressures at the back of Forebay III are slightly less than those for the unvented case; the pressures at locations e and f in Forebay III are about the same as those at the backwall, i.e., location c.

3.2.3 Pressures on the ceiling of the forebay for the condition of: minimum tide and limit waves, and minimum tide and 1981⁺ storm (-2 ft MLLW)

As mentioned earlier, since the elevation of the ceiling of the forebay is -1 ft MLLW and the minimum tide is -2 ft MLLW, it was necessary to conduct pressure measurements for the case of the extreme low tide. Under those conditions large pressures could occur due to the air-water interface in the pump forebays.

In Figures 43 and 44 similar cases for the unvented chamber and the vented chamber for 12 sec regular waves are presented. In Figure 43 the total pressures for the unvented chamber measured at the back of Forebays I, II, III and IV (locations a, b, c, and d) are presented indicating no substantial differences among the chambers and relatively low total pressures. (Recall this is for a case with air at the top of the chamber due to the low water level but no possibility for this air to move in and out of the forebay since there are no openings in the ceiling.) When the chamber is moderately vented, pressures as shown in Fig. 44 occur. The pressures for the moderately vented case are larger than those for the unvented case due to the fact that air is now allowed to flow in-and-out through openings in the ceilings of the forebays. It is noted that for the vented forebay the pressure measurements were made in Forebay III along the centerline of the ceiling. It is reasonable to assume that other forebays would reveal the

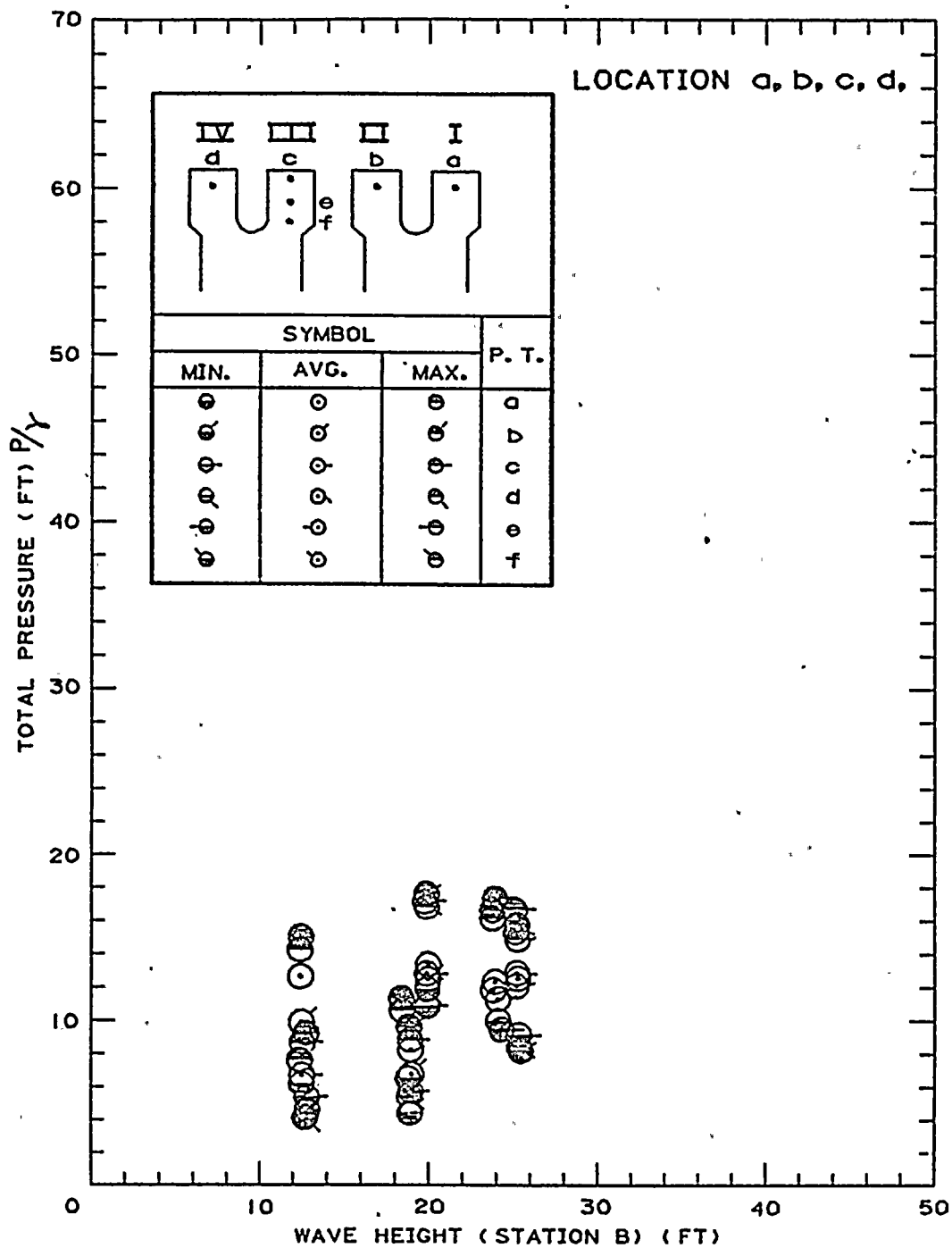


FIGURE 43 Total Pressure on Forebay Ceiling vs. Wave Height: -2 ft MLLW, T=12 sec, 203°Az, Unvented

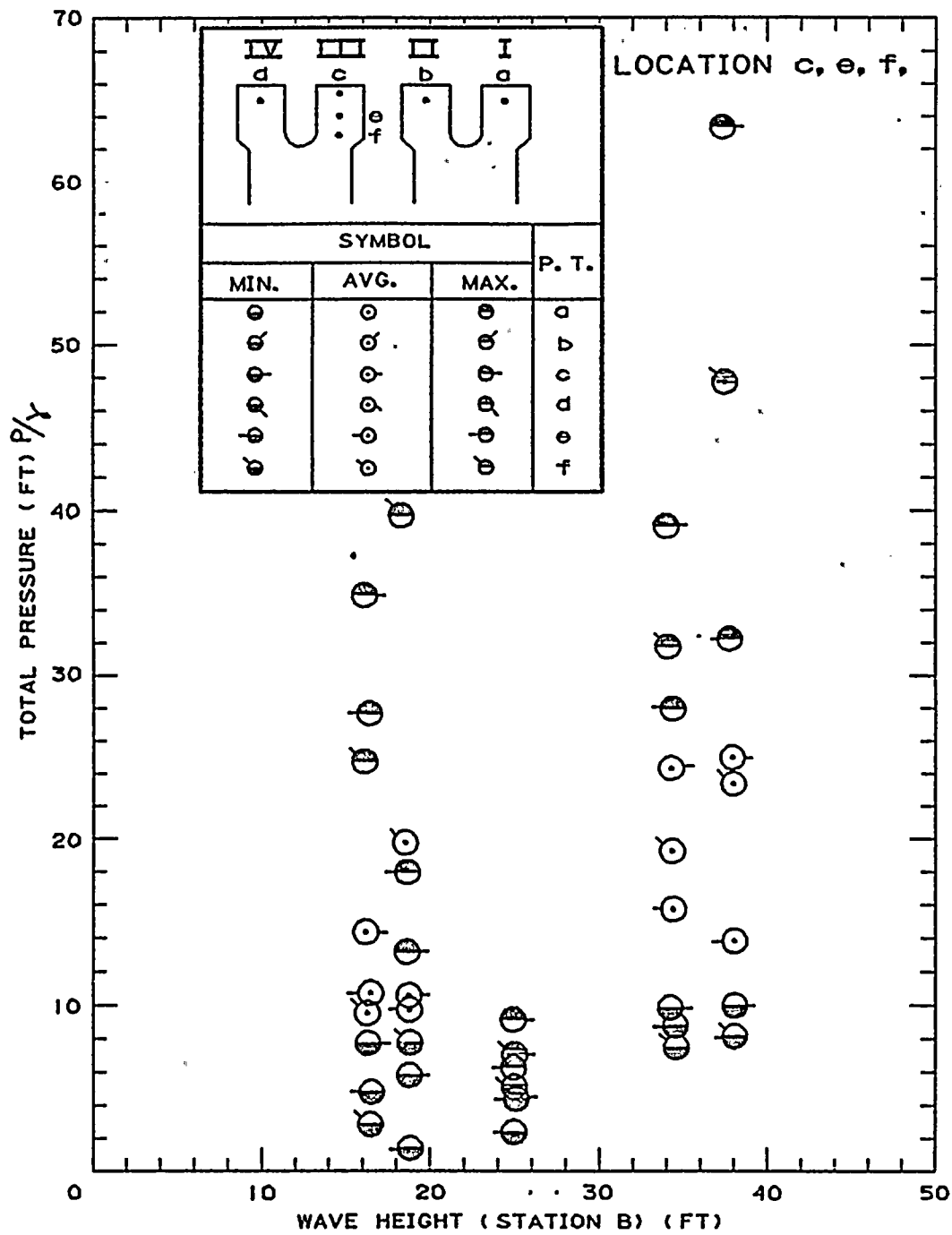


FIGURE 44 Total Pressure on Forebay Ceiling vs. Wave Height: -2 ft MLLW, T=12 sec, 203°Az, Vented (Moderate)

same type of variation, since the variation in pressures among the forebays for the same conditions is small, e.g., see Figure 43. The peak pressure measured during these tests was 64 ft.

In Figures 45 and 46 data are presented on the pressures for the unvented and vented case for periodic 16 sec waves. As before, the pressures for the 16 sec waves are somewhat greater than those for the 12 sec waves for the same physical conditions. For this case only pressures in Forebay III are reported, and the vented case yields somewhat larger pressures for the same wave height compared to the unvented case.

Exploratory experiments were conducted with irregular storm waves corresponding to the 1981⁺ storm. Since this is an unusual case with a minimum tide (-2 ft MLLW) and the consequence of an air-water interface near the ceiling of the auxiliary saltwater pump room, detailed results which correspond to the irregular waves will be presented here. In Figure 47 frequency distributions of normalized pressures are presented for the three cases investigated: unvented, moderately vented (5.6 in. diameter), and fully vented (17 in. diameter). The significant dynamic pressure, $p_{1/3}$, was 15.5 ft, 19.7 ft, and 68.6 ft, respectively, for these three cases. The pressures appear to be more normally than Rayleigh distributed with a larger percentage of higher pressures, for a given number of occurrences, as the leakage increases, i.e., the vent size increases. This emphasizes the need to minimize the leakage in the ceiling of the chamber, as the leakage provides a means for the water to develop a vertical velocity in the chamber and produce large pressures. If the leakage is "moderate" or less, i.e., a leakage opening equivalent to 5.6 in. diameter or less, assuming a normal frequency distribution the probable maximum pressure would be less than about 73 ft. For the unvented case the probable maximum pressure would be about 57 ft. Since these are

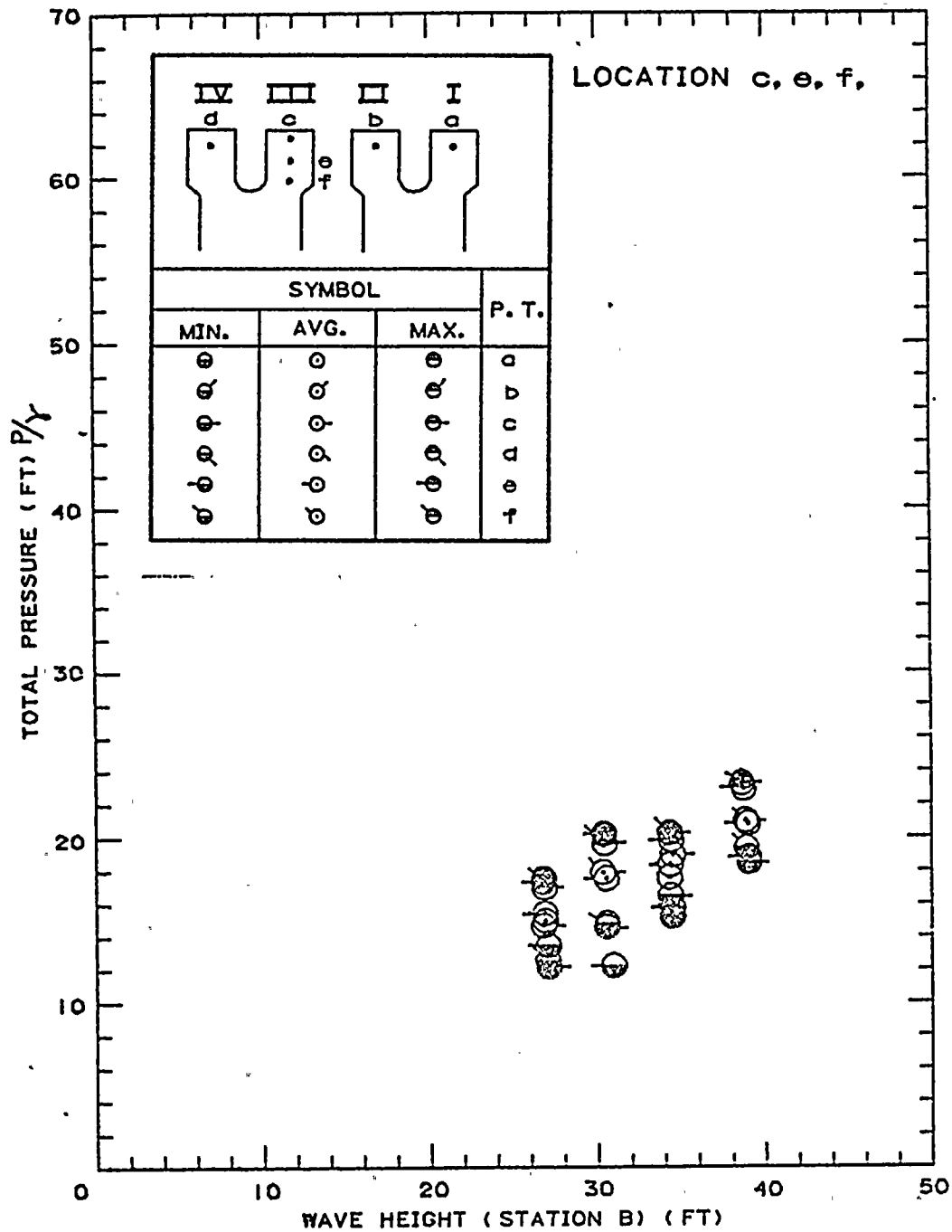


FIGURE 45 Total Pressure on Forebay Ceiling vs. Wave Height: -2 ft. MLLW, T=16 sec, 203°Az, Unvented

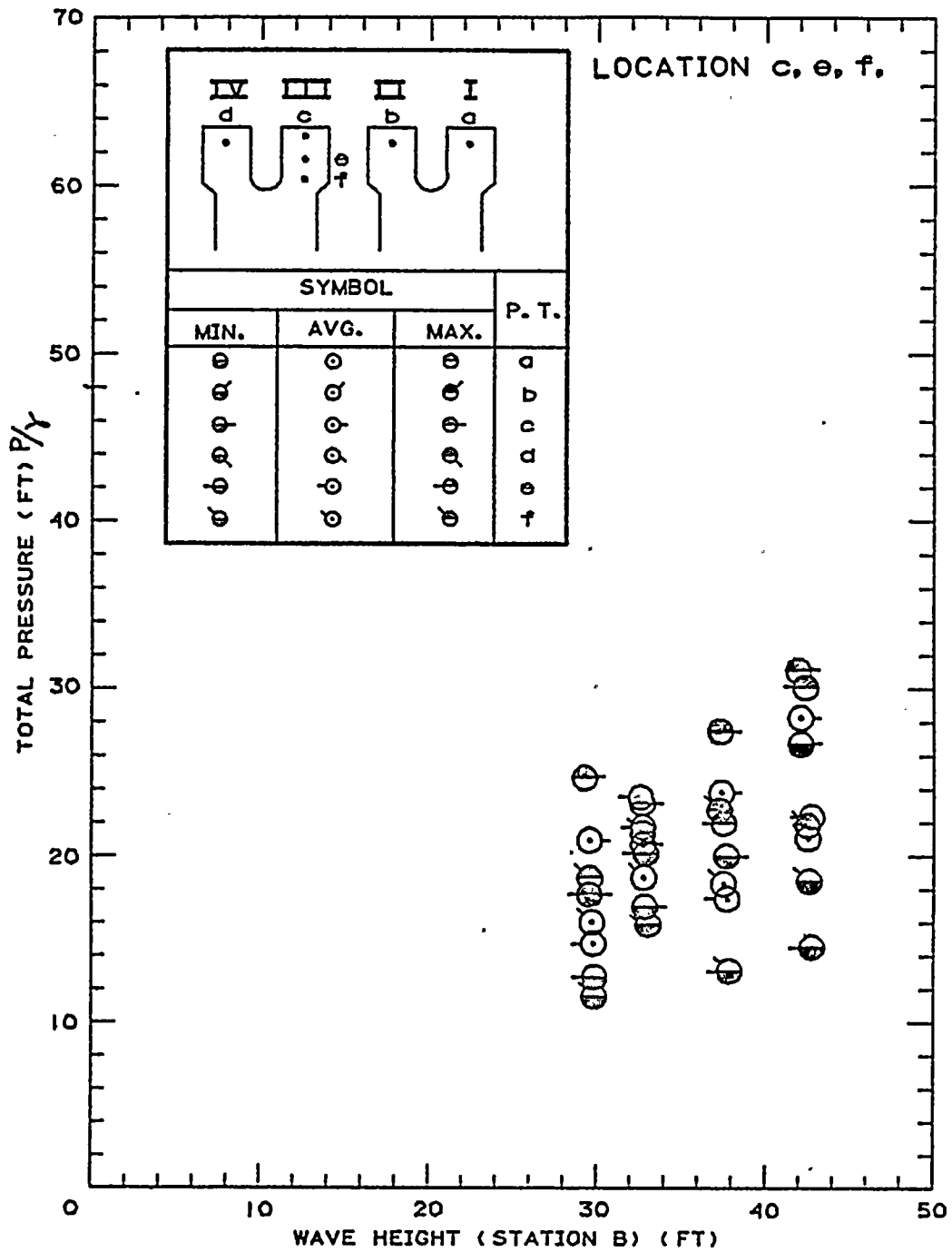


FIGURE 46 Total Pressure on Forebay Ceiling vs. Wave Height: -2 ft MLLW, T=16 sec, 203°Az, Vented (Moderate)

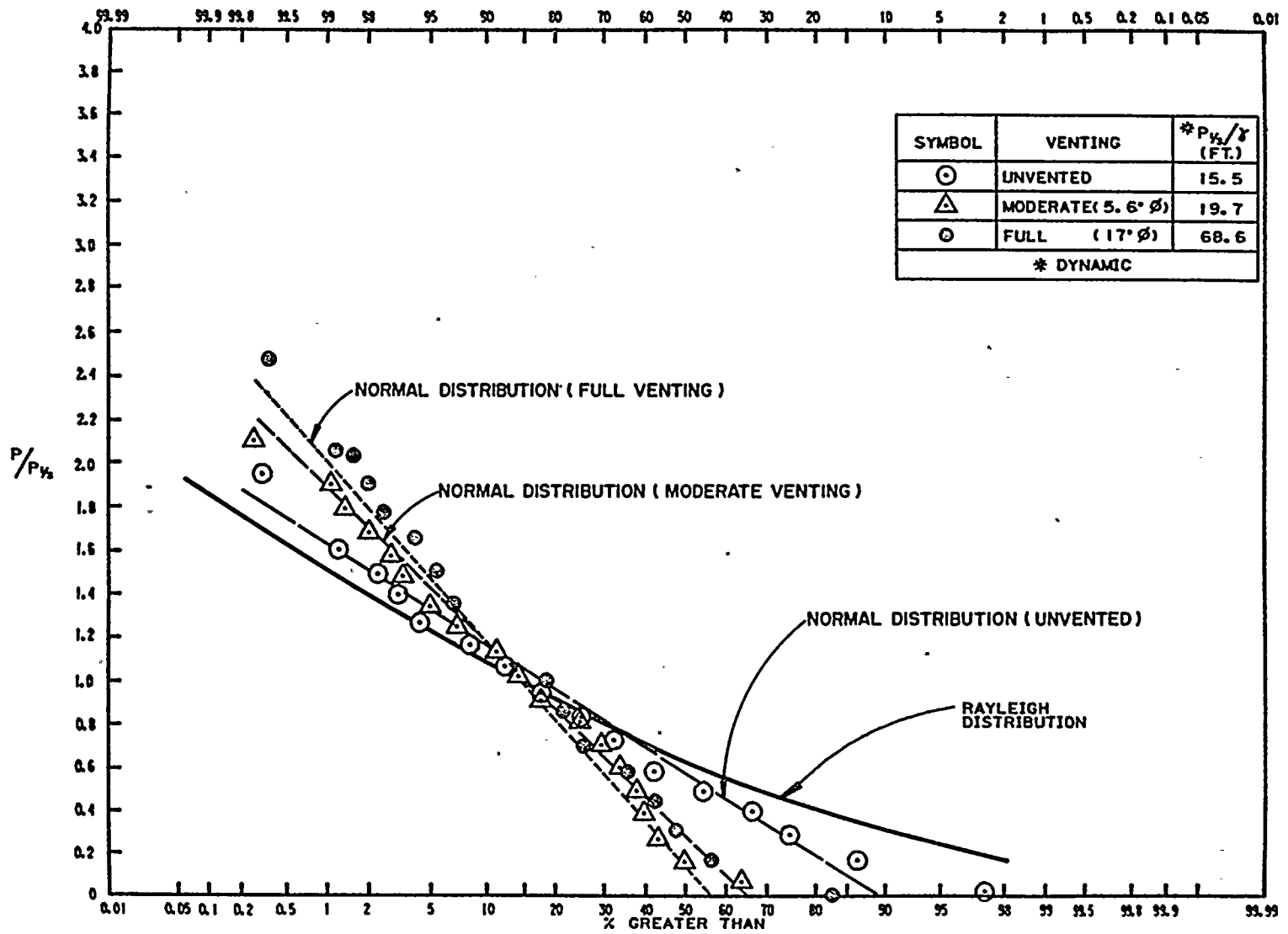


FIGURE 47 Normalized Pressure Frequency Distribution on Forebay Ceiling:
1981⁺ storm, -2 ft MLLW, 203°Az, Unvented, Vented (Moderate), Vented
(Full)

considerably less than the probable maximum pressure of between 88 ft and 97 ft as determined from measurements for the condition of +17 ft MLLW and the 1981⁺ storm the conditions at +17 ft MLLW would still control the loading of the ceiling of the ASWP forebay.

3.3 Velocities at the entrance to the auxiliary saltwater pump forebays

As discussed earlier, a miniature propeller meter was used to measure velocities at the entrance to the auxiliary saltwater pump forebay. Measurements were made in different forebay entrances and at different elevations in the forebay; at no time were measured velocities greater than about 3.9 fps. The data available will be presented in a manner similar to that of the pressure measurements.

3.3.1 Velocities at the entrance to the ASWP forebays for the condition of: tsunami, high tide, meteorological tide, and 1981⁺ storm (+17 ft MLLW).

As before, the 1981⁺ storm approaching from the south (203°) was used as a conservative event in place of the mean annual storm event. A cumulative frequency distribution of these velocities is presented in Figure 48 for the unvented case where the ordinate is the ratio of the velocity measured to the average of the highest one-third of the velocities in the record (the "significant" velocity) and the abscissa is the percent of values which exceed that velocity. (It will be demonstrated later for periodic waves that the unvented case results in somewhat greater velocities than the vented case; hence only results from the unvented case are presented here.) Presented in Figure 48 are the Rayleigh distribution and a normal distribution. It is noted that some values are less than the manufacturer suggested threshold value of 0.7 fps

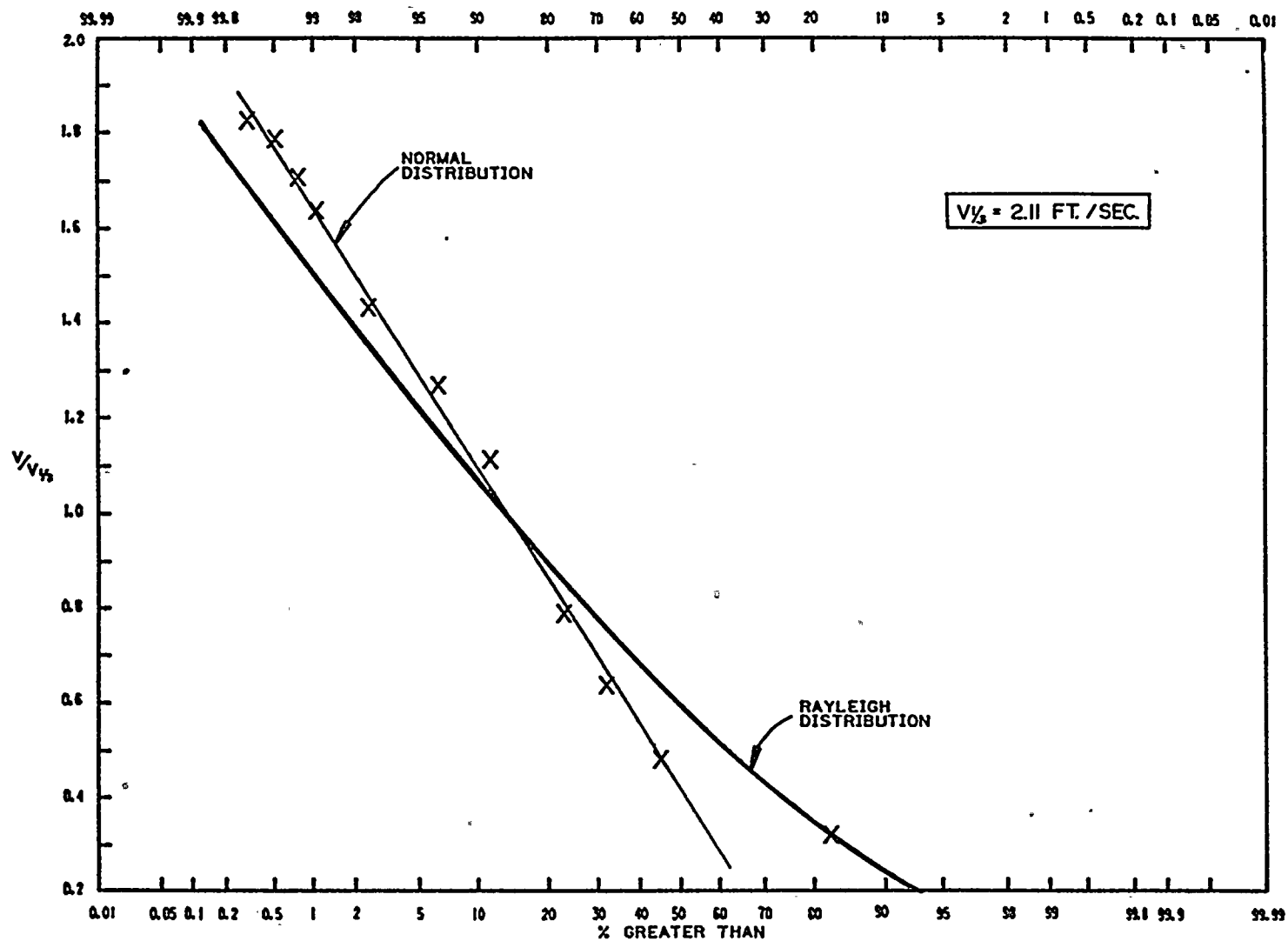
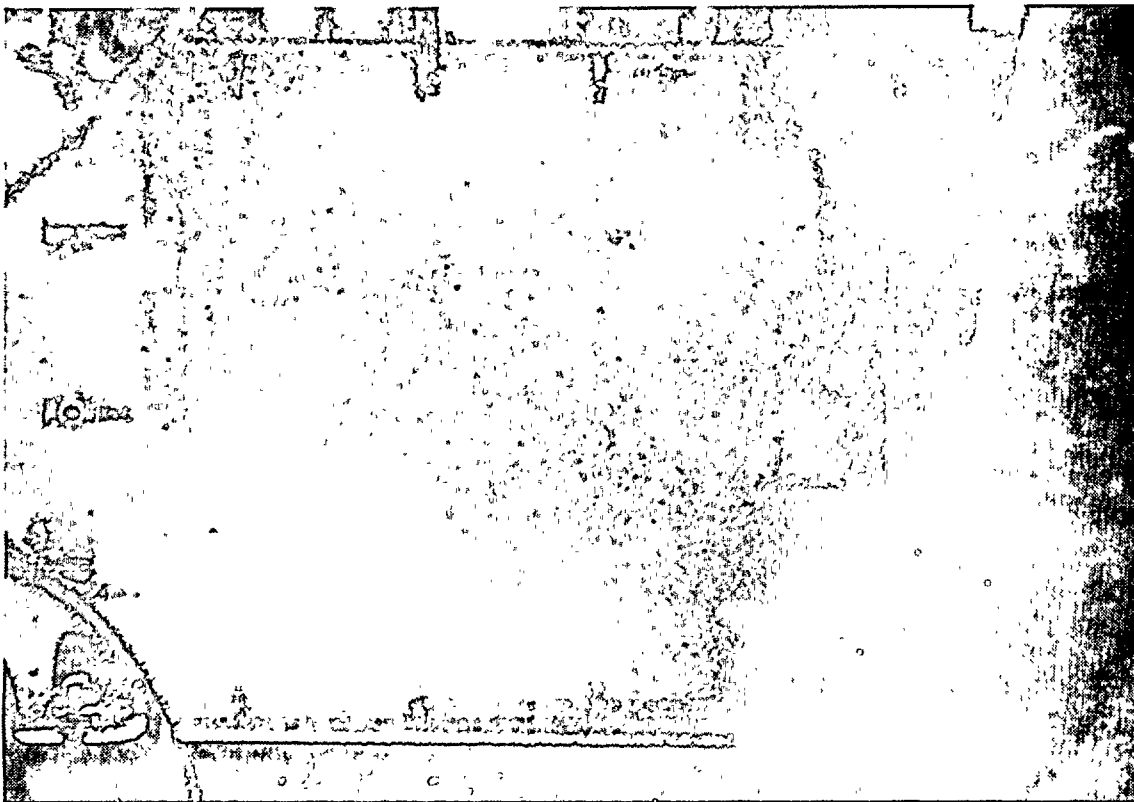


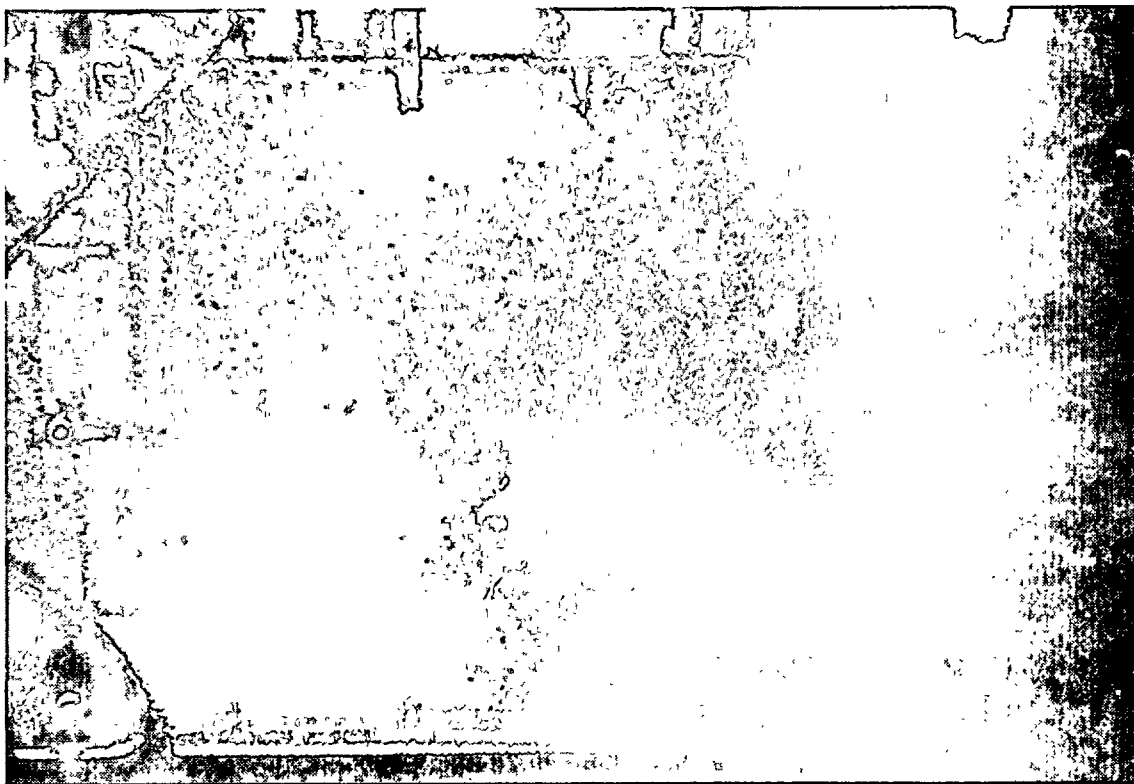
FIGURE 48 Normalized Velocity Frequency Distribution at Entrance to ASWP.
Forebay: 1981⁺ storm, +17 ft MLLW, 203°Az, Unvented

(prototype) and the threshold indicated in the calibration of about 1.3 fps (prototype). The small recorded voltages indicate the propeller of the velocity meter was rotating indicative of the existence of a velocity but of questionable magnitude. Nevertheless, these velocities are included in the data from which Figure 48 was constructed as they represent the presence of small velocities in the population sampled. Due to the lower two points which represent about 20% of the data, these data may follow a frequency distribution between a Rayleigh distribution and a normal distribution with a significant velocity of 2.11 fps. If the ratio of the probable maximum velocity to the significant velocity is taken as 2.5 for a Rayleigh distribution and 3.7 for a normal distribution, the probable maximum velocity at the entrance would be between 5.3 fps and 7.8 fps for this storm. It should be emphasized and recalled that this storm significantly exceeds the intensity of the mean annual storm which NRC specified as occurring simultaneously with the water surface elevation of +17 ft MLLW. This water level can only occur for several minutes. Based on an occurrence of about 3 min there would be a population of only about 12 waves compared to about 2400 waves for a 10 hr exposure; thus, the probable maximum velocity would be significantly reduced even for this extreme storm. For a Rayleigh distribution the probable maximum velocity would be about 4.0 fps and for a normal distribution it would be about 5.7 fps for this reduced number of events.

In Figure 49 two photographs of a side view of the forebays are presented; the pump columns can be seen faintly in these photographs near the back of the forebay. The condition for these photographs was a water surface elevation of +17 ft MLLW with waves from the 1981⁺ storm from 203° and with the forebays unvented. The upper photograph (a) shows



(a)



(b)

FIGURE 49 Sequential Photographs of: (a) Dye injected at entrance to forebay, (b) Dye diffused through forebay, 5 min (prototype) later

dye just introduced at the entrance to the forebay where it remains in a relatively compact dye patch. In the lower photograph (b) taken 5 min (prototype time) later the dye has diffused over nearly two-thirds of the height of the chamber without an indication of stronger velocity filaments in one area compared to another. This is typical of visual observations made at the time of all experiments; hence, the velocities within the chamber must be significantly less than those measured at the entrance.

It has been estimated that, assuming a sliding friction factor of 0.3 between a concrete missile resting on the floor of the chamber and the floor itself and a drag coefficient of unity, a velocity of about 6 fps would be necessary to just move a concrete missile with a dimension in the direction of flow of about 1 ft. Therefore, a velocity much greater than 6 fps would be necessary to entrain such a missile in the flow to an elevation where it could travel about 30 ft and strike the auxiliary saltwater pump column.

3.3.2 Velocities at the entrance to the ASWP forebays for the condition of: maximum tide (and minimum tide) and limit waves (+7.5 ft MLLW and -2 ft MLLW)

The condition for the maximum credible wave event superimposed on the maximum tide (+7.5 ft MLLW) and minimum tide (-2 ft MLLW) with the degraded breakwater (crest at MLLW) was treated using limit periodic waves. The results for the velocities as a function of the incident wave height determined near the wave machines are presented in Figures 50 through 54 for various conditions.

In Figures 50 and 51 the results for the maximum tide (+7.5 ft MLLW) are presented for the unvented case in the form of maximum velocities and mean velocities. The former is for 12 sec waves and the latter is for

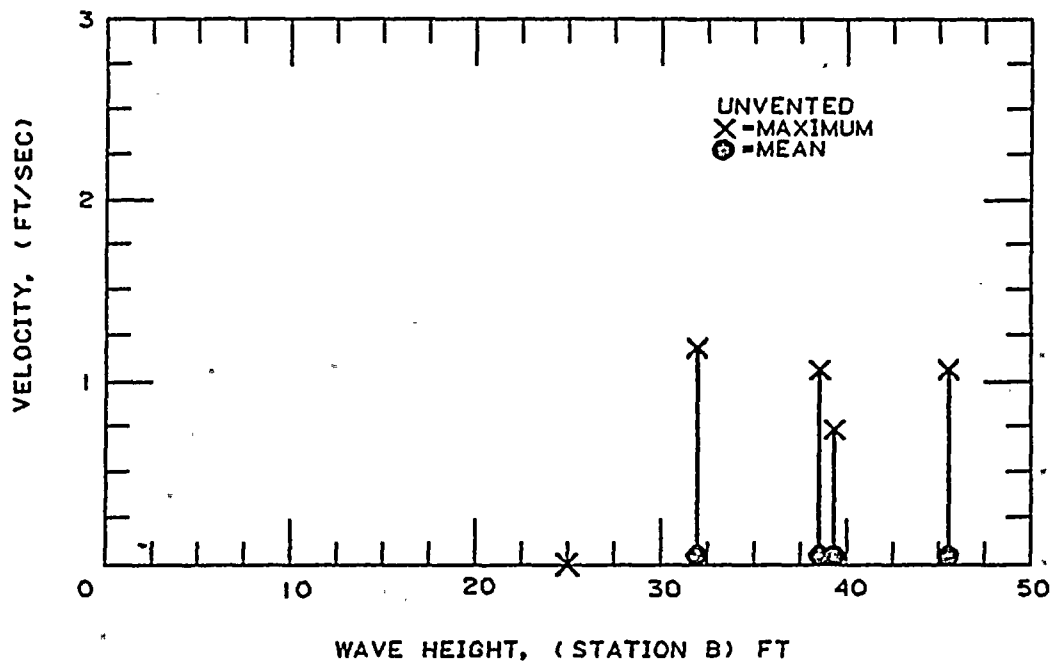


FIGURE 50 Velocity at Entrance to ASWP Forebay: +7.5 ft. MLLW, T=12 sec, 203°Az, Unvented

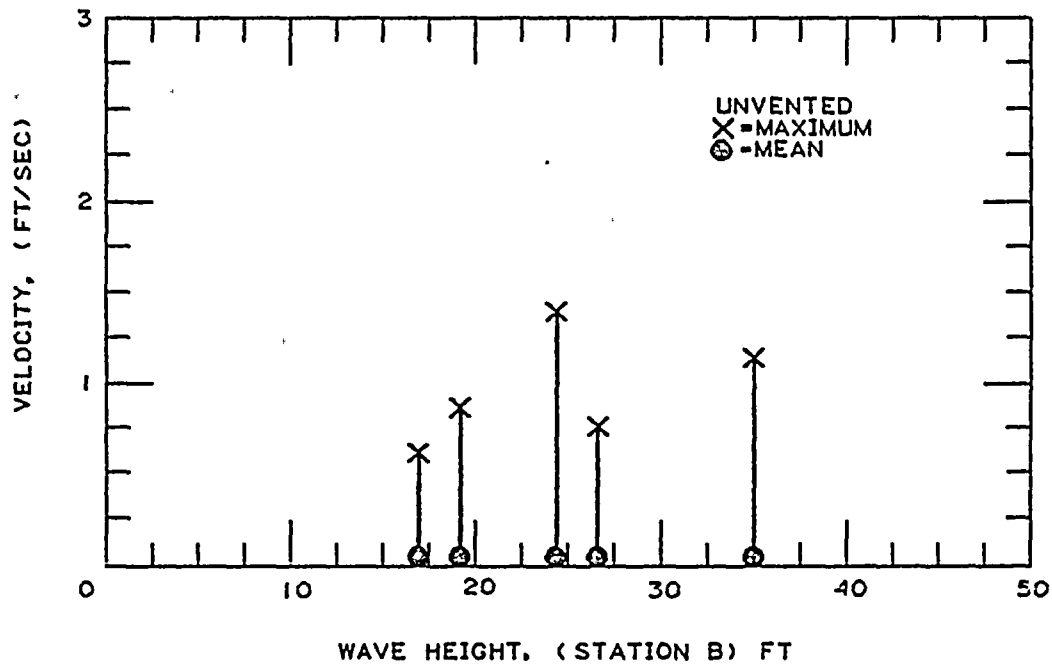


FIGURE 51 Velocity at Entrance to ASWP Forebay: +7.5 ft MLLW, T=16 sec, 203°Az, Unvented

16 sec waves. It should be noted that the mean of the data for each wave height at each period is nearly zero with maximum single values of velocity near 1 fps. In terms of reliable measurements, most maximum values of velocity are near or less than the threshold of the instrument so that one must be careful interpreting these figures; at best one can say the velocities are less than about 1 fps.

In Figures 52, 53, and 54 similar data are presented for the condition of a minimum tide (-2 ft MLLW) and limit waves. Indeed for these experiments also the velocities indicated are insignificant. In addition, it is shown, comparing Figures 53 and 54 for the same wave heights, that the vented case results in lower entrance velocities than the unvented case.

In summary, it appears that limit waves at these two tide levels do not introduce significant entrance velocities and, keeping in mind the discussion in Section 3.3.1 and the photographs of the dye traces within the forebays, the velocities within the chambers for these wave conditions must be less than those measured at the entrances to the forebays.

In addition to these measurements and photographs, observations were made of the motion of lucite cubes which would have equivalent prototype dimensions of about .1 ft on a side for the -2 ft MLLW tide elevation introduced at the entrance to one forebay. The specific gravity of the cubes was about 1.3. Irregular waves corresponding to the 1981⁺ storm were used, and it was observed that the cubes moved very slowly into the forebay always along the floor of the chamber. In the length of time of exposure to waves from this storm (approximately 47 min prototype) the cubes moved only about one-third of the length of the forebay. This is

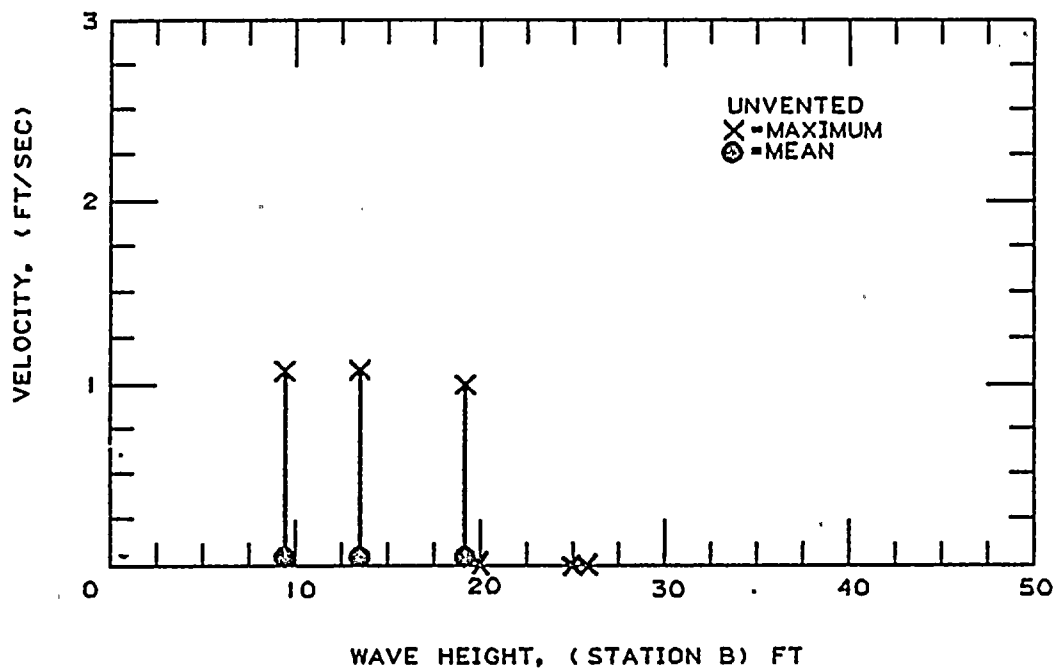


FIGURE 52 Velocity at Entrance to ASWP Forebay: -2 ft MLLW, T=12 sec, 203°Az, Unvented

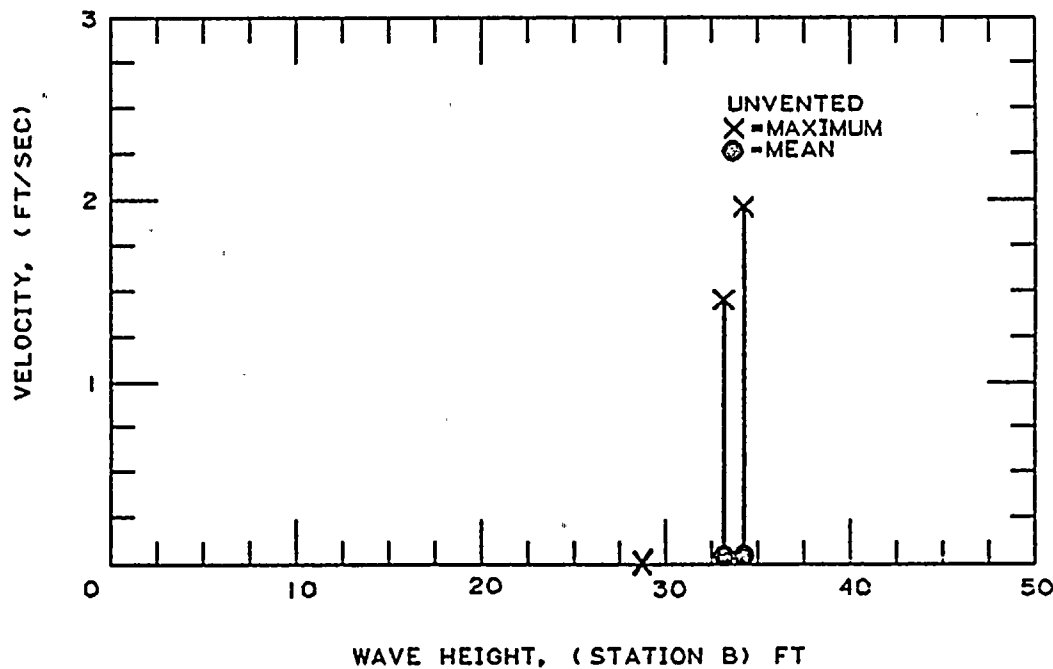


FIGURE 53 Velocity at Entrance to ASWP Forebay: -2 ft MLLW, T=16 sec, 203°Az, Unvented

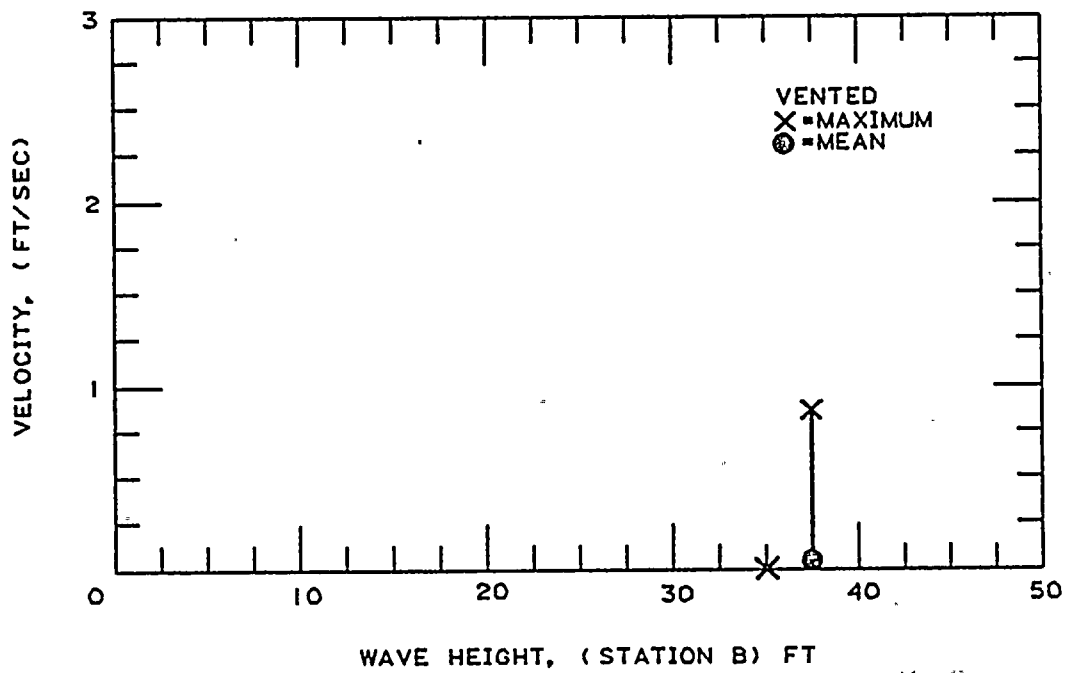


FIGURE 54 Velocity at Entrance to ASWP Forebay: -2 ft MLLW, T=16 sec, 203°Az, Vented (Moderate)

additional support to the observations made that the velocities in the forebays due to waves indeed must be small, and the likelihood of entrainment of missiles is extremely remote.

4. CONCLUSIONS

The following major conclusions can be drawn from this study:

- (1) For all conditions tested, no impact pressures were observed on the seaward face of the curtain wall of the cooling water intake structure.
- (2) In general, the pressure distributions observed were somewhat less than hydrostatic relative to the water level at the front of the curtain wall which occurred simultaneously with the maximum pressures.
- (3) For irregular waves and a still water level of +17 ft MLLW, the frequency distribution of wave heights and pressures on the curtain wall appears to follow a Rayleigh distribution.
- (4) For the 1981⁺ storm and a water surface elevation of +17 ft MLLW, the maximum total pressure measured on the front face of the curtain wall which occurs on the centerline at the lowest elevation was 44 ft. The probable maximum total pressure, obtained from the measurements and probability theory, would be about 59 ft.
- (5) For the pressures measured for the maximum credible wave event at a tide of +7.5 ft MLLW, using the limit wave concept, the loading on the centerline of the front face of the curtain wall was significantly less than for the conditions at +17 ft MLLW. The maximum total pressure measured at the lowest elevation was about 27 ft.
- (6) Impact pressures may occur on the underside of the deck of the intake structure. Tests indicated the pressures would be mitigated by removing the deck section abutting the parapet wall or installing wedge-shaped fillets under the deck in the corner formed by the deck and the curtain wall.

- (7) Impact pressures may occur on the ceiling of the forebay for the fully vented condition. Tests indicated that the pressure would be mitigated by restricting the venting to a moderately vented condition, or eliminating leaks, i.e. the unvented condition.
- (8) For the 1981⁺ storm and a +17 ft MLLW still water level the pressures measured on the ceilings of the four ASWP forebays with the structure vented or unvented were similar. The maximum total pressure measured was 56 ft and the estimated probable maximum total pressure was between 88 ft and 97 ft.
- (9) For still water levels of +7.5 ft MLLW and -2 ft MLLW and for 12 sec and 16 sec periodic limit waves the total pressures measured on the ceiling of the auxiliary saltwater pump forebays were less than 64 ft. For -2 ft MLLW and the 1981⁺ storm the probable maximum pressure would be less than about 57 ft if the chamber is unvented or less than about 73 ft if it is vented by a small opening. (The maximum pressures measured were 30 ft for the unvented case and 41 ft for the moderately vented case.)
- (10) For +17 ft MLLW and the 1981⁺ storm the maximum measured velocity at the ASWP forebay entrances was about 4 fps. The probable maximum velocity inferred from measured cumulative frequency distributions would be between 4.0 fps and 7.8 fps. At extreme high tide (+7.5 ft MLLW) and at extreme low tide (-2 ft MLLW) using limit periodic waves for all conditions investigated the maximum velocities measured were less than 1 fps.
- (11) Photographs and visual observations of dye demonstrate the velocities in the forebays are less than those at the forebay entrance.
- (12) Plastic cubes with a specific gravity of about 1.3 moved only slowly along the floor of the ASWP forebays during irregular wave exposure indicating that missile entrainment would be extremely unlikely.

5. REFERENCES

- Borgman, L.E., "Extremal Analysis of Wave Hindcasts for the Diablo Canyon Area, California made by Mr. R. Strange," Report to O.J. Lillevang, June 18, 1982.
- French, J.A., "Wave Uplift Pressures on Horizontal Platforms," Report KH-R-19, W. M. Keck Laboratory of Hydraulics and Water Resources, Caltech, July 1969.
- Funke, E.R. and Mansard, E.P.D., "On the Synthesis of Realistic Sea States," Proc. of 17th International Conference on Coastal Engineering, 1980.
- Goda, Y., "Numerical Experiments on Wave Statistics with Spectral Simulation," Report of the Port and Harbor Research Institute, Japan, Vol. 9, No. 3, Sept. 1970.
- Goda, Y. and Suzuki, Y., "Estimation of Incident and Reflected Waves in Random Wave Experiments," Proc. of 15th International Conference on Coastal Engineering, 1976.
- Goring, D.G., "Tsunamis - The Propagation of Long Waves Onto a Shelf," Report KH-R-38, W. M. Keck Laboratory of Hydraulics and Water Resources, Caltech, November 1978.
- Goring, D.G. and Raichlen, F., "The Generation of Long Waves in the Laboratory," Proc. of the 17th International Conference on Coastal Engineering, 1980.
- Hwang, L.-S. and Brandsma, M., "Earthquake Generated Water Waves at the Diablo Canyon Power Plant," Tetra Tech Report No. TC-443, September 1974.

Lillevang, O.J., Raichlen, F., and Cox, J.C., "The Height Limiting Effect of Sea Floor Terrain Features and of Hypothetically Extensively Reduced Breakwaters on Wave Action at Diablo Canyon' Sea Water Intake," Report for P.G. & E., March 15, 1982.

Longuet-Higgins, M.S., "On the Statistical Distribution of the Heights of Sea Waves," Journal of Marine Research, Vol. XI, No. 3, 1952.

Ochi, M.K., "On the Prediction of Extreme Values," Journal of Ship Research, 17:29-37, 1973.

Sarpkaya, T. and Isaacson, M., "Mechanics of Wave Forces on Offshore Structures," Van Nostrand Reinhold Co., 1981.

Smiley, R.E., "Water-Pressure Distributions During Landings of a Prismatic Model Having an Angle of Deadrise of $22\frac{1}{2}^\circ$ and Beam Loading Coefficient of 0.48 and 0.97," NACA TN2816, Nov. 1952.

Strange, R.R., "Wave Hindcasts for Diablo Canyon Area, California," Report to O.J. Lillevang, February 1982.